

Dear Prof. Whitehouse,

Please find enclosed a thoroughly revised manuscript based on the excellent reviews we were provided with. We also provide the point-by-point response to each reviewer and a "latexdiff" version highlighting changes from the original submission. You will notice that some minor changes occurred relative to those in our original response to reviewers. This is due to a final extensive internal revision to ensure a more fluid reading and a better connected text. We hope that you can appreciate this difference.

The study now includes an assessment of the effect of horizontal resolution (Fig. S15), which we proposed to include in response to your initial evaluation before the manuscript was accepted for reviews. We performed simulations at several resolutions, refining from 20 km (which we present in the main text) up to 10 km. Simulations at 16 and 15 km are already finished and included in the mentioned figure. Due to technical issues that have been already solved, the computationally expensive simulations at 10 and 12 km had to be re-run and are not yet complete. However, we can already see that none of these additional simulations shows significant changes that affect the conclusions of our study.

We hope that you find our response satisfactory, and the updated manuscript further strengthened.

Yours Sincerely,

Martim Mas e Braga  
(corresponding author)

Dear editor, dear Dr. Schanwell,

We thank the reviewer for his constructive, insightful and helpful evaluation which we feel helped to improve the manuscript. This instigated additional modeling that resulted in numerous refinements, and significant upgrades to the model description and discussion sections. Below, we provide a point-by-point response to each comment, which we numbered in red for easier reference. Our response is structured as follows: Referee comment (*in black italics*), author's response (in green), and proposed changes in the original manuscript text (*in blue italics*) where significant rewriting was done to include the suggested changes. We also add to the end of each figure caption (in blue) their proposed numbering in the revised version of the manuscript.

## Main concerns

**1.** “[...] I suggest to expand section 2.1 to add this required information. To be more specific, what type of stress balance does SICOPOLIS use? What kind of basal friction law do you apply? I know you list the parameters in Table 1, but without the corresponding equation, they are rather useless. Does your basal friction coefficient vary spatially and/or temporally? What are your boundary conditions for your enthalpy equation (e.g. do you specify a geothermal heat flux? Is it spatially constant)? How do you treat calving in the model? There are a number of ways how to parameterise this. Since you talk about this in your results, it is essential to know how this is handled in your model. Also you should mention with what geometry you initialise your model. I believe it is with present-day geometry, but with which dataset (Bedmap2, Bedmachine)? Do you take the bedrock and ocean floor topography from the same dataset?”

**Our response:** We have expanded the model description, including the requested additional information, as can be seen below:

*“For our experiments we employ the 3D thermomechanical polythermal ice-sheet model SICOPOLIS (Greve, 1997, Sato & Greve, 2012) with a 20 km horizontal grid resolution and 81 terrain-following layers. It uses the one-layer enthalpy scheme of Greve & Blatter (2016), which is able to correctly track the position of the cold-temperate transition in the thermal structure of a polythermal ice body.*

*The model combines the Shallow Ice Approximation (SIA) and Shelfy Stream Approximation (SStA) using (c.f. Bernaldes et al., 2017a, Eq. 1)*

$$U = (1 - w) \cdot u_{sia} + u_{sstA}$$

*where  $U$  is the resulting hybrid velocity,  $u_{sia}$  and  $u_{sstA}$  are the SIA and SStA horizontal velocities, respectively, and  $w$  is a weight computed as*

$$w(|u_{sstA}|) = \frac{2}{\pi} \arctan\left(\frac{|u_{sstA}|^2}{u_{ref}^2}\right)$$

*where the reference velocity,  $u_{ref}$ , is set to  $30 \text{ ma}^{-1}$ , marking the transition between slow and fast ice. This hybrid scheme reduces the contribution from SIA velocities mostly in coastal areas of fast ice flow and heterogeneous topography, where this approximation becomes invalid. Basal sliding is implemented within the computation of SStA velocities as a Weertman-type law (cf. Bernaldes et al., 2017a, Eqs. 2--6). The amount of sliding is controlled by a fixed, spatially varying map of friction coefficients that was iteratively adjusted during an initial present-day equilibrium run (cf. Pollard & DeConto, 2012b), such that the grounded ice thickness matches the present-day observations from Bedmap2 (Fretwell et al., 2013) as*

close as possible. Sliding coefficients in sub-ice shelf and ocean areas are set to  $10^5 \text{ ma}^{-1} \text{ Pa}^{-1}$ , representing soft, deformable sediment, in case the grounded ice advances over this region. The initial bedrock, ice base, and ocean floor elevations are also taken from Bedmap2. Enhancement factors for both grounded and floating ice are set to 1, based on sensitivity tests in Bernales et al. (2017b). This choice provides the best match between observed and modelled ice thickness for this hybrid scheme, similar to the findings in Pollard & DeConto (2012a).

Surface mass balance is calculated as the difference between accumulation and surface melting. The latter is computed using a semi-analytical solution of the positive degree day (PDD) model following Calov & Greve (2005). Near-surface air temperatures entering the PDD scheme are adjusted through a lapse rate correction of  $8.0 \text{ }^\circ\text{C km}^{-1}$  to account for differences between the modelled ice sheet topography and that used in the climate model from which the air temperatures are taken. For the basal mass balance of ice shelves, we use a calibration scheme of basal melting rates developed in Bernales et al. (2017b) to optimise a parameterisation based on Beckman & Goosse (2003) and Martin et al. (2011) that assumes a quadratic dependence on ocean thermal forcing (Holland et al., 2008; Pollard & DeConto, 2012; Favier et al., 2019). This optimised parameterisation is able to respond to variations in the applied Glacial Index (GI, Sect. 2.2) forcing. A more detailed description of this parameterisation is given in Sect. 1 of the supplementary material. In our experiments, we prescribe a time lag of 300 years for the ocean response to GI variations, which is considered the most likely lag in response time of the ocean compared to the atmosphere in the Southern Ocean (Yang & Zhu, 2011). At the grounding line, the basal mass balance of partially floating grid cells is computed as the average melting of the surrounding, fully floating cells, multiplied by a factor between 0 and 1 that depends on the fraction of the cell that is floating. This fraction is computed using an estimate of the sub-grid grounding line position based on an interpolation of the current, modelled bedrock and ice-shelf basal topographies. At the ice shelf fronts, calving events are parameterised through a simple thickness threshold, where ice thinner than 50 m is instantly calved away.

Glacial isostatic adjustment is implemented using a simple elastic lithosphere, relaxing asthenosphere (ELRA) model, with a time lag of 1 kyr and flexural rigidity of  $2.0 \times 10^{25} \text{ Nm}$ , which Konrad et al. (2014) found to best reproduce the results of a fully-coupled ice sheet–self-gravitating viscoelastic solid Earth model. The geothermal heat flux applied at the base of the lithosphere is taken from Maule et al. (2005) and is kept constant. All relevant parameters used in the modelling experiments are listed in Table 1.”

**“2. Could you please motivate the ensembles or parameters changes that you are investigating a bit more? As it stands now, it seems like you picked a number of parameters, but there also could an argument be made for a bunch of other parameters to be varied.”**

**Our response:** We picked these ensembles as they are inherent sources of uncertainty that were not addressed by any previous studies that included MIS11. We also performed additional tests to support our parameter choices (such as ocean temperature, lag in its response, and the choice of climate model), which we included in the supplementary material. We justify the choice of ensembles in the last paragraph of the introduction:

*“For this purpose, we perform five ensembles of numerical simulations of the AIS evolution and focus on aspects that remain unaddressed by previous studies. We evaluate the impact on resulting ice volume and extent of the choice of proxy records (including their differences in signal intensity and structure), the choice of sea level reconstruction, and of uncertainties in assumptions regarding the geometry of the AIS at the start of MIS11c.”*

**“3. I find most of the figures (e.g. 4, 6,7,9) not very informative. Looking at integrated quantities is OK, but having five Figures like that is too much. I suggest to combine them into a Figure with several panels. I also find it hard to judge in these volume plots whether differences are small or large (Is 2000 km<sup>3</sup> a lot?). Maybe better to plot it in percent normalised to your starting volume? Also just because your ice volume is similar does not mean you cannot have regional differences in grounding-line position or ice thickness. For example on P16L279 you state “. . . show similar retreat rates...” but I cannot find a Figure where this is actually shown. So I suggest to add some Figures, where we can also look at some spatial differences (a few suggestion in the technical corrections below). For example, you could plot some grounding-line positions from different simulations in 2D on top of each other to see the differences in retreat or lack thereof. I also encourage the authors to discuss their results more in depth. For example, they state in L276ff that different initial ice sheet configurations converge to the same geometry for the same climate forcings. This alone is quite surprising to me and**

at least warrants a discussion why potential feedback mechanisms (e.g. stabilising grounding-line on topographic height) are not triggered in these simulations?”

**Our response:** We have added a compilation of all different GIs as a panel in Fig. 2, which allows us to remove them from Fig. 1 (see Figs. 1 and 2 below). Regarding figures 4, 6, 7, and 9, they were restructured, with their (b) panels being merged into a single figure, and added a line that represents present AIS volume, as suggested by Reviewer 2 (see Fig. 3 below). We have added a new figure (see Fig. 4 below) where we show the grounding lines for each of our core experiments at times of interest: 420, 415, 410, and 405 ka. Regarding the fact that different configurations converge to the same geometry, we have found a tipping point at 412 ka (as pointed out by Reviewer 2 in his comment 47), where the ocean forcing under the main ice shelves (cf. Fig. 8) is strong enough to drive ice sheet retreat in all geometry scenarios. There are two grounding-line stabilising feedbacks not included in our current version of the model: (i) a local sea-level drop caused by a reduced gravitational attraction of a shrinking ice sheet (e.g. Mitrovica et al., 2009), and (ii) the observed faster rebound of the crust due to a lower mantle viscosity in some WAIS locations (Barletta et al., 2018). Even though our ELRA model is set up with a relatively fast response time of 1 kyr (compared to the standard 3 kyr), the resulting bedrock uplift is still not able to trigger a stabilizing effect that compensates for the strong ocean-driven retreat. These feedback mechanisms during MIS11c could be further investigated through the utilization of an Earth-ice coupled model, which is certainly an interesting topic for future research. These points are incorporated in the end of our Discussion section:

*There are, however, two stabilising feedbacks which are not incorporated in our model: (i) a local sea-level drop caused by a reduced gravitational attraction of a shrinking ice sheet (e.g., Mitrovica et al., 2009), and (ii) the observed faster rebound of the crust due to a lower mantle viscosity in some WAIS locations (Barletta et al., 2018). The first effect is probably small based on our model's insensitivity to sea-level changes over these time scales, but we have been unable to robustly test the effect of a faster rebound on AIS response during MIS11c. However, we note that our ELRA model is set up with a relatively short response time of 1 kyr, for which the resulting bedrock uplift is still not able to trigger a stabilizing effect large enough to prevent WAIS collapse.*

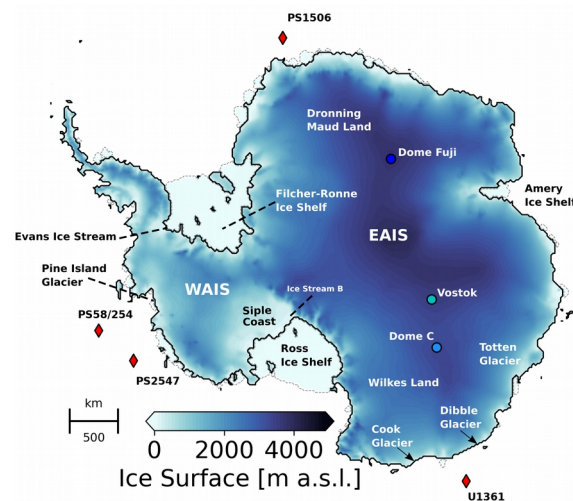


Figure 1: Surface topography of the AIS at the start of our core experiments (425 ka), based on a calibration against Bedmap2 (Fretwell et al., 2013; see Sect. 2.1). The locations mentioned in the text, including the drilling sites of the ice (circles) and sediment (red diamonds) cores on and around Antarctica, are showcased. This is Fig. 1 after the revisions to the manuscript.

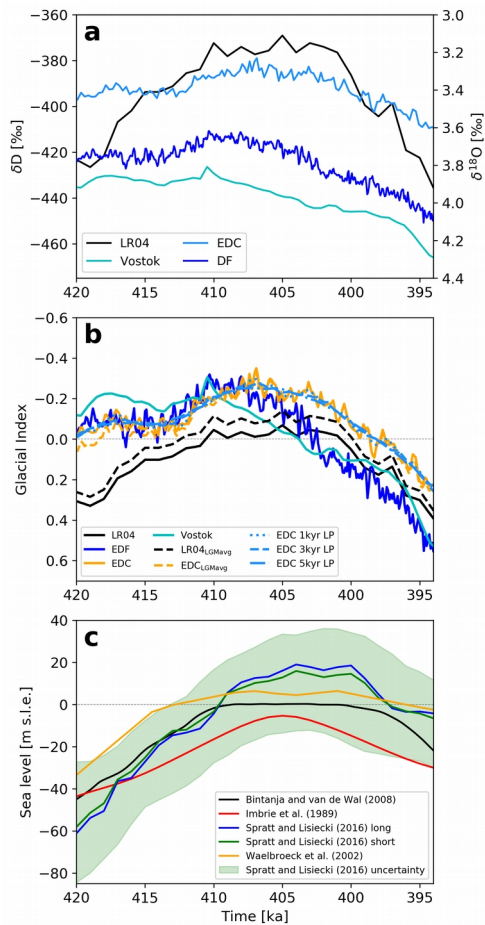


Figure 2: Reconstructions used in this study: (a) LR04  $\delta^{18}\text{O}$  (black) and ice-core  $\delta\text{D}$  [‰]; (b) resulting Glacial Indices from the reconstructions in (a) (cf. Sect. 2 and Table 2); (c) global mean sea level anomaly relative to PI (meter sea level equivalent, m s.l.e.). This is Fig. 2 after the revisions to the manuscript.

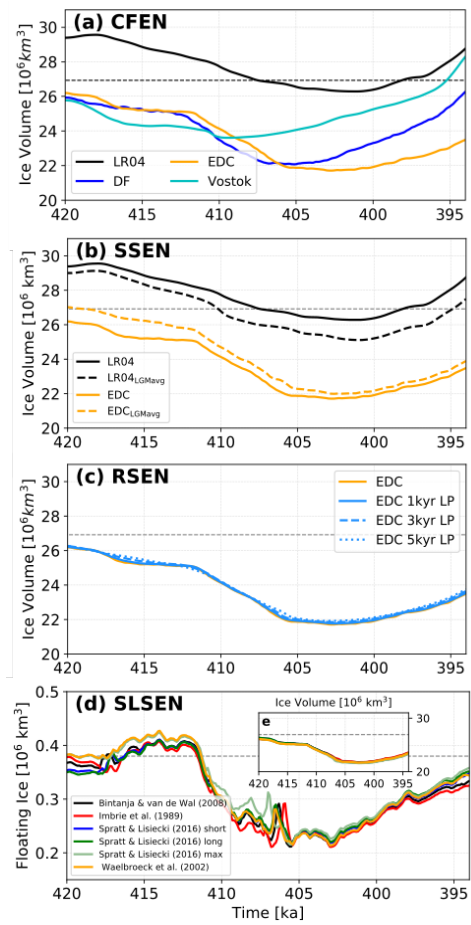


Figure 3: Sensitivity of AIS response (in total ice volume,  $10^3 \text{ km}^3$ ) between 420 ka and 394 ka to (a) CFEN GI reconstructions; (b) SSEN rescaled GI reconstructions; (c) RSEN low-pass filtered GI reconstructions; (d) SLEN sea level reconstructions forced by EDC GI (cf. Table 4). This is Fig. 4 after the revisions to the manuscript.

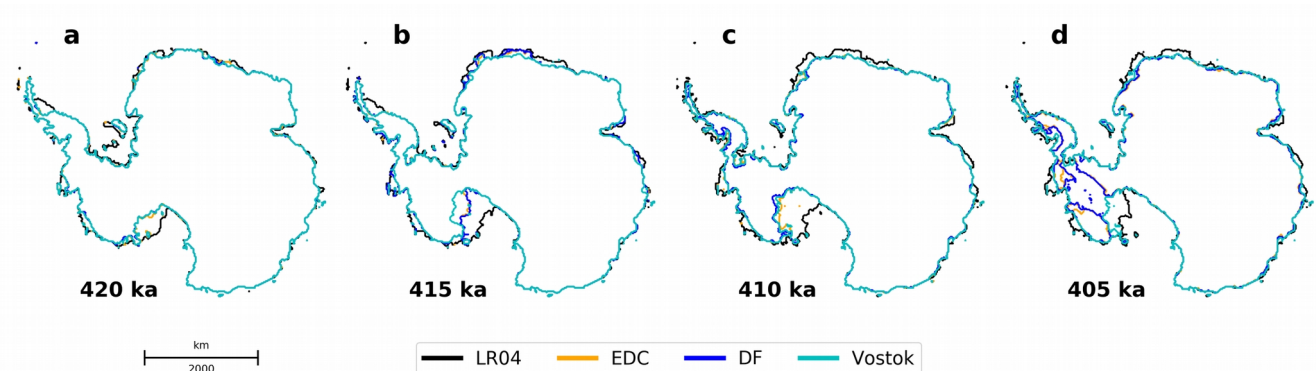


Figure 4: Grounding lines at 420, 415, 410, and 405 ka for the CFEN simulations. This is Fig. 5 after the revisions to the manuscript.

*“4. I think you should scratch your attempt to identify drivers for future change. You have it in your research questions, but other than in the conclusion section you never mention it again. And your statement in the conclusion statement is extremely vague (and we know this already) and to be honest not backed up by your simulation results.”*

**Our response:** We agree with the reviewer regarding the relative weakness of this section, and have removed the mention of drivers for future change from our research questions and the conclusions.

*“5. The abstract in its current form is much too long and too descriptive. Please shorten and make more concise.”*

**Our response:** we have shortened the abstract, and modified it to also account for the analyses suggested by Reviewer 2. It now reads:

*“Studying the response of the Antarctic ice sheets during periods when climate conditions were similar to the present can provide important insights into current observed changes and help identify natural drivers of ice sheet retreat. In this context, the Marine Isotope Substage 11c (MIS11c) interglacial offers a suitable scenario, given that during its later portion, orbital parameters were close to our current interglacial. In particular, ice core data indicate that warmer-than-present temperatures lasted for longer than during other interglacials, and the response of the Antarctic ice sheets and their contribution to sea level rise remain unclear. We explore the dynamics of the Antarctic ice sheets during this period using a numerical ice-sheet model forced by MIS11c climate conditions derived from climate model outputs scaled by three glaciological and one sedimentary proxy records of ice volume. Our results indicate that the East and West Antarctic ice sheets contributed with 3.2 to 8.2 m to the MIS11c sea level rise. In the case of a West Antarctic Ice Sheet collapse, which is the most probable scenario according to far-field sea level reconstructions, the range is further reduced to 6.7--8.2 m, independently of the choices of sea level reconstructions and millennial-scale climate variability. Within this latter range, the main source of uncertainty arises from the sensitivity of the East Antarctic Ice Sheet to a choice of initial configuration. We found that the warmer regional climate signal captured by Antarctic ice cores during peak MIS11c is crucial to reproduce its recorded sea level highstand. Furthermore, we show that a modest 0.4 °C oceanic warming at intermediate depths leads to a collapse of the West Antarctic Ice Sheet if sustained for at least 4 thousand years.”*

*“6. This is more an optional point and maybe a matter of taste, but I think you could also add a model limitations section. There are a few places where you can shorten the main text (see below), so that this would not much increase the length of the manuscript. I always find it helpful in modelling papers to have a section in which limitations and potential future avenues for improvements are discussed. I must admit that as the paper stands now with very little information about the ice-sheet model, it is hard to examine what the benefit of your model setup is?”*

**Our response:** We expect that the changes made in the methods (included as a response to comment 1) help to partly clarify this issue. We have further opted to discuss the model limitations within the context where they were relevant in the discussions, as opposed to giving them their own section.

## **Technical corrections**

**7.** *“L8 I do not think that the Greenland information is necessary in the abstract. Also the latter half of the sentence makes no sense to me “. . . , both configurations of the Antarctic ice sheets. . . ”? What configurations?”*

**Our response:** We have removed the mention of the Greenland Ice Sheet sea-level contribution from the abstract, and we expect that the reformulation presented above (comment 5) has clarified the text.

**8.** *“L12 Does LR04 need to be introduced as an acronym? I did not know straight away what it is.”*

**Our response:** We have removed the LR04 acronym from the abstract while making it more concise and less descriptive as requested (see response to comment 5).

**9.** L17 Here and throughout, I find the term “ice-sheet contraction” unusual. I know what you mean, but I think more commonly it is referred to as “ice-sheet retreat”. Please consider changing it.

**Our response:** We had used “contraction” since the changes seen are both in extent and volume. Nevertheless, we reverted to the usual term as suggested.

**10.** L29-34 This sentence is way too long and confusing. Please split up and make clearer.

**Our response:** We recognise the sentence was indeed too long, and have rewritten the passage. It now reads:

*“However, Dutton et al. (2015) point out that climate modelling experiments with realistic orbital and greenhouse gas forcings fail to fully capture this MIS11c warming despite the fact that orbital parameters were almost identical to Present Day (PD) during its late stage (EPICA, 2004; Raynaud et al., 2005). Earlier studies (e.g., Milker et al., 2013; Kleinen et al., 2014) have shown that climate models also tend to underestimate climate variations during MIS11c, for which ice core reconstructions show the mean annual atmospheric temperature over Antarctica to have been about 2 °C warmer than Pre-Industrial (PI) values.”*

**11.** L43 What do you mean by “reduced stability”? And why would that trigger stronger glacial-interglacial cycles?

**Our response:** Holden et al. (2011) show that a reduced stability of the WAIS (i.e., a higher susceptibility to collapse) through time is caused by an increased bedrock relief as a result of continuous erosion, while Holden et al. (2010) show that the positive feedback of a strong WAIS retreat could contribute to these stronger cycles. We have added the Holden et al. (2010) citation and rewrote this part of the introduction as shown below. We refrained from discussing the mechanisms for the mentioned feedback in detail, since they are not the focus of our work.

*“The unusual length of this interglacial and a transition to stronger glacial-interglacial cycles seen in the subsequent geological record may have been triggered by a reduced stability of the West Antarctic Ice Sheet (WAIS, Fig. 1). The latter may have been due to the cumulative effects of the ice sheet lowering its bed (Holden et al., 2011), which in turn provided a positive climate feedback (Holden et al., 2010).”*

**12.** L49-55 I think this paragraph can be thrown out, as it is irrelevant to the Antarctic simulations in the paper. It suffices to say, I believe, that the ice-sheet history in Antarctica is more uncertain than for Greenland.

**Our response:** We have removed the paragraph, and moved the appropriate references to the beginning of the next paragraph, which we start with

*“The MIS11c history of Antarctica is less constrained than that of Greenland (e.g., Willerslev et al., 2007; Reyes et al., 2014; Dutton et al., 2015; Robinson et al., 2017).”*

**13.** L56-58 The first half of the sentence is confusing. The way it is written, it makes it sound as if Raymo and Mitrovica estimated it to be 6-13 m above present-day? But why is there a reference to Dutton et al. then? Here and throughout, could you please try to keep sentences shorter. It makes it easier to follow for the reader.

**Our response:** We have removed the Dutton et al. reference, as it was misplaced there. We tried to rewrite the sentences to be shorter and easier to follow where necessary.

**14.** L61-64 Again a very long sentence which I do not understand. Please break up the sentence and clarify.

**Our response:** We have rephrased the sentence:

*“Counter-intuitively, the dating of onshore moraines in the Dry Valleys to MIS11c has been used to indirectly support regional ice sheet retreat (Swanger et al., 2017). Swanger et al. (2017) argue that ice sheet retreat in the Ross Embayment provided nearby open-water conditions and therefore a source of moisture and enhanced precipitation, fueling local glacier growth.”*

**15. L65-80** Here, I would like to see what your study adds to studies like the one from Sutter et al. 2019. What is the advantage of your study/model setup ?

**Our response:** Our study has different objectives than that of Sutter et al. (2019), and thus uses different approaches. For example, we focus on MIS11 exclusively, evaluating different transient climate signals and testing for a different set of factors that can influence ice sheet simulations. We made this clearer by rewriting the last two paragraphs of the introduction:

*“As detailed, many modelling studies have investigated AIS responses over time periods that include MIS11. However, so far none has focused specifically on this period. Given the scarce information for MIS11 and conflicting constraints on how Antarctica responded to this exceptionally long interglacial (Milker et al., 2013; Dutton et al., 2015), we here focus on MIS11c, the peak warming period between 420 and 394 ka. Our aim is to reduce the current uncertainties in the AIS behaviour during MIS11c, specifically addressing the following questions:*

*[...]*

*For this purpose, we perform five ensembles of numerical simulations of the AIS evolution and focus on aspects that remain unaddressed by previous studies. We evaluate the impact on resulting ice volume and extent of the choice of proxy records (including their differences in signal intensity and structure), the choice of sea level reconstruction, and of uncertainties in assumptions regarding the geometry of the AIS at the start of MIS11c.”*

**16. L81** I do not agree that you are presenting model reconstructions. What you present are sensitivity experiments. But as far as I can tell, you are not trying to match any geological constraints which is what I understand as model reconstruction.

**Our response:** Geological constraints are very scarce for this period, and we discuss how our simulations match the available constraints throughout the manuscript (e.g., L313-318 and L368-375 in the original submission). Nevertheless, it is a good point that our experiments can be seen as sensitivity experiments. For this reason, we have refrained from using the term and rewrote this sentence also with input from Reviewer 2:

*“Given the scarce information for MIS11 and conflicting constraints on how Antarctica responded to this exceptionally long interglacial (Milker et al., 2013; Dutton et al., 2015), we here focus on MIS11c, the peak warming period between 420 and 394 ka. Our aim is to reduce the current uncertainties in the AIS behaviour during MIS11c, specifically addressing the following questions: [...]”*

**17. L85** As said above, I do not think you really address the last question about future ice-sheet changes. Therefore, I recommend removing it from the manuscript altogether.

**Our response:** We have removed this question.

**18. L106** In addition to the changes suggested above. How do you initialise for the different ice-sheet configurations? Do you use the same temperature spin-up and let it evolve afterwards? Or do you let it evolve to a different geometry and do the temperature spin-up then with a fixed geometry?

**Our response:** In response to your comments and those of Reviewer 2 (comment 33) regarding our different geometries, we have changed our approach. We force the thermally spun up ice sheet with LGM conditions for 5 kyr so it grows to an intermediate stage between PI and LGM extent, and then place the resulting geometry at different points in time: 420, 425 and 430 ka. We then let these transiently evolve from then until 394 ka, and analyse the period between 420 and 394 ka, as in the original submission. We made changes to the text (see below) and to Table 3 to reflect this new approach:

*“In order to create a representative range of initial geometries at 420 ka, we use a common starting geometry, but vary the relaxation time. For this purpose, we first create an ancillary geometry by perturbing the thermally spun-up AIS with a constant LGM climate (air temperature and precipitation rates) and no sub ice-shelf melting over a 5 kyr period. The resulting ancillary ice sheet (which has an extent that sits between PI and LGM configurations) is then placed at 420, 425 and 430 ka and runs transiently (following the respective GIs) until 394 ka. This creates a representative range of starting geometries at 420 ka (Fig. 3), and each initial ice sheet geometry is labelled gmt1 to gmt3 (Fig. 3a-c; shortest relaxation is gmt1, longest is gmt3). The gmt1 initial topography is generally more extensive and thinner than the control. Its grounding*

line advanced at the southern margin of the Filcher-Ronne Ice Shelf and at Siple Coast, but the ice sheet interior is on average 200 m thinner than the control and up to 500 m thinner across particular regions such as the dome areas of the WAIS and Wilkes Land (Dome C). It is, however, about 200 m thicker at its fringes, which results in a gentler surface gradient towards the ice sheet margins. The *gmt2* initial topography is less than 100 m thinner than control over the EAIS interior, and about 100 m thicker over the WAIS interior and at the EAIS margins. Finally, the *gmt3* initial topography is overall thicker than control, though not by more than 100 m except at the western side of the Antarctic Peninsula and the WAIS margins, where some regions are up to 300 m thicker (Fig. 3c).”

**19. L106** *From where do you get your surface temperature distribution? An ice core only provides you with temperature changes with respect to a certain baseline. Please add this to this section.*

**Our response:** Based on this comment and on comment 20, which led us to slightly alter our approach (as detailed in the answer to comment 20), we have rewritten the paragraph for increased clarity:

“All ensembles cover a period from 420 to 394 ka. After the calibration for basal sliding mentioned above, we initialise the AIS by performing a thermal spin-up over a period of 195 kyr from 620 to 425 ka, i.e., apply a transient surface temperature signal from the EDC ice core (Jouzel et al., 2007) as an anomaly to our PI climate (described in the next section) while keeping the ice sheet geometry constant at our previously calibrated Bedmap2-based configuration. We then let the AIS freely evolve for 5 kyr, between 425 and 420 ka, applying transient GI forcing during the relaxation period (Fig. S12). We chose 425 ka as the starting point for relaxation because it is when the MIS11c oxygen isotope values in the EDC ice core are closest to PI. In summary, we ignore the first 5 kyr (425--420 ka) to avoid a shock from suddenly letting the ice-sheet topography freely evolve at the start of our period of interest.”

**20. L107-109** *This means you just move this shock outside of your time period of interest? This is in general OK, but raises the following questions: What forcing do you apply for the 5 ka in which the ice geometry is allowed to freely evolve? And how far away do you get from your initial geometry? And I am also missing a plot where you show that your ice sheet is close to steady state. I would appreciate if you could add a plot for this.*

**Our response:** We had initially applied the same GI forcing based on the EDC core for all simulations during the relaxation stage, so that they all had the same geometry at 420 ka. This proved to be a problem for the LR04-forced simulation, since it significantly deviates in its isotope values from the others. Consequently, and in response to the review, we now apply the GI forcing during the relaxation stage that corresponds to the forcing during the main experiments (i.e., the 425-420 ka DF GI for the DF-forced runs, EDC GI for the EDC-forced runs, and so on). A figure showing the spread in initial geometries during this period is now provided in the supplement (see Fig. 5 below). We do not provide a plot showing that the ice sheet is close to steady state because the point of the thermal spin-up is precisely to remove the effects of the initial steady state (attained during the calibration of the model) from our simulations, and offer a more realistic internal thermal structure for the AIS. All figures shown already contain the new simulations, and the corresponding part in the Methods section is also revised as shown in comment 19.

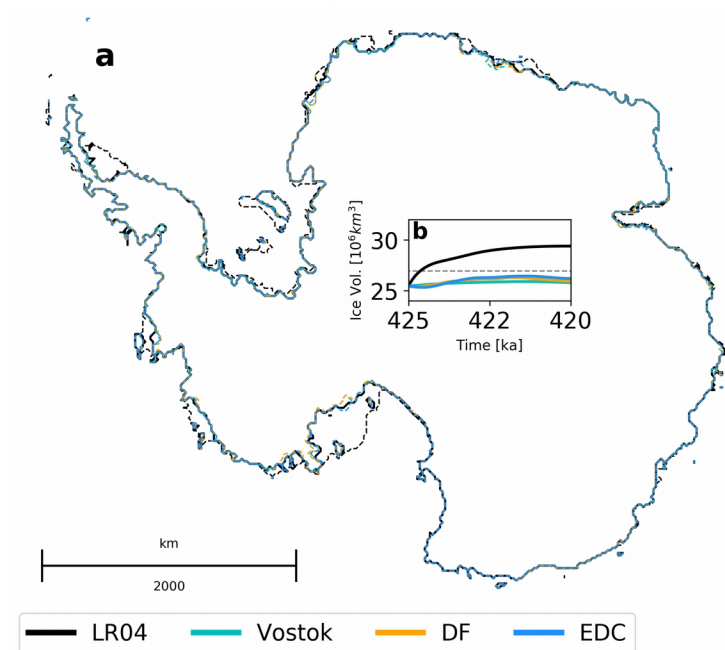


Figure 5: Relaxation period between 425 and 420 ka for all four CFEN members. (a) shows the grounding line at 420 ka (solid line) and at 425 ka for each member (dashed lines); (b) shows the evolution of total ice volume [10<sup>6</sup> km<sup>3</sup>] during this 5 kyr period for each member. Dashed line shows the volume of the present-day AIS according to Bedmap2. This is Fig. S12 after the revisions to the supplement.

**21.** L129, equation (2): From this equation I gather that you apply the same temperature differences to the ocean as you do to the atmosphere? And you also do not apply a time lag to the ocean warming/cooling? Is that really realistic giving the long response time of the ocean compared to the atmosphere? At the very least, this choice should be discussed somewhere in the text.

**Our response:** We do not apply the same temperature differences to ocean and atmosphere, but modulate them with the same index. The differences are obtained by the ocean temperature and atmospheric temperature fields from the climate forcing. We appreciate this criticism regarding the ocean lag, also voiced by Reviewer 2 (in his comment 4), and have acted accordingly. We have introduced a lag to the ocean forcing of 300 years, as this is the timescale of response of the Southern Ocean (Yang & Zhu, 2011). We additionally present in the supplement an ensemble of sensitivity tests to different time lags in the ocean forcing (see Fig. 6 below), which shows their effect to be very small compared to the timescales of this study. We tried to clarify the concern about the differences applied by rewriting the last sentence before Eq. (4):

“The atmospheric and ocean temperature ( $T$ ) fields at time  $t$  are reconstructed based on their respective PI and LGM reference fields ( $T_{PI}$  and  $T_{LGM}$  respectively) using: [...]”

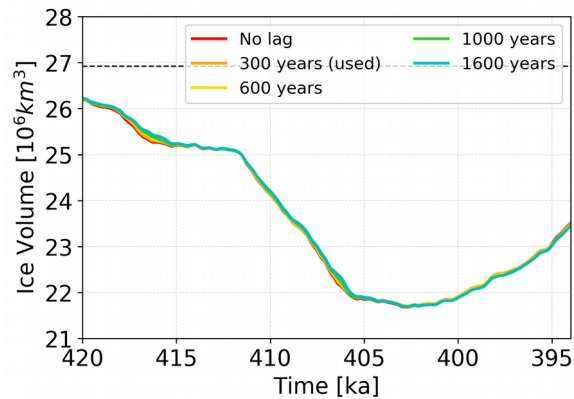


Figure 6: Sensitivity of the AIS response expressed in total ice volume [ $10^6 \text{ km}^3$ ] to a range of lags (0-1600 years) between the atmospheric forcing and the ocean forcing between 420 and 394 ka. This is Fig. S11 after the revisions to the supplement.

**22.** L137 To me all headers in this section should rather read “Model sensitivity to XXX”. Because this is ultimately what you do in this paper, rather than rigorously quantifying uncertainties.

**Our response:** We have changed it accordingly. We thank for this good suggestion as it also makes it consistent with the headers in section 3 (results).

**23.** L139-141 This sentence needs rewriting. I am not sure I understand what you are saying.

**Our response:** We have rewritten this section, also based on an additional request from Reviewer 2 (comment 30):

“Because different approaches have been used to transform the isotope curves into a GI, we assess the sensitivity to the choice of the scaling procedure by performing an additional scaling using another reference value for  $\delta X_{LGM}$ . In the new scaling procedure,  $\delta X_{LGM}$  is the average (between 19 ka and 26.5 ka) rather than the peak value. We compare the effects of using these two procedures when applied to the EDC ice core  $\delta D$  and the LR04 stack  $\delta^{18}O$  records. We call this ensemble the Scaling Sensitivity Ensemble (SSEN).”

**24.** L154 should be “mean sea level”

**Our response:** We have corrected as requested.

**25.** L166 Here I believe you say that you also initialise with present-day conditions, but this needs to come much earlier and with more info as to what datasets you used for this.

**Our response:** We expect that the changes made to the Methods section as described above (comment 1) have successfully addressed this issue. Hence, in this paragraph we merely provide a reference to section 2.1:

“Similar studies that assess AIS changes over glacial and interglacial cycles often adopt a PI or PD starting geometry (e.g., Sutter et al., 2019, Tigchelaar et al., 2019, Albrecht et al., 2020). We have followed the same approach in our CFEN experiments (see Sect. 2.1)”

**26.** L221 you state: “. . . ice sheet contraction is associated with strong basal melting close to the grounding lines ...”. First of all this comes a bit out of the blue. Secondly, you show little evidence that this is actually the case. In Fig. 5 you show that basal melting is dominating, but if you have different SMB rates, the basal melt rate could be either 1.5m/yr or 6 m/yr. Please also avoid relative terms like “strong” without giving any numbers. Do you mean 5, 50, or 500 m/yr when you say “strong” melting. Related to this, do you apply melting to partially grounded grid cells or only to fully floating? This makes a big difference how much your grounding line retreats for similar melt rates.

**Our response:** Based on this and other comments from the reviewers, we have moved this paragraph to the Discussion section, where it is more fitting and does not “come out of the blue”. We added the information about the basal melting to the Methods section (shown above in our response to comment 1). Also, we expect that changes made to Fig. 5 in the original manuscript (see Fig. 7 below) further help clarify the regions where SMB or ice-shelf basal melting dominates.

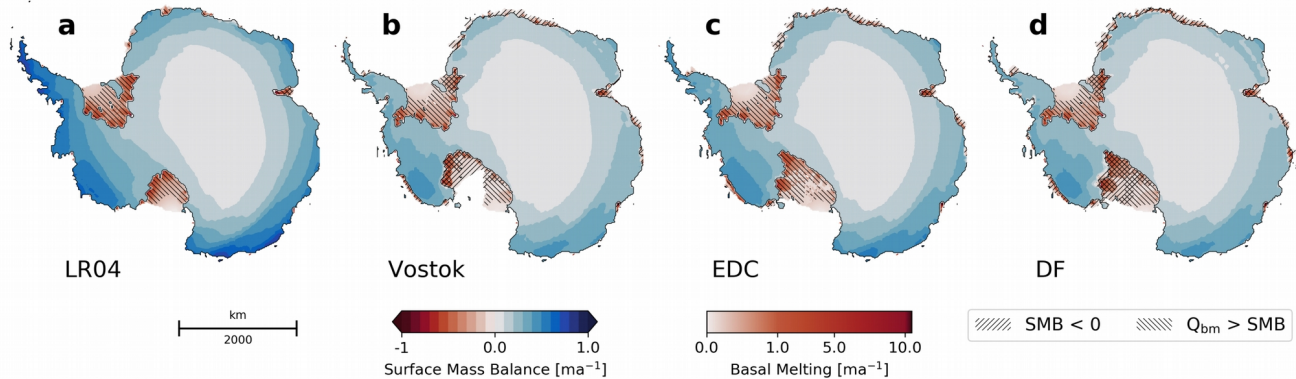


Figure 7: Surface mass balance (SMB,  $\text{ma}^{-1}$ ) for the grounded ice and basal melting ( $Q_{\text{bm}}$ ,  $\text{ma}^{-1}$ ) for the ice shelves for the CFEN simulations at 415 ka. Hatched areas show where basal melting dominates over surface mass balance and where surface mass balance is positive (i.e., where surface ablation occurs). Everywhere where  $Q_{\text{bm}} > \text{SMB}$ , ice shelves are thinning. This is Fig. 8 after the revisions to the manuscript.

27. L222 should read “. . . Siple Coast, at the Ross Ice Shelf, and underneath ...”

**Our response:** We thank the reviewer for spotting the typo and have corrected it.

28. L223-224 & L227 Since your basal melt rate is a quadratic function of your ocean temperature, stating that it is a combination of warming of the upper ocean layer and high melt rates is saying the same thing. Please reformulate.

**Our response:** This sentence has been removed, and we focus our discussion on the thermal forcing under the ice shelves, as opposed to the distribution of SMB vs. ice-shelf basal melting (Figs. 7, and 8).

29. L228 Two things here. First, since you have a separate results and discussion section, I was expecting only a description of the results. However, here and in other places (e.g. L245, L256-259) in your results section you are interpreting and discussing your results already. So either you have a combined results and discussion section or you move this material to your discussion section. Secondly, I cannot confirm your statement that ice loss is dominated by surface ablation on Amery in Fig.5. First of all, the panels are too small, so I am not sure if Amery is hatched or not? I do not really understand the purpose of Fig. 5, but to me Amery looks pretty red which means to me that there is a lot of ablation in this area. So why would it not retreat there and why is ablation so high in this region compared to basal melting?

**Our response:** Thank you for highlighting these points. We have moved this part to the discussion as suggested. As described in comment 26, Fig. 7 in this response letter shows significant improvements related to Fig. 5 in the original manuscript, and now better highlights the regions affected by basal melting and surface ablation. In combination with a new figure provided (see Fig. 8 below), we were able to see that Amery is indeed, contrary to what we originally stated, dominated by basal melting. However, the difference between surface ablation and basal melting is not as pronounced as in the larger ice shelves, such as Ross and Filchner-Ronne. We made the necessary adjustments to the text.

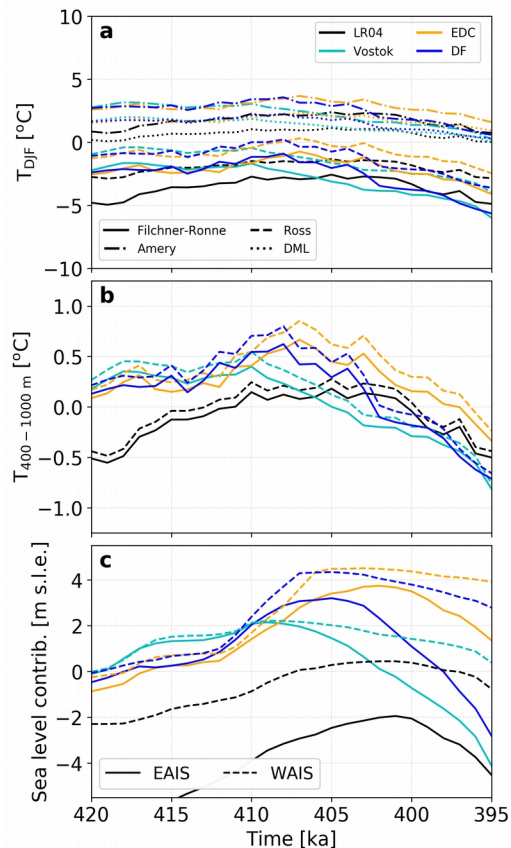


Figure 8: Evolution throughout MIS11 for each CFEN member for (a) Summer surface air temperature [°C] averaged over the main Antarctic ice shelves; (b) ocean temperatures averaged between 400 and 1000 m [°C] for the Filchner-Ronne and Ross ice shelves; (c) sea level contribution by EAIS and WAIS. Colours denote the respective CFEN member, while line styles in panels (a,b) denote each ice shelf, and each ice sheet in panel (c). DML refers to all smaller ice shelves along the Dronning Maud Land margin. This is Fig. 9 after the revisions to the manuscript.

**30.** L237 “. . . , the resulting ice sheet histories are quite similar.” This is true for the integrated ice volume, but again I find this quite superficial and it could be different when we look at 2D fields.

**Our response:** We have included a new figure (Fig. 4 above) to show the evolution of the grounding lines of each ensemble member at key times, and that further supports this statement that their histories are indeed fairly similar.

**31.** L242 If it is problematic why did you include it?

**Our response:** We have removed these from our study, as also requested by Reviewer 2.

**32.** L256-259 This is discussion for me (see comment above).

**Our response:** Indeed, we agree and have moved it to the discussion.

**33.** L268-L274 This paragraph should rather be part of your experimental design section. By now there are so many simulations that you performed that I think it is really necessary to add a table where you list all the simulations with important forcing parameters in a table. It is really hard to keep track of the simulations.

**Our response:** We agree with the reviewer; this paragraph felt out of place and was essentially recapping part of what we described in the methods. We have removed it. We appreciate the suggestion for a summary table, which we added to the end of the Methods section.

Table 4. Summary of performed experiments grouped by ensemble, listing their respective GI forcings, used sea level reconstruction and choice of initial geometry. LGMavg denotes that the GI was rescaled using the average LGM value as opposed to the peak value (cf. Sect. 2.3.1 and Table 4). The SGEN experiments were grouped for better visualisation, but each SGEN row corresponds to 3 experiments, one starting from each geometry (1 to 3).

Ensemble	Experiment	GI forcing	Sea level reconstruction	Initial Geometry
CFEN	lr04	LR04	Bintanja and van de Wal (2008)	control
CFEN	edc	EDC	Bintanja and van de Wal (2008)	control
CFEN	df	DF	Bintanja and van de Wal (2008)	control
CFEN	vos	Vostok	Bintanja and van de Wal (2008)	control
SSEN	lr04lgmavg	LR04 <sub>LGMavg</sub>	Bintanja and van de Wal (2008)	control
SSEN	edclgmavg	EDC <sub>LGMavg</sub>	Bintanja and van de Wal (2008)	control
RSEN	lp1bx	EDC (1 kyr low pass)	Bintanja and van de Wal (2008)	control
RSEN	lp3bx	EDC (3 kyr low pass)	Bintanja and van de Wal (2008)	control
SLSEN	lp5bx	EDC (5 kyr low pass)	Bintanja and van de Wal (2008)	control
SLSEN	s16l	EDC	Spratt and Lisiecki (2016) long	control
SLSEN	s16s	EDC	Spratt and Lisiecki (2016) short	control
SLSEN	s16u	EDC	Spratt and Lisiecki (2016) upper uncertainty	control
SLSEN	spm	EDC	Imbrie et al. (1989)	control
SLSEN	wae	EDC	Waelbroeck et al. (2002)	control
SGSEN	edcgmt[1-3]	EDC	Bintanja and van de Wal (2008)	gmt1-3
SGSEN	dfgmt[1-3]	DF	Bintanja and van de Wal (2008)	gmt1-3
SGSEN	vosgmt[1-3]	Vostok	Bintanja and van de Wal (2008)	gmt1-3

**34.** L276 To me that is really surprising. From my experience, the initial geometry is quite important with regard to what your results look like at the end of the simulation. You glance over this, but this needs a discussion. Why do you think this is the case?

**Our response:** The insensitivity to the choice of initial geometry of the WAIS seems to stem from the fact that the ocean is able to trigger its collapse regardless of its initial state. The EAIS, for example, showed a clear sensitivity to the initial geometry. We have included this in our discussion:

*“In this case, the EAIS contribution is the largest source of uncertainty, being most sensitive to the choice of starting ice geometry. This effect is strongest over Wilkes Land, where the spread in position of the grounding line is wider, and ice thickness is more variable than for other basins (Fig. 7). While nearby drainage basins, such as those of Totten and Dibble glaciers, become more stable given the larger ice sheet configurations of the alternative geometries (Figs. 3b,c), Cook glacier, emanating from Wilkes Subglacial basin, appears to thin regardless of the choice of initial geometry (Figs. 7a-c). Overall, the EAIS contributes 1.1 to 3.7 m s.l.e. at 405 ka (Fig. 11). Conversely, the WAIS was rather insensitive to the choice of starting geometry (yielding 4.3--4.5 m s.l.e. at 405 ka in the case of a collapse, and 2.0--2.1 otherwise) due to the stronger role played by the sub-shelf ocean forcing after 412 ka.”*

**35.** L279 “. . . also show similar rates of retreat ...”. Again this is nowhere shown. I mean in Fig. 10 it looks like they actually have exactly the same grounding-line position. Is that true?

**Our response:** We modified Figs. 3 and 10 of the original manuscript (Figs. 9 and 10 presented below), also based on comment 43. The grounding lines are indeed close to each other, but are not at the same position. Also, by “rates” we mean their pacing, and not the starting and final volumes, which

can be seen in Fig. 9 in the original submission. We have changed the phrasing in the text to avoid misunderstanding.

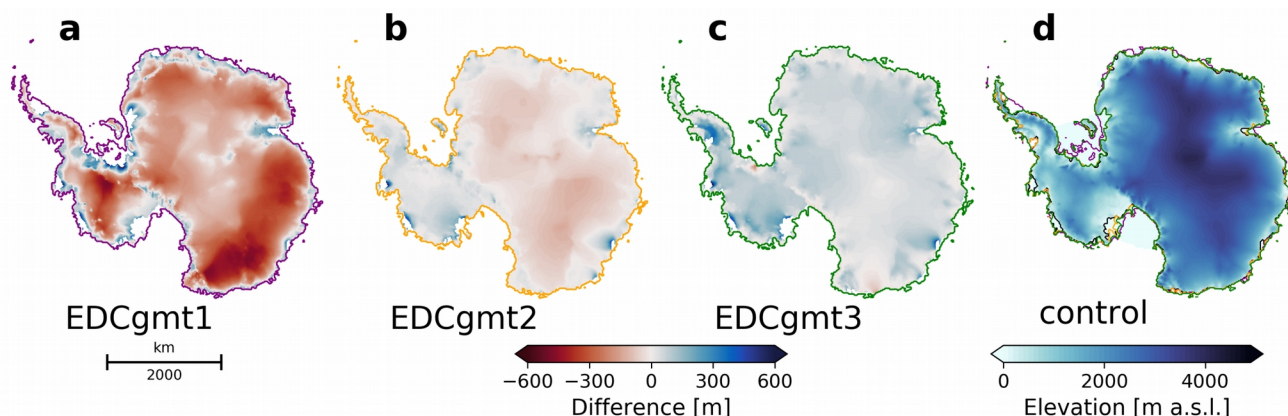


Figure 9: (a-c) Three different starting ice sheet geometries at 420 ka for the EDC CFEN member (gmt1-3). Color scheme shows differences in surface elevation between each geometry and the control for 420 ka (d). Differences are only shown where the ice is grounded in both geometries, and coloured lines show the respective grounding lines in gmt1-3, also overlain in (d). This is Fig. 3 after the revisions to the manuscript.

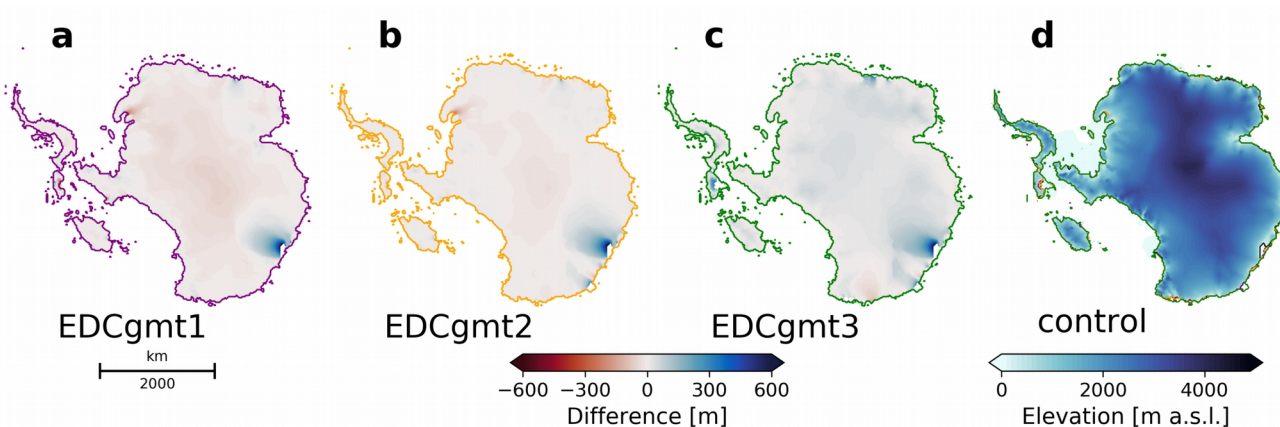


Figure 10: (a-c) ice sheet geometries at 405 ka for the EDC CFEN member using three different starting geometries at 420 ka (Fig. 3). Color scheme shows differences in surface elevation between each geometry and the control for 405 ka (d). Differences are only shown where the ice is grounded in both geometries, and coloured lines show the respective grounding lines in gmt1-3, also overlain in (d). This is Fig. 7 after the revisions to the manuscript.

**36.** L282 Could you please add these locations to the respective Figure for better orientation.

**Our response:** These locations were added to Fig. 1 (see our response to comment 3), so that it can be used as a reference for the locations cited in the manuscript, while the remaining figures can be less cluttered with text. Some glacier locations were also reviewed based on comment 12 from Reviewer 2, as we were originally pointing to adjacent glaciers instead.

**37.** L289-301 This is a weak introduction to the discussion and repeats most of the material that you covered in the introduction. Consider removing it.

**Our response:** We have removed it, while significantly reordering and rewriting most of the discussion, in light of the comments from both reviewers.

**38.** L321 “. . . it seems that ice-shelf calving plays a role just as big”. This again comes totally out of the blue and at the moment there is no way to check this statement as it is simply not described how calving is handled in the model. I also do not quite follow the explanation for this. Could the authors please elaborate on this?

**Our response:** Calving in our model is done by a simple thickness threshold, where ice thinner than 50 m is calved out instantly. We have included this in our methods section (see our response to comment 1). Furthermore, in the rewriting of the discussion, this passage was removed. It no longer made sense to discuss calving there.

**39.** L393 delete objective

L406-407 Delete last sentence (see comment above).

**Our response:** We have removed the sentence and the word “objective”.

**40.** Comment hyphenation: I noticed that throughout the manuscript your use of hyphenation is inconsistent. You write ice-shelf calving, but then grounding line advance without hyphen. I am not sure what the TC policy is, but please make sure that you are at least consistent throughout the manuscript

**Our response:** We thank the reviewer for noticing it, and have addressed the mistakes.

## Figures

**41.** Fig. 1: Please add a scale bar. Glacial index plots and their labels could be bigger.

**Our response:** We have added a scale bar. The GI plots were removed from Fig 1 (see our response to comment 3).

**42.** Fig. 2: Why do you show the time series until present-day? I think a zoom in into the period of interest would be better.

**Our response:** Thank you for this suggestion. We have zoomed in to our period of interest, and added the GI plots from Fig. 1 in the original submission as Fig. 2b in this response letter.

**43.** Fig. 3: It is really hard to see any differences in the upper panel (a-d) with the current colour scale. Also the grounding-line position should be made more prominent (thicker line or different color). In general there is too much white space and subplot labels (a-g) are too small. Please make each subplot bigger for better readability. Please also add a scale bar.

**Our response:** The reviewer has a good point that it is hard to see differences in the upper panel, and a rescaling of the colorbar did not satisfactorily improve it. Thus, we have changed the figure to show only the control topography, and kept the difference plots to compare with the other geometries. We added thicker and colored lines for the grounding lines, which are plotted over their respective difference plot and over the control plot for an easier comparison. We have also added a scale bar as suggested. The same was applied to Fig. 10, which had the same style. Both figures were presented earlier in this letter as Figs. 9 and 10 (under our response to comment 35).

**44.** Fig. 4: In the lower plot it looks like your model run for LR04 is not really in steady state or is your initial perturbation that large compared to your spin-up forcing? As mentioned above, I do not find the current y-axis units very intuitive for the lower panel. Labels (a,b) are too small.

**Our response:** We never intended for it to be in steady state before this period, which is why we performed a thermal spin-up and gave it a relaxation period. Given the changes to the relaxation stage mentioned above, this figure has changed substantially, as shown in Fig. 3 of this response letter. A reference line indicating present-day Antarctic ice volume, suggested by Reviewer 2 (comment 36), helps put the presented numbers into perspective.

45. Fig. 5: I do not really understand the point of this Figure as I do not get any information about the magnitudes of basal melting or the SMB. This Figure also needs a scale bar.

**Our response:** We find that the changes incurred have improved the figure (see Fig. 7 in this letter, our responses to comments 26 and 29). We now show SMB for the grounded ice sheet, basal melting for the ice shelves, and added different hatching to where ablation occurs, and to where basal melting dominates over SMB at the ice shelves.

46. Fig. 6: See Fig. 4

47. Fig. 7: Labels (a,b) are too small.

48. Fig. 8: Labels (a,b) are too small.

**Our response:** We have increased the font size of all figures.

### References cited in this letter that were not listed under the original manuscript submission

Barletta, Valentina R., et al. "Observed rapid bedrock uplift in Amundsen Sea Embayment promotes ice-sheet stability." *Science* 360.6395 (2018): 1335-1339.

Calov, Reinhard, and Ralf Greve. "A semi-analytical solution for the positive degree-day model with stochastic temperature variations." *Journal of Glaciology* 51.172 (2005): 173-175.

Holden, P. B., et al. "Interhemispheric coupling, the west Antarctic ice sheet and warm Antarctic interglacials." *Climate of the Past* 6.4 (2010): 431-443.

Maule, Cathrine Fox, et al. "Heat flux anomalies in Antarctica revealed by satellite magnetic data." *Science* 309.5733 (2005): 464-467.

Mitrovica, Jerry X., Natalya Gomez, and Peter U. Clark. "The sea-level fingerprint of West Antarctic collapse." *Science* 323.5915 (2009): 753-753.

Pollard, David, and R. M. DeConto. "A simple inverse method for the distribution of basal sliding coefficients under ice sheets, applied to Antarctica." *The Cryosphere* 6.5 (2012b): 953.

Waelbroeck, Claire, et al. "Sea-level and deep water temperature changes derived from benthic foraminifera isotopic records." *Quaternary Science Reviews* 21.1-3 (2002): 295-305.

Yang, Haijun, and Jiang Zhu. "Equilibrium thermal response timescale of global oceans." *Geophysical research letters* 38.14 (2011).

Dear editor, dear reviewer,

We thank the reviewer for their constructive, insightful and helpful evaluation which we feel helped to improve the manuscript. This instigated additional modeling that resulted in numerous refinements, and significant upgrades to the model description and discussion sections. Below, we provide a point-by-point response to each comment, which we numbered in red for easier reference. Our response is structured as follows: Referee comment (*in black italics*), author's response (in green), and proposed changes in the original manuscript text (*in blue italics*) where significant rewriting was done to include the suggested changes. We also add to the end of each figure caption (in blue) their proposed numbering after the changes made to the original submission of the manuscript.

Finally, we would like to draw the reviewer's attention to the correct reference to the first author's last name, as it is "Mas e Braga" and not "Braga".

## General Comments

**1.** *"I find inconclusive the set of experiments to determine whether or not the duration of the interglacial is responsible for AIS retreat rather than a warm peak as for MIS5. This is because the index derived from ice core records mainly impact on the oceanic forcing of the simulation which generates a tipping point. Once the tipping point is crossed, then the duration of the interglacial does not matter at all to explain the amplitude of ice sheet retreat in the simulations. In simulations using Vostok-GI, ice volume is lower but because the GI does not yield too warm temperature."*

**Our response:** The reviewer has a very good point, which we missed in our original submission. We have made sufficient changes to our analyses to address the possible tipping point mentioned by the reviewer. First, we have added a figure (Fig. 1 in this letter) that shows the ocean temperatures under the main ice shelves as requested in comments 53 and 54, compared to the Summer atmospheric temperatures. Based on what this figure shows, there is indeed a tipping point where the ocean starts to rapidly warm up at around 412 ka, reaching temperatures up to 0.6 °C warmer than PI at intermediate depths (between 400 and 1000 m). To investigate whether this is a tipping point, we performed four new experiments. Two are based on the EDC ice core, one where we keep the climate constant before and after the suspected tipping point (at 416 and 410 ka respectively). The other two are based on the Vostok ice core, one where we keep the climate constant at its peak GI value, and one where we instantly move the climate from its peak back to constant pre-peak conditions at 411 ka. These are shown below in Fig. 2. We have reformulated our discussion in light of these new results, which essentially show that the duration of warming was key for instigating strong WAIS retreat, while warming intensity (peak) allowed the retreat to be accelerated or delayed. There is indeed a threshold of 0.4 °C relative to PI at these intermediate depths, which must be crossed for the WAIS to collapse. We have included the following in our discussion:

*The average intermediate-depth ocean temperatures under the Filcher-Ronne and Ross ice shelves peak between 0.4 and 0.85 °C for the three ice core-forced CFEN members (Fig. 9b). This happens at 410 ka for Vostok, 408 ka for DF, and 407 ka for EDC. Strong WAIS retreat, however, starts before the peak in forcing, supporting the presence of a tipping point at 412 ka. To further test whether this tipping point is the trigger of WAIS collapse, we have performed four additional experiments: (i) forced by EDC GI, but keeping the GI constant after 416 ka (i.e., before the threshold found in ocean temperatures), (ii) forced by EDC GI, but keeping the GI constant after 410 ka (i.e., just after the sudden increase in ocean temperatures, cf. Fig. 9b), (iii) forced by Vostok GI, where climate forcing is kept constant at its peak condition at 410 ka, and (iv) forced by Vostok GI where, after the 410 ka peak, GI is brought back to its 411 ka value (i.e., between the peak and the observed tipping point) and kept constant. Figures 10a,b show that keeping the EDC-derived climate constant at 416 ka conditions prevents the WAIS from collapsing, while keeping it constant at 410 ka conditions delays its collapse by almost 5 kyr compared to the core CFEN run. The Vostok-based simulations (Figs. 10e-h) show that there is indeed a threshold, which is of approximately 0.45 °C for the Filchner-Ronne ice shelf, and 0.54 °C for the Ross ice shelf. However, our results also imply that this threshold must be sustained for at least 4 kyr to cause a collapse (compare red and blue dashed lines in*

Figs. 10f-h). A short peak at this threshold and subsequent cooling prevents the WAIS from collapsing, compared to keeping it constant at the same peak value (Fig. 10e,f). Comparing these values to PI temperatures averaged over the same extent of the water column, the magnitude of warming necessary to cross this threshold is 0.4 °C. In other words, a warming of this magnitude can be understood as the condition necessary for WAIS collapse (Figs. 10c,d,g,h).

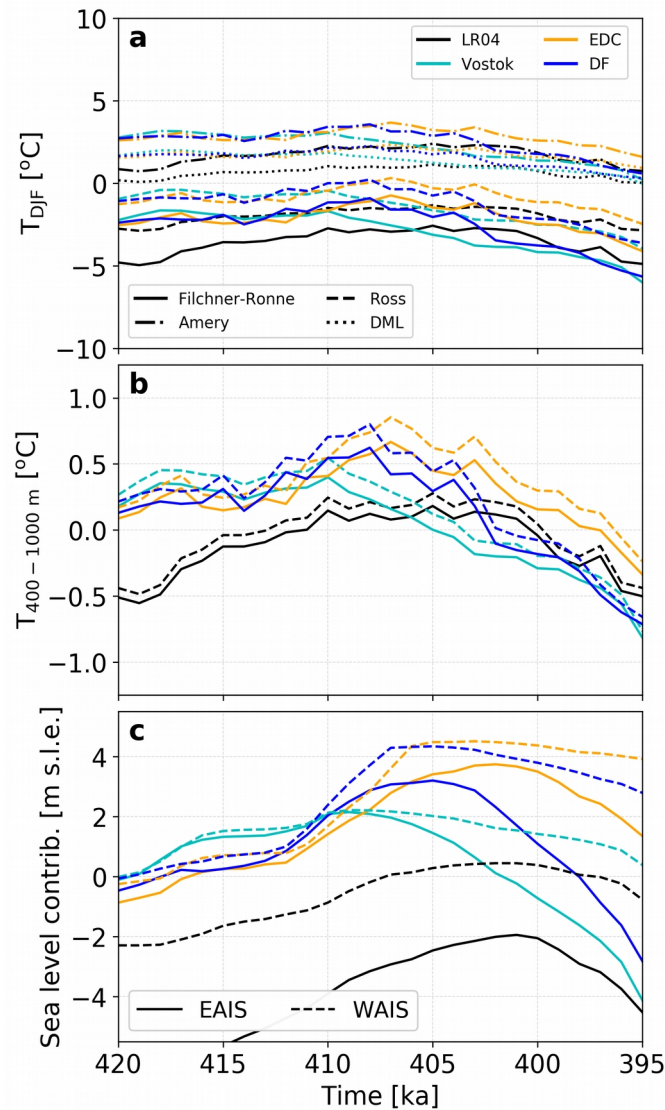


Figure 1: Evolution throughout MIS11 for each CFEN member for (a) Summer surface air temperature [°C] averaged over the main Antarctic ice shelves; (b) ocean temperatures averaged between 400 and 1000 m [°C] for the Filchner-Ronne and Ross ice shelves; (c) sea level contribution by EAIS and WAIS. Colours denote the respective CFEN member, while line styles in panels (a,b) denote each ice shelf, and each ice sheet in panel (c). DML refers to all smaller ice shelves along the Dronning Maud Land margin. This is Fig. 9 after the revisions to the manuscript.

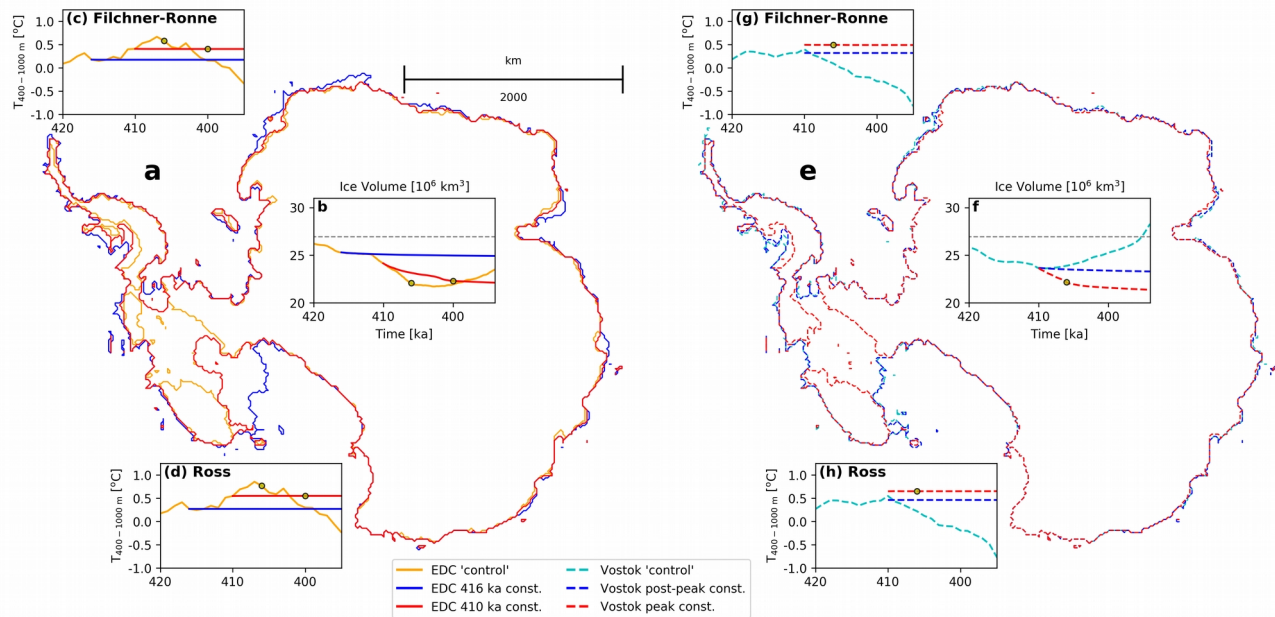


Figure 2: Thresholds for WAIS collapse. (a,e) grounding lines at 405 ka for three EDC-based (solid lines) and three Vostok-based (dashed lines) experiments, respectively (see below for explanation); (b,e) ice volume ( $10^6 \text{ km}^3$ ), (c,d; g,h) intermediate-depth (400–1000 m) ocean temperatures [ $^{\circ}\text{C}$ ] for the Filchner-Ronne and Ross ice shelves, respectively. Time series cover the period between 420 and 395 ka for both EDC (solid lines) and Vostok-based (dashed lines) experiments. Orange line shows the EDC control run, while cyan line shows the Vostok control run. Blue lines show EDC and Vostok simulations where climate was kept constant and the WAIS did not collapse, while the red lines show EDC and Vostok simulations where climate was kept constant and the WAIS collapsed. Yellow circles show the moment when the WAIS breaks down and an open-water connection between the Ross, Weddell and Amundsen seas is established. This is Fig. 10 after the revisions to the manuscript.

2. Actually, in question 2, ocean forcing is not mentioned at all as a potential driver of the ice sheet retreat. Same for ocean forcing: I would like to see a Figure in the supplementary of the oceanic forcing derived with the GI for the main ice shelves

**Our response:** This is a good follow-up to the previous point. We now mention oceanic forcing in question 2, and Figs 1 and 2 in this response letter (which are added to the revised manuscript) now show ocean temperatures under the main ice shelves. These figures underpin a discussion of our results regarding oceanic forcing, as suggested by the reviewer here and in subsequent comments, and form the main basis for our discussion in the manuscript.

3. You should discuss the impact to force WAIS with EAIS ice core records on the amplitude and timing of this retreat. For example, comparing them with WAIS divide ice core record.

**Our response:** The WAIS divide record only spans the last 68 kyr, making a comparison between it and the used EAIS ice cores impossible for MIS11. What we suspect the reviewer is suggesting is that we add to our discussion that the WAIS could have responded sooner to changes in climate than the EAIS, as the WAIS Divide ice core record shows a more than 2 kyr lead over the EAIS records (WAIS Divide Project members, 2013). We included this in our discussion.

4. In those simulations, all forcing co-vary: your surface climate forcing and your oceanic forcing are modulated with the same index. It is likely not the case as atmosphere cools or warms faster than

ocean does. This is not accounted for here. You could perform some interesting tests that would provide a nice discussion about the interaction between ocean and ice sheet. A plot showing air and ocean temperature forcing versus WAIS ice volume evolution; same for EAIS for all simulations is really necessary to support or explain better some aspect of this manuscript and provide answers to questions 1 and 2.

**Our response:** The reviewer offers another good point. To address this issue, we have added a lag to the ocean index (Fig. 3 below). We also performed three sensitivity experiments, one where its forcing is dampened by 50%, and two where the ocean is overall colder by 0.5 and 1.0 °C (Figs. 4 and 5). Figure 1 presented above also shows how air temperatures and the thermal forcing vary throughout the study period, and how they relate to changes in WAIS and EAIS ice volume. These results and the other suggestions provided will also be incorporated in the discussion. Finally, because we added a lag of 300 years to the ocean response in all our experiments (which was the most probable response time of the ocean for this latitude; Yang & Zhu, 2011) we re-ran all the simulations shown in the manuscript.

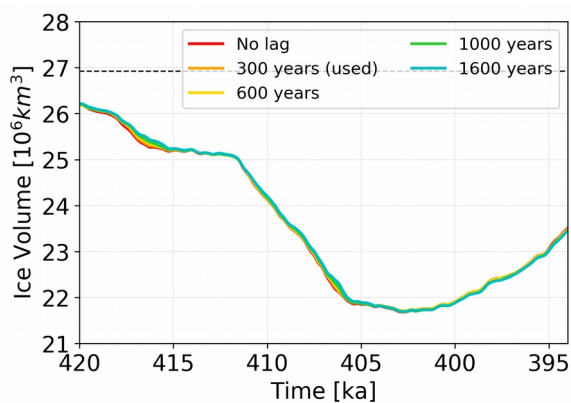


Figure 3: Sensitivity of the AIS response expressed in total ice volume [ $10^6 \text{ km}^3$ ] to different lags in the GI applied to the ocean between 420 and 394 ka. This is Fig. S11 after the revisions to the supplement.

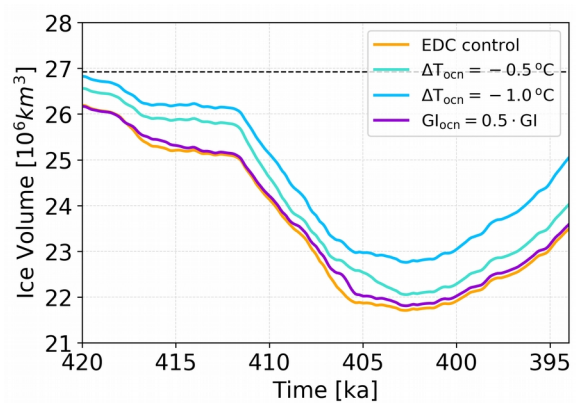


Figure 4: Sensitivity of the AIS response expressed in total ice volume [ $10^6 \text{ km}^3$ ] to three simulations where we test for the ocean sensitivity for a collapse. In two runs we apply a  $\Delta T$  of -0.5 and -1.0 °C, and in a third a reduction of the ocean GI amplitude by 50%. This is Fig. S6 after the revisions to the supplement.

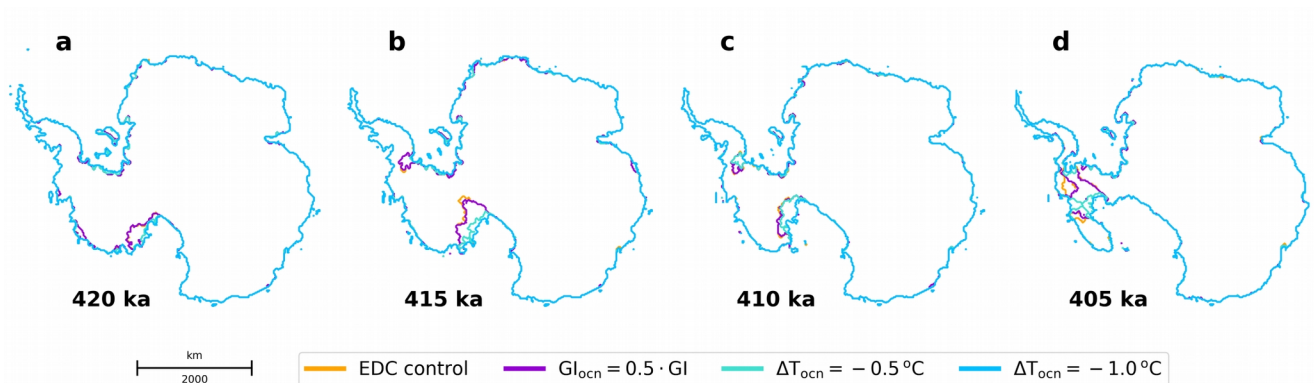


Figure 5: Grounding lines of the experiments presented in Fig. 4 at times of interest throughout the simulation. This is Fig. S7 after the revisions to the supplement.

5. *I would like to see a comparison between present-day simulated climate forcing and ocean forcing and observation from ERA5, and not between simulated PI and present-day ERA5.*”

**Our response:** We appreciate the reviewer’s concern here. We are unable to compare our model using present-day (PD) climate because we use an in-house simulation which does not have PD time slices. However, the difference between PI and PD in climate models is an order of magnitude smaller than the difference between either PI or PD and observational/reanalysis data (Otto-Bliesner et al., 2006, Fig. 2). Thus, we expect that not much would be gained if we were to compare the PD state as opposed to PI. We have, however, changed the comparison to CCSM3 from ERA5 to RACMO2 (see Fig. 15 in our response to comment 42), because the latter is a more accurate product for Antarctica (van Wessem et al., 2018). This change is also motivated by the changes based on the responses to comments 28 and 42.

## Comments

6. *Line 47: please cite cite Tzedakis, P. C., et al. "Interglacial diversity." Nature Geoscience 2.11 (2009): 751-755.*

**Our response:** This paragraph was removed from our manuscript in response to comment 12 by Reviewer 1.

7. *Line 74: please cite De Boer et al. (2015) PLISMIP-ANT paper on which Dolan et al (2018) is largely based.*

**Our response:** We struggled to see how this citation fits in line 74 because we address ice-core reconstructions for MIS11c, while de Boer et al.’s paper is about model reconstructions for the Pliocene. We decided to add the reference to the previous sentence, which makes more sense.

8. *Line 74: please correct with “agree with how ANTARCTIC surface air temperature evolved”*

**Our response:** We have made the correction as requested.

9. *Lines 79-82: I strongly disagree with this paragraph. Lost of long-term transient simulations have been performed, including MIS11, and you cite all those contributions in your introduction. I think what you mean is that no study really tried to improve the current simulations of MIS11-AIS, neither with climate forcing or ice sheet modeling, in absence of geological constraints on both climate and ice dynamics. Please reformulate this way, this much more honest. State that your aim is to improve by exploring aspects on which nobody really focused on so far (e.g. the two questions you pose at the end of this paragraph).*

**Our response:** Thank you for this suggestion for better phrasing/framing. We rewrote the last two paragraphs of the introduction, also based on comments 15 and 16 from Reviewer 1.

*“As detailed, many modelling studies have investigated AIS responses over time periods that include MIS11. However, so far none has focused specifically on this period. Given the scarce information for MIS11 and conflicting constraints on how Antarctica responded to this exceptionally long interglacial (Milker et al., 2013; Dutton et al., 2015), we here focus on MIS11c, the peak warming period between 420 and 394 ka. Our aim is to reduce the current uncertainties in the AIS behaviour during MIS11c, specifically addressing the following questions:*

*[...]*

*For this purpose, we perform five ensembles of numerical simulations of the AIS evolution and focus on aspects that remain unaddressed by previous studies. We evaluate the impact on resulting ice volume and extent of the choice of proxy records (including their differences in signal intensity and structure), the choice of sea level reconstruction, and of uncertainties in assumptions regarding the geometry of the AIS at the start of MIS11c.”*

**10.** Line 89: correct as follows “of uncertainties in sea level reconstruction, and of uncertainties of the geometry. . .”

**Our response:** Corrected.

**11.** Figure 1: If the starting AIS topography is present-day (BEDMAP2 or other) please state it in this caption as well.

**Our response:** We mention it is based on Bedmap2, and refer to the section in the Methods where we explain our approach to creating it.

**12.** Figure 1: Are you sure that the glacial tongue in the Wilkes Land corresponds to Ninnis Glacier and not to Mertz Glacier instead?

**Our response:** Thank you for making us re-examine the precise features of Wilkes Land that were most affected, and their location in Figure 1: after more careful analysis, we conclude that these areas corresponded to neither Mertz nor Ninnis. The mainly affected glaciers in Wilkes Land are Totten, Dibble, and Cook. We have updated the text, figure, and caption.

**13.** Lines 101-102: please invert the order of the two sentences (put together everything about ocean forcing and then put the rest).

**Our response:** We removed the mention of salinity from the Methods section, moving it to the Supplementary Material. Please consult our response to comments 17-20, where the changes to the Methods section are detailed.

**14.** Line 105: “i.e., apply a transient surface temperature signal from the EDC ice core (Jouzel et al., 2007)”. But Jouzel et al. only provide a temperature anomaly, what is your baseline climate forcing here for this thermal spin-up tase and then for the 5,000 kyrs geometry adjustment afterward?

**Our response:** We had initially applied the EDC core GI forcing to all simulations during the relaxation stage, so that they all had the same geometry at 420 ka. After this feedback (and from Reviewer 1, comment 20), we now apply the same GI forcing during the relaxation stage as the forcing during the main experiments (i.e., DF GI for the DF-forced runs, EDC GI for the EDC-forced runs, and so on). We have updated the text to reflect these changes and further clarify the point raised by the reviewer. It now reads:

*“All ensembles cover a period from 420 to 394 ka. After the calibration for basal sliding mentioned above, we initialise the AIS by performing a thermal spin-up over a period of 195 kyr from 620 to 425 ka, i.e., apply a transient surface temperature signal from the EDC ice core (Jouzel et al., 2007) as an anomaly to our PI climate (described in the next section) while keeping the ice sheet geometry constant at our previously calibrated Bedmap2-based configuration. We then let the AIS freely evolve for 5 kyr, between 425 and 420 ka, applying transient GI forcing during the relaxation period (Fig. S12). We chose 425 ka as the starting point for relaxation because it is when the MIS11c oxygen isotope values in the EDC ice core are closest to PI. In summary, we ignore the first 5 kyr (425--420 ka) to avoid a shock from suddenly letting the ice-sheet topography freely evolve at the start of our period of interest. Figure 1 shows the thermally spun-up ice sheet configuration at 425 ka, from which the simulations start.”*

**15.** Line 107: geometry is that of present-day, please specify which one and cite the reference (BEDMAP2, ALBMAP. . .).

**Our response:** We now specify using Bedmap2, as shown above for comment 14.

**16.** Line 107: “We then let the AIS freely adjust for 5 kyr, between 425 and 420 ka”: what is the ocean forcing for this 5,000 years free run? It seems to me that the topography shown in Fig1 is really

present-day. Is this really the AIS topography that you obtain after those 5,000 years of geometry evolution?

**Our response:** We believe we have addressed this concern in the rewritten text shown above for comment 14. We have also updated Fig. 1 in the manuscript to show the post spin-up configuration of the ice sheet.

**We group comments 17-20 because these are all addressed in the updated model description in the Methods section.**

**17.** Line105-107: Please detail ALL the forcing, boundary conditions (geothermal heat fluxes, etc..) used for the entire spin-up procedure this 5000 years (even in the supplementary if you prefer). All experiments presented here, including the spin-up, must be reproducible.

**18.** Table 1: Do you really use only one enhancement factor (the same for both SIA and SStA)? If yes please indicate it within the Table.

**19.** Table 1: what about calving? How is this done?

**20.** Table 1: Why is the relaxation time set at 1 kyr while characteristic time is 3 kyr? Please provide a detail description in the supplementary about the choice of your parameters. Also provide a description of the sliding law, surface mass balance in the Supplementary.

**Our response:** We thank the reviewer for highlighting the need to further clarify our setup. We present an updated methods section including all information requested by both Reviewers (see also comments 1, 26, and 38 from Reviewer 1). We added information to Table 1, highlighting the use of the same enhancement factor, with a justification for this in the Methods section. For calving, we use a thickness threshold of 50 m, where ice at the calving front that is thinner than the threshold is instantly calved. We also refer Konrad et al. (2014), from which we obtain our ELRA parameters. Konrad et al., (2014) found them to yield the closest results to a fully-coupled ice-sheet-self-gravitating viscoelastic model. The expanded model description is shown below:

*“For our experiments we employ the 3D thermomechanical polythermal ice-sheet model SICOPOLIS (Greve, 1997, Sato & Greve, 2012) with a 20 km horizontal grid resolution and 81 terrain-following layers. It uses the one-layer enthalpy scheme of Greve & Blatter (2016), which is able to correctly track the position of the cold-temperate transition in the thermal structure of a polythermal ice body.*

*The model combines the Shallow Ice Approximation (SIA) and Shelfy Stream Approximation (SStA) using (c.f. Bernaldes et al., 2017a, Eq. 1)*

$$U = (1 - w) \cdot u_{sia} + u_{sstA}$$

*where  $U$  is the resulting hybrid velocity,  $u_{sia}$  and  $u_{sstA}$  are the SIA and SStA horizontal velocities, respectively, and  $w$  is a weight computed as*

$$w(|u_{sstA}|) = \frac{2}{\pi} \arctan\left(\frac{|u_{sstA}|^2}{u_{ref}^2}\right)$$

*where the reference velocity,  $u_{ref}$ , is set to  $30 \text{ m a}^{-1}$ , marking the transition between slow and fast ice. This hybrid scheme reduces the contribution from SIA velocities mostly in coastal areas of fast ice flow and heterogeneous topography, where*

this approximation becomes invalid. Basal sliding is implemented within the computation of SStA velocities as a Weertman-type law (cf. Bernales et al., 2017a, Eqs. 2--6). The amount of sliding is controlled by a fixed, spatially varying map of friction coefficients that was iteratively adjusted during an initial present-day equilibrium run (cf. Pollard & DeConto, 2012b), such that the grounded ice thickness matches the present-day observations from Bedmap2 (Fretwell et al., 2013) as close as possible. Sliding coefficients in sub-ice shelf and ocean areas are set to  $10^5 \text{ ma}^{-1} \text{ Pa}^{-1}$ , representing soft, deformable sediment, in case the grounded ice advances over this region. The initial bedrock, ice base, and ocean floor elevations are also taken from Bedmap2. Enhancement factors for both grounded and floating ice are set to 1, based on sensitivity tests in Bernales et al. (2017b). This choice provides the best match between observed and modelled ice thickness for this hybrid scheme, similar to the findings in Pollard & DeConto (2012a).

Surface mass balance is calculated as the difference between accumulation and surface melting. The latter is computed using a semi-analytical solution of the positive degree day (PDD) model following Calov & Greve (2005). Near-surface air temperatures entering the PDD scheme are adjusted through a lapse rate correction of  $8.0 \text{ }^\circ\text{C km}^{-1}$  to account for differences between the modelled ice sheet topography and that used in the climate model from which the air temperatures are taken. For the basal mass balance of ice shelves, we use a calibration scheme of basal melting rates developed in Bernales et al. (2017b) to optimise a parameterisation based on Beckman & Goosse (2003) and Martin et al. (2011) that assumes a quadratic dependence on ocean thermal forcing (Holland et al., 2008; Pollard & DeConto, 2012; Favier et al., 2019). This optimised parameterisation is able to respond to variations in the applied Glacial Index (GI, Sect. 2.2) forcing. A more detailed description of this parameterisation is given in Sect. 1 of the supplementary material. In our experiments, we prescribe a time lag of 300 years for the ocean response to GI variations, which is considered the most likely lag in response time of the ocean compared to the atmosphere in the Southern Ocean (Yang & Zhu, 2011). At the grounding line, the basal mass balance of partially floating grid cells is computed as the average melting of the surrounding, fully floating cells, multiplied by a factor between 0 and 1 that depends on the fraction of the cell that is floating. This fraction is computed using an estimate of the sub-grid grounding line position based on an interpolation of the current, modelled bedrock and ice-shelf basal topographies. At the ice shelf fronts, calving events are parameterised through a simple thickness threshold, where ice thinner than 50 m is instantly calved away.

Glacial isostatic adjustment is implemented using a simple elastic lithosphere, relaxing asthenosphere (ELRA) model, with a time lag of 1 kyr and flexural rigidity of  $2.0 \times 10^{25} \text{ Nm}$ , which Konrad et al. (2014) found to best reproduce the results of a fully-coupled ice sheet-self-gravitating viscoelastic solid Earth model. The geothermal heat flux applied at the base of the lithosphere is taken from Maule et al. (2005) and is kept constant. All relevant parameters used in the modelling experiments are listed in Table 1.”

**21. Table 1: Units for salinity is “PSU”, please fill the missing units.**

**Our response:** We understand the reviewer’s concern and confusion regarding salinity units, which is often very tricky. In the Practical Salinity Scale, introduced in 1978 (PS1978) salinity is a unitless quantity, since it follows a scale. The Practical Salinity Unit (PSU) was unofficially introduced and is invalid despite being accepted in some academic journals. Practical Salinity is calculated by its conductivity compared to Standard Seawater. Standard Seawater, in turn, is a reference manufactured by Ocean Scientific International Limited (OSIL). A brief review on salinity units, along with a list of technical papers on the matter can be found in OSIL’s website, in the following link: <https://osil.com/category/seawater-technical-papers/>.

**22. Table 1: Please explain in the Supplementary how you choose the value for the thermal mixing coefficient (it varies quite a lot and this one of the main important parameter of oceanic parameterisation)**

**Our response:** We use the value of  $10^{-4} \text{ ms}^{-1}$  as it is the one presented in the original work of Beckman & Goosse (2003) and used in the ice-sheet model implementation of this parameterisation in Martin et al. (2011). This is clarified in the Supplementary Material.

**23. Table 2: Please substitute “Age scale” with “Age model”.**

**Our response:** Done.

24. Table 2: please provide a more detailed caption for this Table. What does “Age (ka)” corresponds to?

**Our response:** We have updated the table caption, which now reads:

“Ice and sediment cores reference values used in Eq. (1), together with the age (in thousand years before present; ka) from which the reference values were obtained. The respective age models of each core, and their references, are listed.”

25. Table 2: Add a column to state what is the nature of the record (either dO18 or dD and it record is glaciological or marine).

**Our response:** We added a new column to Table 2 where we show the core type (ice/sediment) and isotope ( $\delta^{18}\text{O}/\delta\text{D}$ ).

26. Subsection 2.2: In this paper your focus is on MIS11. Can you explain why you chose to scale the ice cores isotopic records to the difference between LGM and PI? Thus because of this, how much do your glacial index scaled surface temperature differs from the temperature from ice core records at DF, EDC and Vostok? I would like to see a Figure showing the derived surface air temperature for each GI and in comparison with each temperature reconstructions from dD for each ice cores used in this study.

**Our response:** We chose LGM and PI for the scaling because they are the two best constrained periods available, which is especially important when combining the records with climate model forcings. The comparison between ice-core-inferred and GI-climate-model reconstructed temperatures was already given in Fig. S6. We have, however, improved the figure by removing the curves that were not related to this comparison (see Fig. 6 below). We updated the discussion to bring attention to this figure.

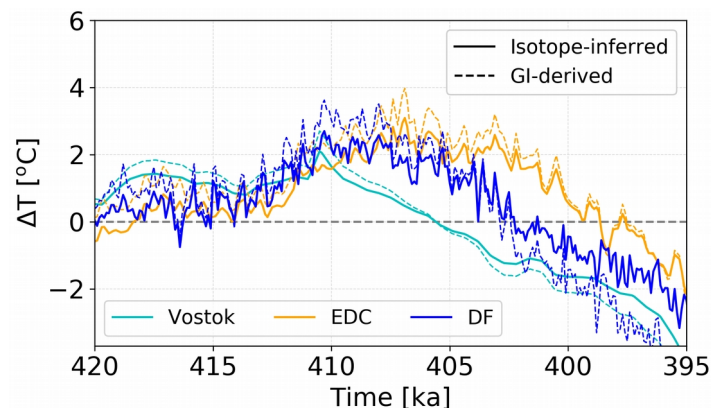


Figure 6: Comparison between surface atmospheric temperature anomalies ( $\Delta T$ ) obtained by the ice cores GI scaling and those inferred from their respective  $\delta\text{D}$  values. This is Fig. S14 after the revisions to the supplement.

27. Lines 123-124: I don't understand the choice of CCSM3 since many other runs from CCSM4, even earlier versions of CESM, were released by Otto-Bliesner's group for contribution to PMIP3 on CMIP5 platform for both PI and LGM, run by NCAR, on the same computer. CCSM4 presents strong improvements relative to CCSM3. I would like to see a discussion about this and related literature for both version CCSM3 and CCSM4 in the Supplementary.

**Our response:** During early stages of this study we carried out both CCSM3- and CESM1.2-driven simulations, forced by the EDC-derived GI. In the end, we decided to use CCSM3 rather than CESM1.2 for two important reasons, which we also include in our supplementary material:

1. With CESM1.2 forcing (in-house simulations, see Bakker et al., 2020), the ice-sheet model failed to match the geological constraints for MIS11c by Raymo & Mitrovica (2012), i.e., not showing a volume loss that would cause the expected contribution from the AIS to sea level rise for this period (Fig.7, “CESM”). In order to understand what exactly caused this difference in performance between the two

versions, we ran a series of sensitivity experiments where we replaced one forcing field (air temperature, ocean temperature, or precipitation; Fig.7) or two forcing fields (e.g. air temperature + ocean temperature; not shown) from CCSM3 by their CESM1.2 equivalent. We found that the evolution of the ice sheet throughout MIS11c was most sensitive to the differences in precipitation. The differences in precipitation fields show that CESM1.2 precipitation rates are, in general, lower than those of CCSM3 during MIS11c, especially in key areas of the WAIS, such as East of Siple Coast. As a consequence, the calibration of the ice sheet model to CESM1.2 forcing fields resulted in the need for a higher basal friction (relative to CCSM3) to compensate for the reduced precipitation in order to match the modern reference observational data sets. In turn, the combination of this higher basal friction and the higher precipitation rates during MIS11c compared to PI results in a much reduced sensitivity of the ice sheet to MIS11c warming, thus not capturing the AIS contribution to sea level rise shown by the geological record (Raymo & Mitrovica, 2012).

2. Several studies have shown that CCSM3 does a reasonably good job in simulating Southern Ocean conditions during glacials and interglacials, which is important for the simulation of the AIS. It has been shown that CCSM3 correctly simulates characteristics of water masses produced in the Southern Ocean (AABW, AAIW) for the LGM (Otto-Bliesner & Brady, 2008; Ronge et al., 2015) and the transition into the Holocene (Ronge et al., 2020). Moreover, Marzocchi & Jansen (2017) have shown that CCSM3 has a better skill in simulating glacial Antarctic sea ice and deep-ocean circulation than CCSM4.

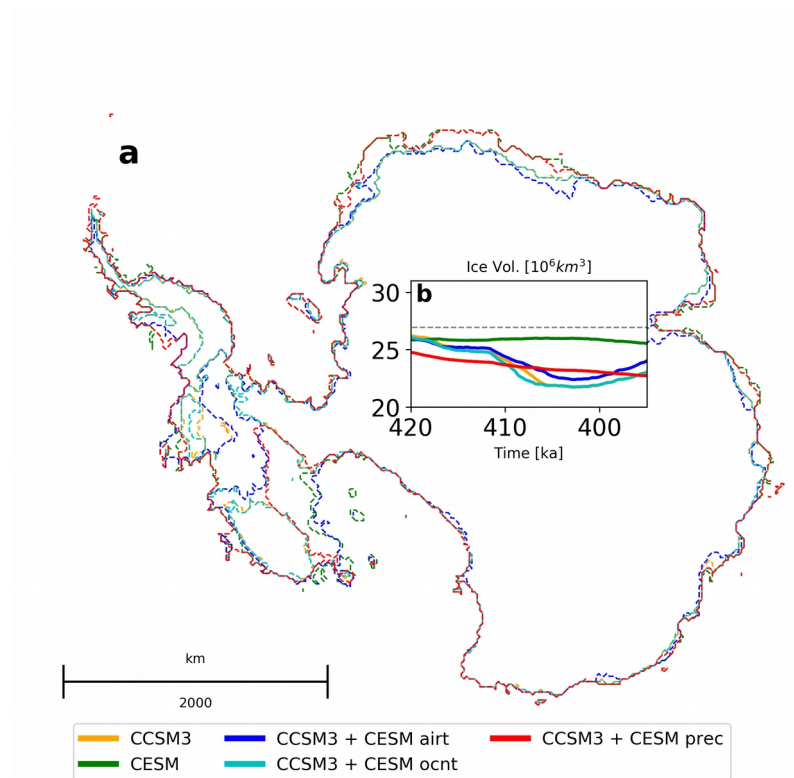


Figure 7: (a) Grounding lines (dashed for an easier comparison) at 405 ka (i.e., the MIS11c sea level highstand), and (b) ice volume [10<sup>6</sup> km<sup>3</sup>] throughout MIS11c for a series of CESM1.2 and CCSM3 runs. ‘airt’, ‘ocnt’ and ‘prec’ denote atmospheric surface temperature, ocean temperatures, and precipitation rates respectively, and these refer to the runs where CCSM3 forcing variables were replaced by equivalent CESM1.2 variables (e.g., ‘CCSM3 + CESM airt’ means that all variables

were from CCSM3, except for atmospheric surface temperatures, which were from CESM1.2). This is Fig. S3 after the revisions to the supplement.

**28.** Lines 126-127: On the contrary, I would like to see a few panels about simulated Antarctic climate and associated biases since it is also highly important to your study. Thus I am expecting you to also provide a bias correction to your forcing field (assuming the bias correction propagates linearity back in time). This is something that you did not do, but it needs to be done. I also expect to see a figure of surface air temperature over Antarctica and comparison with all available ice core records for LGM (not only the few that you consider here), to have a comprehensive view of the performance of your climate forcing.

**Our response:** As requested, we provide a map of the mean annual surface air temperature difference between LGM and PI, as simulated by CCSM3 (Fig. 8) along with temperature differences derived from ice cores (Werner et al., 2018). The CCSM3 results suggest a stronger cooling than the proxy data, which is likely related to a too thick Antarctic Ice Sheet prescribed in the LGM (PMIP2) simulations, and hence does not substantially affect our ice-sheet forcing due to lapse rate correction.

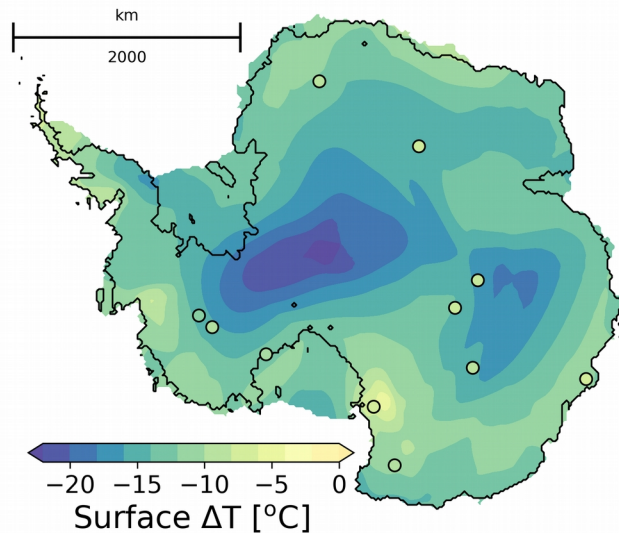


Figure 8: Surface atmospheric temperature difference ( $\Delta T$  in  $^{\circ}\text{C}$ ) between CCSM3 LGM and PI time slices. Circles show the  $\Delta T$  values derived from isotopes presented by Werner et al. (2018). This is Fig. S4 after the revisions to the supplement.

To assess how our forcing's biases impact our results, we have now performed an EDC-GI-forced simulation using RACMO2 as our modern reference fields, with CCSM3 providing the anomalies and ocean forcing. We also include a similar experiment using RACMO2 modern fields and CESM1.2 anomalies and ocean forcing (for the sake of completeness to the assessment presented in comment 27). In Fig. 9 we show how they differ from the simulations fully forced with CCSM3 (which we used in the manuscript) and CESM1.2 (which we presented in Fig. 7). Differences do exist between RACMO2 and CCSM3, but are relatively small and most evident during the time of sea level highstand at 405 ka. This difference in ice volume at 405 ka means that the RACMO2 runs contribute 1.1 m less to global mean sea level. The position of the grounding line shows that this difference seems to relate mainly to the fringes of the EAIS (particularly in Dronning Maud Land) and to the WAIS sector just south of the

Peninsula. The runs in which CESM1.2 anomalies were applied yield a rather insensitive ice sheet. As already discussed in our response to comment 27, and considering that basal sliding conditions in these simulations were calibrated to RACMO2 climate, the ‘RACMO+CESM’ experiment further confirms that its precipitation anomalies are what makes it not capture the sea level contribution constraints for MIS11c in Raymo & Mitrovica (2012). Overall, the RACMO2-forced simulations do not decisively change our results, except for final sea level contribution calculations. This analysis is also added to the Supplementary Material.

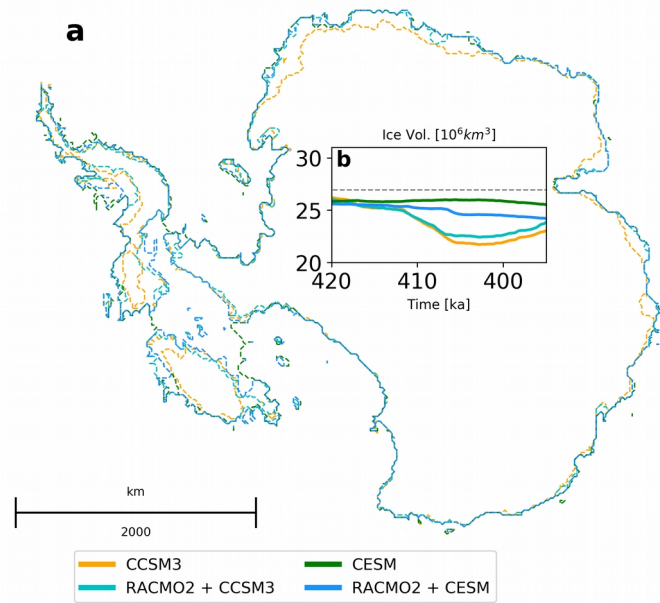


Figure 9: (a) grounding lines (dashed for an easier comparison) at 405 ka (i.e., the MIS11c sea level highstand), and (b) ice volume [ $10^6 \text{ km}^3$ ] throughout MIS11c for the bias assessment runs for CCSM3 and CESM1.2, where we test for the impact of using RACMO2 atmospheric fields as our modern reference, while keeping the ocean field and all anomalies from CCSM3 and CESM1.2. This is Fig. S5 after the revisions to the supplement.

**29.** Line 134: Please substitute “age scale” with “age model”.

**Our response:** We have made the requested change.

**30.** Line 140-141: I don’t understand how you can compare  $dO18$  from marine sediments and  $dD$  from ice cores and deduce that Holocene temperature history is inconsistent between those two. First of all, it is not straightforward to compare marine and glacial records together. To me this figure 2a does not make any sense, remove it.

**Our response:** We changed Fig. 2 in the manuscript (based on comment 42 from Reviewer 1) by (i) zooming-in on the MIS11c period and (ii) by adding a panel with the different derived GI curves (see response to comment 3 by Reviewer 1). The idea is to provide a comparison between the isotope curves and their respective rescaled GIs (amplitude and structure), not a comparison between different isotopes. We removed comparisons between isotopes, such as referenced by the reviewer, from the manuscript, made changes to the text, and also removed the GI plots from Fig. 1 to avoid duplicating information.

**31.** Subsection 2.3.2: Please refer to Figure 7 to show the filtered GI.

**Our response:** We refer to Fig. 2b instead, as this is the panel where the filtered GI is shown after the revisions mentioned in comment 30.

**32. Subsection 2.3.3:** I find the choice of your sea level curve a bit awkward. Why not considering also Waelbroeck et al (2002) which also encompasses MIS11 and which is one of the best curve we have with Bintanja et al. (2008).? Actually, many other new isotopic reconstructions have been done (e.g. Sutter et al., 2019), which is performed with more recent versions of models that Bintanja. Please redo some simulations also considering at least Waelbroeck et al (2002) in your ensemble.

**Our response:** We added the Waelbroeck et al. (2002) record to our ensemble (SLEN, Fig. 10). Our results were not impacted by introducing this new simulation (which is hardly surprising, given that this is what this ensemble showed in the first place).

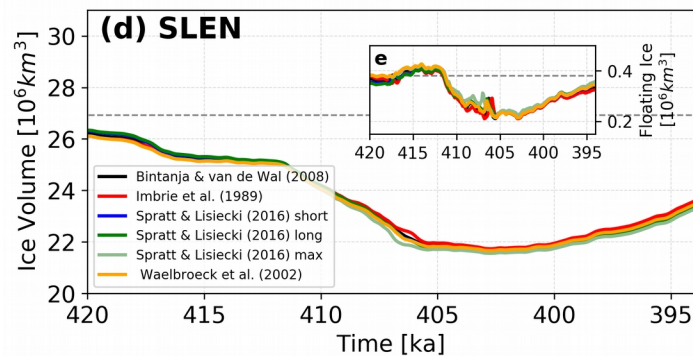


Figure 10: Sensitivity of AIS response (in total ice volume,  $10^6 \text{ km}^3$ ) between 420 ka and 394 ka to the SLEN sea level reconstructions forced by EDC GI. These are Figs. 4d,e after the revisions to the manuscript.

**33. Subsection 2.3.4:** The methodology to provide intermediate geometries is definitely highly science-fiction. One can provide geometries, even though idealised, but with a more appropriate approach. For example: you could have done an equilibrium simulation with LGM conditions scaled with your GI for a few tens of thousands of year, and then transiently vary your climate forcing as in your control experiment until beginning of MIS11. This is a much better alternative than what you propose here. Or, alternatively, you can start one glacial cycle ahead and transiently vary your climate forcing with your GI. Then you could have used your the various GI generated with your scaling ensemble to vary the slope of transition from glacial to MIS 11. I strongly suggest you to try this way since, at least, you can justify much better your geometry ensemble than how you defined it currently.

**Our response:** In light of the reviewer's suggestions, we have changed to a more conservative approach regarding the creation of our different initial geometries, which is close to the first approach proposed by the reviewer. We now use constant LGM conditions and no ice shelf basal melt to grow the ice sheet towards an intermediate extent between PI and LGM in 5 kyr. We then place this intermediate-sized ice sheet at 420 ka (as was our old 'gmt1' ensemble member), at 425 ka, and at 430 ka, and let them transiently evolve since then. We have updated the figures accordingly, but overall, this change did not impact our results (see Figs. 11 and 12 below, which are updated version of Figs. 3 and 10 in the original submission). We have made the changes to Table 3, recalculated all the sea level contributions, and changed the text accordingly. The description of how we create our spread in initial geometry now reads:

*"In order to create a representative range of initial geometries at 420 ka, we use a common starting geometry, but vary the relaxation time. For this purpose, we first create an ancillary geometry by perturbing the thermally spun-up AIS with a constant LGM climate (air temperature and precipitation rates) and no sub ice-shelf melting over a 5 kyr period. The*

resulting ancillary ice sheet (which has an extent that sits between PI and LGM configurations) is then placed at 420, 425 and 430 ka and runs transiently (following the respective GIs) until 394 ka. This creates a representative range of starting geometries at 420 ka (Fig. 3), and each initial ice sheet geometry is labelled *gmt1* to *gmt3* (Fig. 3a-c; shortest relaxation is *gmt1*, longest is *gmt3*). The *gmt1* initial topography is generally more extensive and thinner than the control. Its grounding line advanced at the southern margin of the Filcher-Ronne Ice Shelf and at Siple Coast, but the ice sheet interior is on average 200 m thinner than the control and up to 500 m thinner across particular regions such as the dome areas of the WAIS and Wilkes Land (Dome C). It is, however, about 200 m thicker at its fringes, which results in a gentler surface gradient towards the ice sheet margins. The *gmt2* initial topography is less than 100 m thinner than control over the EAIS interior, and about 100 m thicker over the WAIS interior and at the EAIS margins. Finally, the *gmt3* initial topography is overall thicker than control, though not by more than 100 m except at the western side of the Antarctic Peninsula and the WAIS margins, where some regions are up to 300 m thicker (Fig. 3c).”

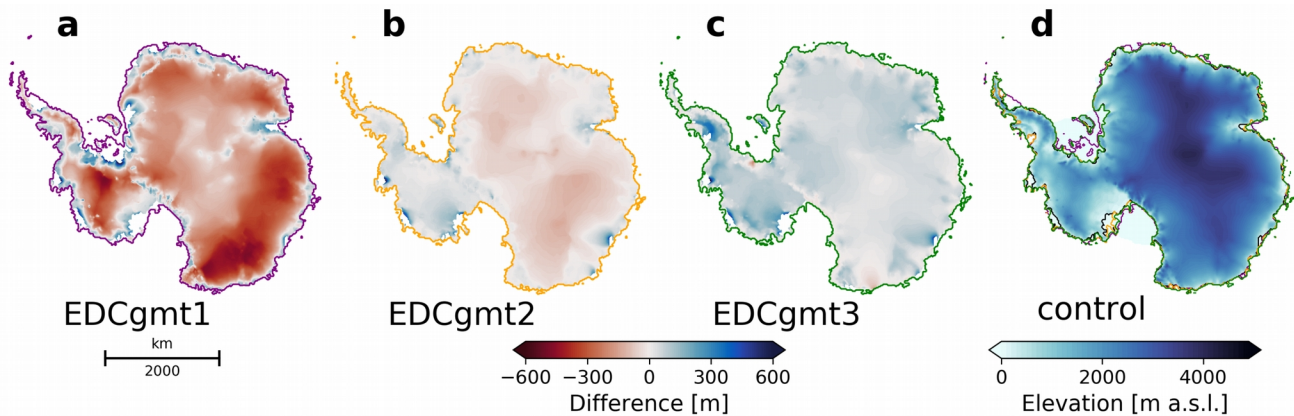


Figure 11: (a-c) Three different starting ice sheet geometries at 420 ka for the EDC CFEN member (*gmt1-3*). Color scheme shows differences in surface elevation between each geometry and the control for 420 ka (d). Differences are only shown where the ice is grounded in both geometries, and coloured lines show the respective grounding lines in *gmt1-3*, also overlain in (d). This is Fig. 3 after the revisions to the manuscript.

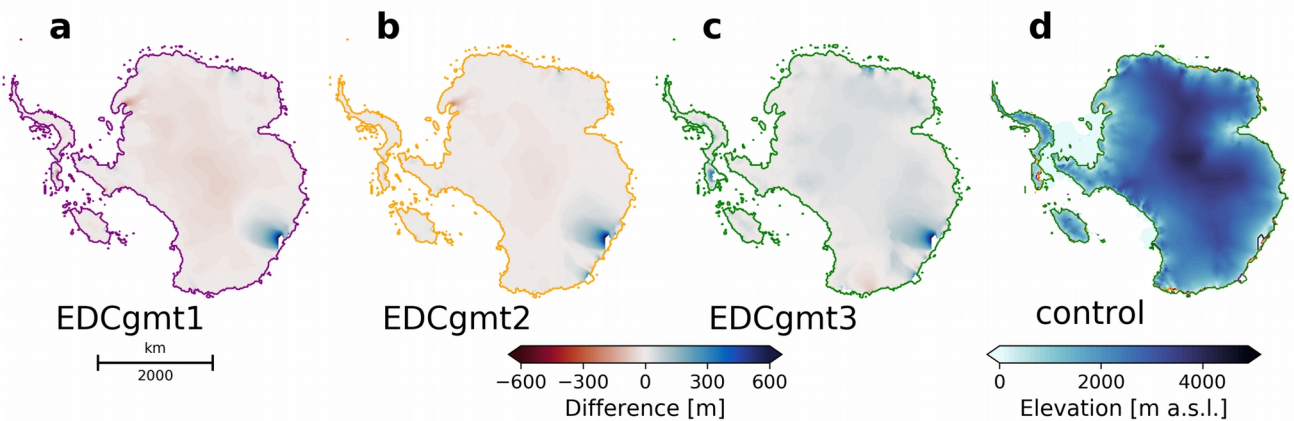


Figure 12: (a-c) ice sheet geometries at 405 ka for the EDC CFEN member using three different starting geometries at 420 ka (Fig. 11). Color scheme shows differences in surface elevation between each geometry and the control for 405 ka (d). Differences are only shown where the ice is grounded in both geometries, and coloured lines show the respective grounding lines in *gmt1-3*, also overlain in (d). This is Fig. 7 after the revisions to the manuscript.

34. Line 194: I think that the Figure number is wrong, it should not be Fig. 6.

**Our response:** We thank the reviewer for spotting this typo.

**35.** Line 191-204: I am not sure in which Figure I can see the corresponding GI. Figure 4? If yes, I don't understand why you say that LR04-GI does not warm above PI temperature. PI temperature in Fig4a is given by 0 (the dashed horizontal line) right? To me LR04-GI goes beyond, even if not a lot.

**Our response:** The reviewer is right. We have updated the corresponding section:

*“Considering the four adopted isotope curves (Fig. 2a,b), although similar at first sight, the GI reconstructions are different from one another, and therefore offer a range of modelled ice-sheet responses. The LR04 GI reconstruction is generally colder, showing conditions warmer than PI only for the warmest period of MIS11c (i.e., between ca. 410 ka and 400 ka).”*

**36.** Figure 4: Please put a horizontal dashed line corresponding to present-day AIS volume ( $26.9 \times 10^6 \text{ km}^3$ ).

**Our response:** We have added a dashed line, and reference Bedmap2, which we believe is the source of the number suggested by the reviewer (and which we use as our model's initial topography).

**37.** Lines 205-213: Actually, the amplitude of  $T^\circ$  increase between al curve is broadly the same, as shown on your Figure 4a. The difference resides in the fact that LR04-GI starts with colder conditions than the others. However the ice volume evolution also decreases for a long time event with LR04-PI, however, because initially it the AIS grows, then it can not retreat beyond present-day extent during the peak of MIS11c. Vostok-GI yields a decrease in ice volume of the same order than LR04-GI, about  $2 \times 10^6 \text{ km}^3$ .

**Our response:** As the reviewer highlighted, the main problem behind LR04 is that it is consistently colder than the other ensemble members during MIS11c. The relatively colder values we obtain are consistent with a bias towards Northern Hemisphere temperatures, which were found to be colder than PI during MIS11c. In line with the reviewer, and based on our results, it seems possible that an LR04-forced simulation would yield a WAIS collapse if its GI was somehow shifted towards the warmer conditions captured by the ice cores. However, at present we have no justification for adding such a shift. We reinforce this in our discussion by adding the following:

*“The fact that MIS11c marine records show oxygen isotopic values similar to the Holocene (Lisiecki and Raymo, 2005) despite geological evidence showing that there was a contribution to higher-than-Holocene sea levels from both Greenland and Antarctica (Scherer et al., 1998; Raymo and Mitrovica, 2012) implies that, if true, the ocean must have been colder. Indeed, paleoceanographic records from the Nordic Seas, for example, indicate that they were colder than present during MIS11 (Bauch et al., 2000; Kandiano et al., 2016; Doherty and Thibodeau, 2018). Southern Ocean records remain equivocal about a warming of MIS11 relative to the Holocene (e.g., Droxler et al., 2003). Hence, the inclusion of many Northern Hemisphere records in the LR04 stack could explain why it fails to capture the Antarctic warming during MIS11c seen in the ice cores. This also helps explain why the different criteria adopted for changing its scaling procedure had little effect on the results (Fig. 2b). A possible way of circumventing this problem could be to adopt a similar scaling approach to Sutter et al. (2019), who combined the LR04 stack and EDC ice-core temperature records, which, in their study, also led to WAIS collapse during MIS11c.”*

**38.** Line 218: What I see on Fig 4b is that there is a tipping point, a threshold from which the AIS retreats very fast. Thus, instead of warming rates, I see that when temperature reaches a certain threshold, the ice sheet reacts fast. For example, the Vostok curve is initially the warmest and thus the initial crease in volume is the strongest. Then the GI stabilises compared to the other and the volume decreases slow down. I would thus reformulate the analysis more in terms of tipping points and thresholds.

**Our response:** The reviewer is absolutely right, and we are thankful that we were directed towards this important observation. We have updated our figures (Figs. 1 and 2 in this response letter), and the discussion so the analyses are more focused on the tipping points and thresholds observed in the oceanic forcing.

39. Line 224: What about surface melt? Do you have any in your simulations? What method is used to calculate surface melt? Please provide detail about it in the Supplementary.

**Our response:** We used a PDD model as described in Calov & Greve (2005). This was added to the model description, which was included as a response to comment 20. Based on Figs. 1 and 13 of this response letter, we show that some areas do experience surface melt, and that it is most relevant along the Dronning Maud Land margin. This is now mentioned in the discussion, also comparing this region to the main ice shelves.

*“In all our CFEN simulations, ice sheet retreat is associated with stronger basal melting close to ice shelf grounding lines, especially at Siple Coast, and in the Ross and Filchner-Ronne ice shelves (Fig. 8). Surface ablation seems to be significant only over the fringes of the EAIS, notably at Dronning Maud Land (DML) and the Amery ice shelf, where surface temperatures reach positive values during summer (Fig. 9a). Nevertheless, they show limited retreat compared to the former two in the WAIS regions.”*

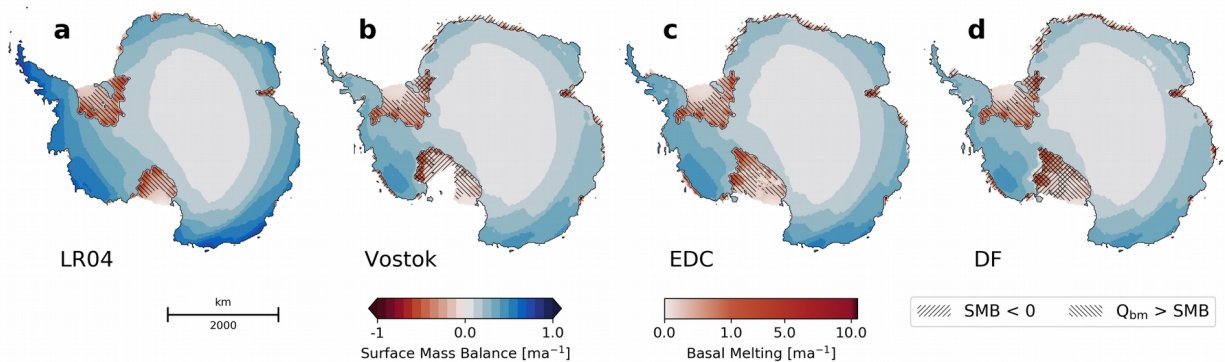


Figure 13: Surface Mass Balance (SMB) for the grounded ice and basal melting ( $Q_{bm}$ ) for the ice shelves for the CFEN simulations at 415 ka. Hatched areas show where basal melting dominates over surface mass balance and where surface mass balance is negative (i.e., where surface ablation occurs) Everywhere where  $Q_{bm} > SMB$  ice shelves are thinning. This is Fig. 8 after the revisions to the manuscript.

40. Line 223-228: Could you provide a figure.

**Our response:** We have addressed this with the changes made to Fig. 5 of the original submission, shown above as Fig. 13.

41. Figure 5: I would be nice to have a contour for  $SMB = 0m/yr$ , so to understand which area are subject to surface melt.

**Our response:** We agree with the Reviewer, but have added hatching where  $SMB < 0$  (see Fig. 13 above), which makes it easier to see these regions.

42. Figure S2: you can't comparison between PI climate and ERA5 fields. . .this makes no sense. Please modify this figure and show a comparison between present-day CCSM3 fields and ERA5 instead. Same for basal melting comparison: you can't use PI fields and compare with present-day inferred basal melt rates from Rignot et al. By the way, Which reference did you used in c) for basal melt rates?

**Our response:** The first part of this reviewer's comment was addressed in comment 5. We have added the reference to the present-day basal melt rates as requested, which were from Rignot et al. (2013), and now compare our fields to RACMO2 instead of ERA5, which is a more accurate representation of the Antarctic climate (Fig. 14). Including RACMO2 suits its use in other additions to the supplementary material following comment 28.

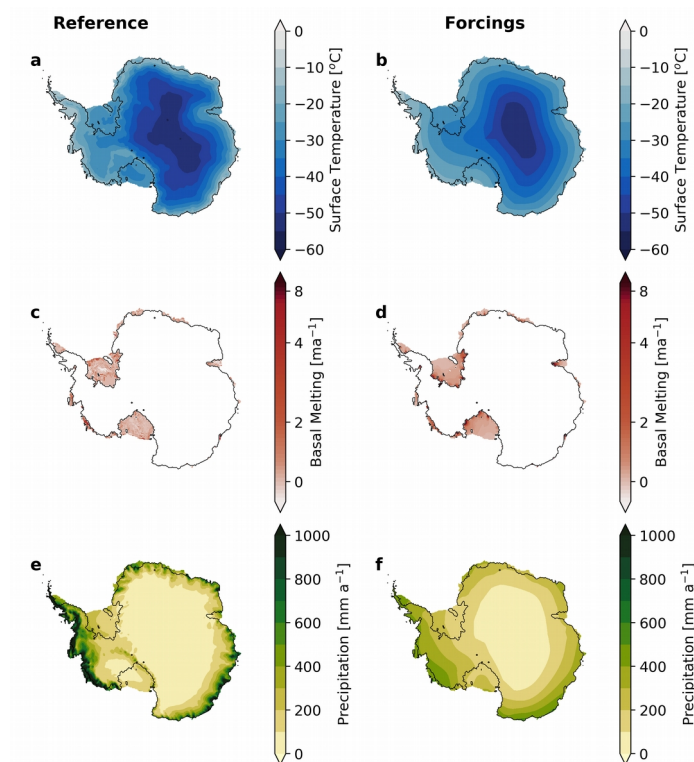


Figure 14: Comparison of CCSM3 forcings (right) to reference data (left) from RACMO2 (a,e; van Wessem et al., 2014) and of the calibrated basal melting to those of Rignot et al. (2013). (a,b) surface temperature [°C]; (c,d) basal melting [ma<sup>-1</sup>]; (e,f) annual precipitation [mm a<sup>-1</sup>]. This is Fig. S2 after the revisions to the supplement.

**43.** Line 241-244: *Thus why did you use an average over the last 10 kyrs. . .this does not make sense, because orbitals are varying so much. Please remove the corresponding results from the manuscript.*  
**Our response:** We have removed these results.

**44.** Line 249: *I disagree. Trajectories are the same, they are only delayed, please reformulate.*  
**Our response:** We have removed this sentence because of the changes in our ensemble and for reasons explained in the comment below.

**45.** Line 254: *“This effect seems to be non-physical, and a result of the delay introduced by the low-pass filter. “* → *The effect is physical, this is the result of your delayed curve. Please remove this sentence. Because it is not the point here.*  
**Our response:** This was pointed out by the Editor during the first screening process. We considered that the best way to address this was to use an alternative method for low-pass filtering, and re-run this ensemble of simulations using a box-filter, which does not yield the delay seen. Figure 15 shows the new results, which do not impact our inferences regarding the impact of high-frequency variability. Sect. 3.3 now reads:

*“The trajectories of each ensemble member in RSEN agree very well with one another (Fig. 4c), showing slightly increased delays in retreat due to the filtering process. Also, although it is possible to see slight differences in ice sheet volume between each ensemble member (the volume is larger the more filtered the forcing is), it is negligible compared to the overall changes in volume experienced by the entire ensemble.”*

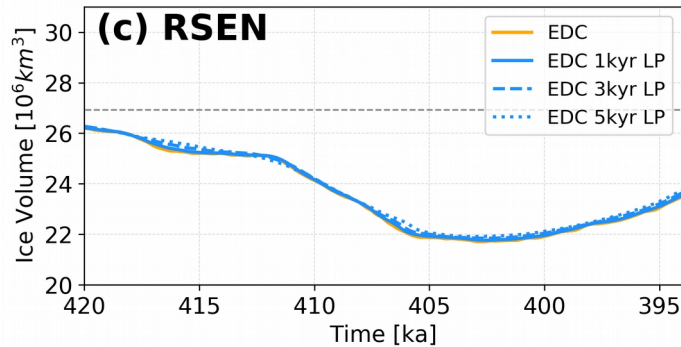


Figure 15: Sensitivity of AIS response (in total ice volume,  $10^6 \text{ km}^3$ ) between 420 ka and 394 ka to the RSEN low-pass filtered GI reconstructions. This is Fig. 4c after the revisions to the manuscript.

**46.** Line 256-259: “The 1 kyr low-pass GI is the only one that still preserves some higher-frequency variability “. I don’t this on the Figure, I disagree. None of the filtered curve preserve the high frequency visible on the original EDC record.

**Our response:** The reviewer is right, and this has been addressed with the changes shown above.

**47.** Subsection 3.5: the only difference visible is before the threshold at 412k for EDC and DF index. This is because there is this threshold that initial geometry does not impact on your results. Basically, ocean forcing is driving all your scenarios. To see the difference in initial ice sheet geometry, you should turn-off the ocean forcing. But this wouldn’t make sense. So the conclusion here is that ocean forcing is driving the initial trajectories until 412k, the tipping point. Thus is it not surprising that initial geometry does not matter too much. There is one thing you have not tested though here, is the variation in ocean forcing. Those tests makes also a lot of sens because ocean forcing has this tremendous effect on your simulations. Thus I would like to see a couple of other transient simulations with lower ocean forcing. And thus, try again your geometry scenarios with the difference ocean forcing rather than with EDC-GI or DF-GI.

**Our response:** We appreciate the highlighted importance of ocean forcing, and the lack of sensitivity experiments. Hence, we address this concern by performing an ensemble forced by the EDC GI with three simulations: Two where we lower the ocean temperature by 0.5 and 1.0 °C, and one where we reduce the ocean GI amplitude by 50%. We include the original ensemble member for comparison. We show the resulting ice volume (Fig. 4) and the grounding lines (Fig. 5) at different times of interest (see our response to comment 4). In short, the tipping point at ca. 412 ka still persists despite the fact that the ocean is substantially colder, but a total collapse of the WAIS is not achieved using a forcing with reduced temperatures. In light of these results, we believe that the ocean is driving our simulations after 412 ka (as evidenced by Figs. 1 and 16), which is why the different ice-sheet configurations converge to a similar geometry.

In our tests for different oceanic forcings, there is no connection between the Ross and Weddell seas at 405 ka for the  $\Delta T_{\text{ocn}} = -0.5 \text{ °C}$  run (Fig. 5d), but a narrow passage is established between the Ross and Amundsen seas. A comparison of the thermal forcing below the Ross and Filchner-Ronne ice shelves (Fig. 16) shows the stronger effect in the Ross sector and further strengthens a 0.4 °C warming below the ice shelves relative to PI as the threshold for which WAIS collapse is possible, as we postulate in the original manuscript and in our response to comment 1. This discussion is added to the supplementary material.

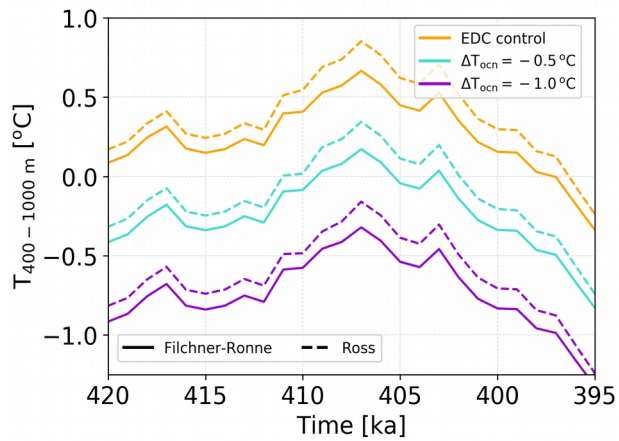


Figure 16: Average ocean temperatures between 400 and 1000 metres depth [°C] averaged under the Ross and Filchner-Ronne ice shelves for the  $\Delta T$  experiments presented in Figs. 4 and 5. This is Fig. S8 after the revisions to the supplement.

48. I also would like to see a figure in the supplementary showing the  $T_{forcing}$  for each GI.

**Our response:** We have added the requested figure to the supplement, and below as Fig. 17.

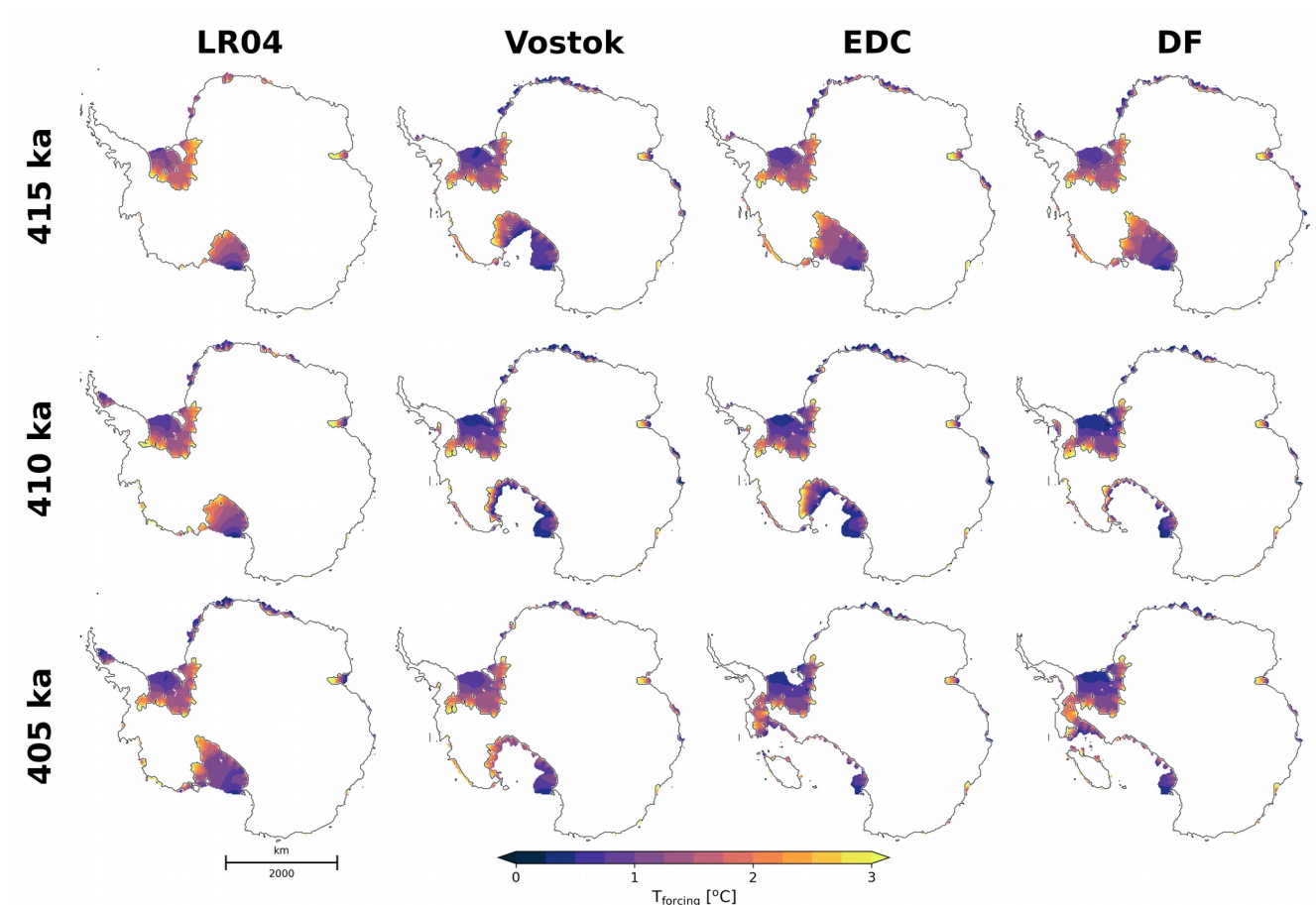


Figure 17: Thermal forcing (i.e., the difference between the ocean temperature and the ice shelf base temperature) at time steps of interest for each of the CFEN members. This is Fig. S9 after the revisions to the supplement.

49. Figure 12: Please also add total AIS sea level contribution on the figure for each geometry.

**Our response:** We have added the total AIS sea level contribution for each geometry to the figure (see Fig. 18 below).

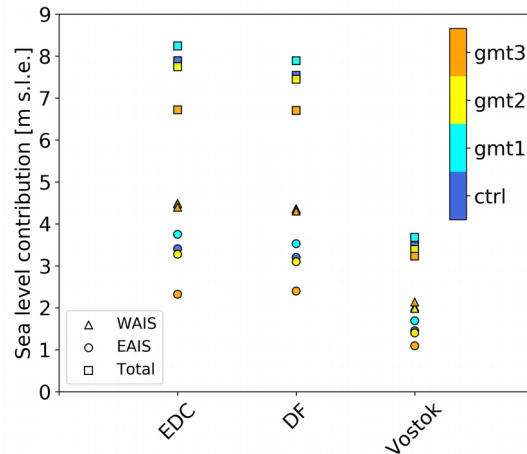


Figure 18: Sea level contribution (in m s.l.e.) of each SGSEN member during the global sea level highstand at 405 ka. This is Fig. 11 after the revisions to the manuscript.

50. Line 321-323: Please show some calving fluxes against oceanic warmth because you never really discuss calving, neither describe the calving method used here. Put this in the supplementary.

**Our response:** Figure 19 shows the calving fluxes for the main ice shelves. The mention of how calving is treated in our model is presented in the response to comments 17-20. We have added the requested calving plot to the Supplementary Material, which can be compared against Fig. 1b.

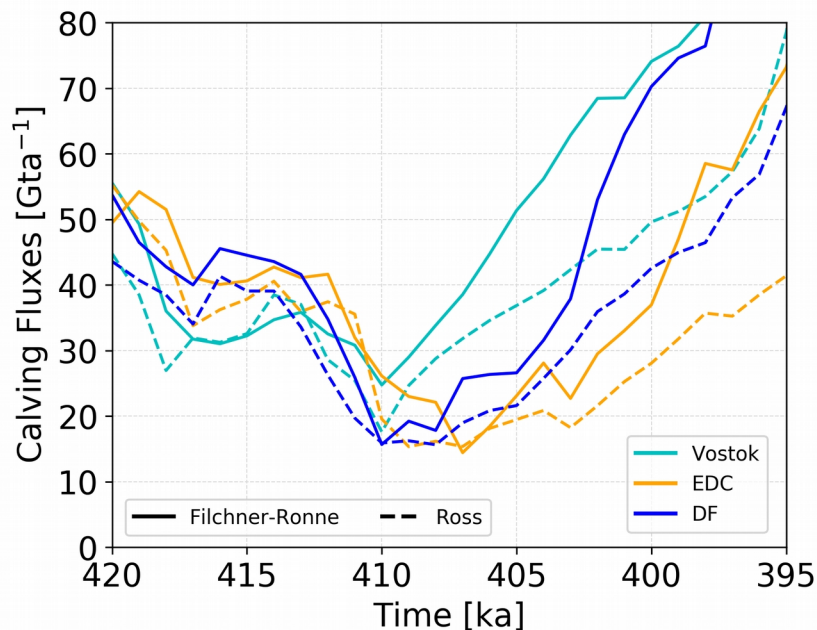


Figure 19: Calving fluxes (in Gt/a) integrated along the Filchner-Ronne and Ross ice shelves calving fronts. This is Fig. S10 after the revisions to the supplement.

51. Line 340-353: I really would like to see a specific figure in the Supplementary of temperature forcing derived from GI for each ice core records and compared with the temperature reconstructed from  $dD$  of those ice cores.

**Our response:** This has been addressed in comment 26.

**52.** Line 349-350: *I completely disagree with this statement. On your Figure 1, you can definitely see that this is because EDC-GI and DF-GI yield temperature warmer than those I Vostok and thus it is a matter of tipping point rather than duration. . .*

**Our response:** The reviewer offers a very good point. After a renewed assessment (see response to comment 1), we show that a collapse is possible for temperatures above the mentioned threshold if they are sustained for long enough. In short, there is indeed a threshold that must be crossed (which happens after the tipping point at 412 ka mentioned by the reviewer in comment 47), but it needs to be sustained for long enough to trigger the collapse.

**53.** Line 391-392: *“WAIS collapse was caused by the duration rather than the intensity of warming “. I don't see how you can conclude this here. I find the entire set of simulations rather inconclusive for this aspect. There is a tipping point in all the simulations shown in Figure 4. However, the amplitude of contribution to sea level is determined then by the magnitude of the warmth during the peak rather than the duration of the peak itself. Actually the ice sheet retreat in a very comparable way when using EDC and DF, which have a different peak duration. . .IN fact there is almost no significant difference between them in Figure 12 as well.*

**Our response:** The reviewer is right about the existence of a tipping point. As we showed in our responses to comments 1, 4, and 47, this marks the point when the ocean forcing becomes the main driver of retreat. However, as shown in our response to comment 1, the length of warming is still a decisive factor for the WAIS collapse, but both EDC and DF fulfill this criterion. EDC has a longer warmth period, and thus contributes slightly more to sea level. We included the importance of tipping points and the relationship between length and volume changes in our discussion.

**54.** Line 395-400: *Instead of just stating it, show it. Plot air and ocean temperature forcing versus WAIS ice volume evolution; same for EAIS*

**Our response:** We have provided this information in Fig. 1 in this response letter, which also helps restructure our discussion around possible tipping points and thresholds.

## References cited in this letter that were not listed under the original manuscript submission

Bakker, Pepijn, et al. "Hypersensitivity of glacial summer temperatures in Siberia." *Climate of the Past* 16.1 (2020): 371-386.

Bauch, Henning A., et al. "A paleoclimatic evaluation of marine oxygen isotope stage 11 in the high-northern Atlantic (Nordic seas)." *Global and Planetary Change* 24.1 (2000): 27-39.

Calov, Reinhard, and Ralf Greve. "A semi-analytical solution for the positive degree-day model with stochastic temperature variations." *Journal of Glaciology* 51.172 (2005): 173-175.

Danabasoglu, Gokhan, et al. "The CCSM4 ocean component." *Journal of Climate* 25.5 (2012): 1361-1389.

De Boer, B., et al. "A continuous simulation of global ice volume over the past 1 million years with 3-D ice-sheet models." *Climate Dynamics* 41.5-6 (2013): 1365-1384.

Doherty, John M., and Benoit Thibodeau. "Cold water in a warm world: Investigating the origin of the Nordic Seas' unique surface properties during MIS 11." *Frontiers in Marine Science* 5 (2018): 251

Droxler, André W., et al. "Unique and exceptionally long interglacial Marine Isotope Stage 11: window into Earth warm future climate." *Geophysical Monograph Series* 137 (2003): 1-14.

Kandiano, Evgenia S., et al. "A cold and fresh ocean surface in the Nordic Seas during MIS 11: Significance for the future ocean." *Geophysical Research Letters* 43.20 (2016): 10-929.

Marzocchi, Alice, and Malte F. Jansen. "Connecting Antarctic sea ice to deep ocean circulation in modern and glacial climate simulations." *Geophysical Research Letters* 44.12 (2017): 6286-6295.

Maule, Cathrine Fox, et al. "Heat flux anomalies in Antarctica revealed by satellite magnetic data." *Science* 309.5733 (2005): 464-467.

Otto-Bliesner, Bette L., et al. "Climate sensitivity of moderate-and low-resolution versions of CCSM3 to preindustrial forcings." *Journal of Climate* 19.11 (2006): 2567-2583.

Otto-Bliesner, B. L., and E. Brady. "PMIP2 climate model-proxy data intercomparisons for the LGM." *PAGES News* 16.2 (2008): 18-20.

Pollard, David, and R. M. DeConto. "A simple inverse method for the distribution of basal sliding coefficients under ice sheets, applied to Antarctica." *The Cryosphere* 6.5 (2012b): 953.

Rignot, Eric, et al. "Ice-shelf melting around Antarctica." *Science* 341.6143 (2013): 266-270.

Ronge, Thomas A., et al. "Pushing the boundaries: Glacial/interglacial variability of intermediate and deep waters in the southwest Pacific over the last 350,000 years." *Paleoceanography* 30.2 (2015): 23-38.

Ronge, Thomas A., et al. "Radiocarbon evidence for the contribution of the Southern Indian Ocean to the evolution of atmospheric CO<sub>2</sub> over the last 32,000 years." *Paleoceanography and Paleoclimatology* 35.3 (2020): e2019PA003733.

Tzedakis, P. C., et al. "Interglacial diversity." *Nature Geoscience* 2.11 (2009): 751-755.

Van Wessem, Jan Melchior, et al. "Modelling the climate and surface mass balance of polar ice sheets using RACMO2: Part 2: Antarctica (1979-2016)." *Cryosphere* 12.4 (2018): 1479-1498.

Van Wessem, J. M., et al. "Improved representation of East Antarctic surface mass balance in a regional atmospheric climate model." *Journal of Glaciology* 60.222 (2014): 761-770.

Waelbroeck, Claire, et al. "Sea-level and deep water temperature changes derived from benthic foraminifera isotopic records." *Quaternary Science Reviews* 21.1-3 (2002): 295-305.

WAIS Divide Project Members. "Onset of deglacial warming in West Antarctica driven by local orbital forcing." *Nature* 500.7463 (2013): 440-444.

Werner, Martin, et al. "Reconciling glacial Antarctic water stable isotopes with ice sheet topography and the isotopic paleothermometer." *Nature communications* 9.1 (2018): 1-10.

Yang, Haijun, and Jiang Zhu. "Equilibrium thermal response timescale of global oceans." *Geophysical research letters* 38.14 (2011).

# Sensitivity of the Antarctic ice sheets to the peak warming of Marine Isotope Stage 11

Martim Mas e Braga<sup>1,2</sup>, Jorge Bernales<sup>3</sup>, Matthias Prange<sup>3</sup>, Arjen P. Stroeven<sup>1,2</sup>, and Irina Rogozhina<sup>3,4</sup>

<sup>1</sup>Geomorphology & Glaciology, Department of Physical Geography, Stockholm University, Stockholm, Sweden

<sup>2</sup>Bolin Centre for Climate Research, Stockholm University, Stockholm, Sweden

<sup>3</sup>MARUM - Center for Marine Environmental Sciences, University of Bremen, Bremen, Germany

<sup>4</sup>Department of Geography, Norwegian University of Science and Technology, Trondheim, Norway

**Correspondence:** Martim Mas e Braga (martim.braga@natgeo.su.se)

**Abstract.** Studying the response of the Antarctic ice sheets ~~to past climate conditions during periods when climate conditions were~~ similar to the present ~~day~~ can provide important insights ~~for understanding its current~~ into current observed changes and help identify natural drivers of ice sheet retreat. ~~The~~ In this context, the Marine Isotope Substage 11c (MIS11c) interglacial ~~is one of the best candidates for an in-depth analysis given that at~~ offers a suitable scenario, given that during its later portion,   
5 ~~orbital parameters were close to our current interglacial. However, Antaretic~~ In particular, ice core data indicate that ~~although MIS11c CO<sub>2</sub> levels were close to Pre-Industrial,~~ warmer-than-present temperatures ~~(of about 2C) lasted for much~~ lasted for longer than during other interglacials. ~~Since the global mean sea level is thought to have been 6–13 m higher than today, there should have been some contribution from Antarctica. While substantial work has been conducted regarding,~~ and the response of the ~~Greenland Ice Sheet to the MIS11c climate, which is believed to have contributed with 3.9–7.0 m to global sea level, both~~ configurations of the Antarctic ice sheets and their contribution to sea level rise remain ~~poorly constrained. We use a numerical ice-sheet model to shed light on the response unclear. We explore the dynamics~~ of the Antarctic ice sheets ~~to during this period using a numerical ice-sheet model forced by~~ MIS11c climate conditions ~~obtained from a combination of a suite of Antaretic ice cores and the LR04 global stack of deep-sea sediment records and climate model outputs, while assessing the model sensitivity to the uncertainties in~~ derived from climate model outputs scaled by three glaciological and one sedimentary proxy records of   
15 ice volume. Our results indicate that the East and West Antarctic ice sheets contributed with 3.2 to 8.2 m to the MIS11c sea level rise. In the case of a West Antarctic Ice Sheet collapse, which is the most probable scenario according to far-field sea level reconstructions, ice-sheet initial configuration, and multi-centennial the range is further reduced to 6.7–8.2 m, independently of the choices of sea level reconstructions and millennial-scale climate variability. Within this latter range, the main source of uncertainty arises from the sensitivity of the East Antarctic Ice Sheet to a choice of initial configuration. We found that the   
20 warmer regional climate signal ~~of the MIS11c peak warming in Antarctica captured by the ice core records is necessary for the captured by Antarctic ice cores during peak MIS11c is crucial to reproduce its~~ recorded sea level highstand ~~to be reproduced,~~ and that warming length was more important than magnitude. However, there is a threshold for a West Antaretic Ice Sheet collapse that lies within an envelope of 1.6 and 2.1. Furthermore, we show that a modest 0.4 °C warmer-than-pre-industrial regional climate conditions. Sea level forcing and multi-centennial variability were found to have played virtually no role in   
25 driving ice-sheet contraction, but the choice of initial configuration of the East oceanic warming at intermediate depths leads

~~to a collapse of the West Antarctic Ice Sheet provided a large source of uncertainty in the quantification of MIS11e Antarctic peak sea level contribution, which falls between 6.4 and 8.8 m. if sustained for at least 4 thousand years.~~

## 1 Introduction

Marine Isotope ~~Stage 11 stands out in the Quaternary history since one of its substages, substage~~ Substage 11c (hereafter MIS11c), was ~~an interglacial period different from the preceding and subsequent interglacials of the Quaternary. First a remarkable interglacial~~ because it lasted for ~~ea. as much as~~ 30 thousand years (kyr), between 425 and 395 thousand years ago (ka; Lisiecki and Raymo, 2005; Tzedakis et al., 2012), thus making it the longest interglacial of the Quaternary. It also marked the transition from weaker to more pronounced glacial-interglacial cycles (EPICA Community Members, 2004). Its long duration is attributed to a modulation of the precession cycle, resulting in CO<sub>2</sub> levels that were high enough to suppress the cooling of the climate system due to the low eccentricity and thus reduced ~~solar radiation insolation~~ (Hodell et al., 2000). Moreover, ocean sediment cores (e.g., Hodell et al., 2000) and climate models (e.g., Rachmayani et al., 2017) show that the MIS11c global overturning circulation was at an enhanced state, resulting in asynchronous warming of the southern and northern high latitudes (~~Steig and Alley, 2002~~) (i.e., ~~they did not reach their warming peak at the same time; Steig and Alley, 2002~~). However, Dutton et al. (2015) ~~surmise that,~~ ~~point out that climate modelling experiments with realistic orbital and greenhouse gas forcings fail to~~ fully capture this MIS11c warming despite the fact that orbital parameters ~~in MIS11e~~ were almost identical to Present Day (PD) ~~at during~~ its late stage (~~EPICA Community Members, 2004; Raynaud et al., 2005~~) and (~~cf. EPICA Community Members, 2004; Raynaud~~ . Earlier studies (e.g., Milker et al., 2013; Kleinen et al., 2014) have shown that climate models also tend to underestimate climate variations during MIS11c, for which ice core reconstructions show the mean annual atmospheric ~~temperatures~~ temperature over Antarctica to have been ~~ea. about~~ 2 °C warmer than ~~Pre-Industrial~~ Pre-Industrial (PI) values, ~~climate modelling experiments with realistic orbital and greenhouse gas forcings fail to fully capture this MIS11e warming, as they tend to underestimate climate variations during the interglacial~~ (Milker et al., 2013; Kleinen et al., 2014).

A better understanding of the climate dynamics during ~~the~~ Quaternary interglacials, especially those that were warmer than today, is critical because they can help assess Earth's natural response to future environmental conditions (Capron et al., 2019). Among these periods, MIS 5e (also referred to as the Eemian, Last Interglacial, or LIG; Shackleton et al., 2003) was originally proposed to be a possible analogue for the future of our current interglacial (Kukla, 1997). More recently, MIS11c has been considered ~~an even better another suitable~~ candidate, since its orbital conditions were closest to PD (Berger and Loutre, 2003; Loutre and Berger, 2003; Raynaud et al., 2005). Furthermore, ice core evidence indicates that Termination V (i.e., the deglaciation that preceded MIS11) was quite similar to the last deglaciation in terms of rates of change in temperature and greenhouse gas concentrations (EPICA Community Members, 2004). The ~~unusual~~ length of this ~~unusual interglacial and the interglacial and a~~ transition to stronger glacial-interglacial cycles seen in the ~~recent subsequent~~ geological record may have been triggered by a reduced stability of the West Antarctic Ice Sheet (~~WAIS, Fig. ??; Holden et al., 2011~~), and its long duration was (~~WAIS, Fig. 1~~). The latter may have been due to the cumulative effects of the ice sheet lowering its bed (Holden et al., 2011), which in turn provided a positive climate feedback (Holden et al., 2010). The long duration of MIS11 was also shown to be

~~key to a key condition to triggering~~ the massive retreat of the Greenland Ice Sheet (GIS; Robinson et al., 2017). Elucidating  
60 the response of the Antarctic ice sheets (AIS) to past interglacials can also help identify various triggers ~~that are able to drive~~  
~~of~~ ice sheet retreat. This is because each interglacial has its unique characteristics: for example, while MIS11c was longer than  
the LIG, the latter was significantly warmer (Lisiecki and Raymo, 2005; Dutton et al., 2015).

~~Compared to more recent interglacials such as the LIG, information for MIS11c is scanty (Dutton et al., 2015; Capron et al., 2019)~~  
~~and pertains primarily to the GIS. The MIS11c behaviour of the GIS, constrained through numerical modelling and empirical~~  
65 ~~evidence, includes a strong retreat of its ice margin followed by vegetation expansion across southern Greenland (Willerslev et al., 2007; Reyes et al. (2014) report a probable GIS contribution of 4.5 to 6 m of sea level rise based on simplified model simulations~~  
~~driven by MIS5e climate forcings that best fit their geological constraints for MIS11c, while Robinson et al. (2017) provide an~~  
~~estimated range of 3.9–7.0 m (and 6.1 m as their most likely value) of sea level rise based on targeted numerical simulations~~  
~~for MIS11c.~~

70 The MIS11c history of Antarctica is less constrained than that of Greenland (e.g., Willerslev et al., 2007; Reyes et al., 2014; Dutton et al.  
. Whereas Raymo and Mitrovica (2012) consider that the WAIS had collapsed and that the East Antarctic Ice Sheet (EAIS,  
Fig. ??1) provided a minor contribution based on their estimate of MIS11c global sea levels of 6 to 13 m above PD (Dutton et al., 2015)  
~~, studies regarding the response of the AIS~~, ~~studies directly assessing the AIS response~~ have been elusive. For example, sed-  
imentary evidence has been inconclusive regarding the possibility of a collapse of the WAIS during ~~certain some~~ Quaternary  
75 interglacials (Hillenbrand et al., 2002, 2009; Scherer, 2003), and ~~only recently~~ evidence for the instability of marine sectors  
of the EAIS has ~~been provided (Wilson et al., 2018)~~ ~~only recently been provided (Wilson et al., 2018; Blackburn et al., 2020)~~  
. Counter-intuitively, ~~perhaps, the onshore dating of the dating of onshore~~ moraines in the Dry Valleys ~~back to MIS11c~~  
~~is has been~~ used to indirectly support regional ice sheet ~~contraction, which would result in retreat (Swanger et al., 2017).~~  
~~Swanger et al. (2017) argue that ice sheet retreat in the Ross Embayment provided~~ nearby open-water conditions and ~~thus~~  
80 ~~therefore~~ a source of moisture and enhanced precipitation, fueling local glacier ~~advances (Swanger et al., 2017)~~ ~~growth~~. Previ-  
ous numerical modelling experiments that encompass MIS11 also ~~do not show lack~~ a consensus regarding AIS volume changes.  
For example, Sutter et al. (2019) report an increased ice volume variability from MIS11 onwards, caused by ~~the~~ stronger at-  
mospheric and oceanic temperature variations, while Tigchelaar et al. (2018) only obtained significant volume changes during  
the last 800 kyr when increasing their ocean temperatures to ~~unrealistically high values (i.e., applying a ca. values as high as~~  
85 ~~4 C surface warming anomaly to their experiments)~~ °C. Conversely, de Boer et al. (2013) report higher sea level contributions  
during MIS ~~15.5, 9, and 13~~ ~~15e, 13, and 9~~, and weaker contributions during MIS ~~11 and 5.5~~.

~~Apart from the LIG, when 11c and 5e. Among the past interglacials, the LIG and Pliocene are considered to be the closest~~  
~~analogues to MIS11c, and~~ studies acknowledge the possibility of a WAIS collapse (e.g., Hearty et al., 2007; Pollard and DeConto, 2009)  
~~, the closest comparable period to MIS11c is the Pliocene, when the WAIS is also thought to have collapsed (Naish et al., 2009; Pollard and~~  
90 ~~in both periods (e.g., Hearty et al., 2007; Naish et al., 2009; Pollard and DeConto, 2009).~~ However, Pliocene model results were  
shown to be highly dependent on the choice of climate and ice-sheet models (Dolan et al., 2018). ~~Similarly, reconstructions~~  
~~(de Boer et al., 2015; Dolan et al., 2018).~~

The MIS11c climate is also loosely constrained. Reconstructions from different ice cores do not fully agree on how Antarctic surface air temperature evolved during MIS11c. For example, the Vostok ice core surface air temperature reconstruction (Petit et al., 1999; Bazin et al., 2013) reveals a much shorter and weaker period of peak warming (about  $2.16^{\circ}\text{C}$  higher than PD-PI around 410 ka) than that inferred from the EPICA Dome C (EDC; Jouzel et al., 2007) and Dome Fuji (DF; Uemura et al., 2018) ice cores, which have a lower uncertainty, and. The latter show a longer duration (ca. 15 kyr) of warmer-than-present temperatures (peaking at almost  $4^{\circ}\text{C}$ , peaking at over  $2.7^{\circ}\text{C}$  above PI around 407–406 ka for EDC, and  $2.7$ – $2.5^{\circ}\text{C}$  above PI at about 410–407 ka for DF, (locations are shown in Fig. ??1).

Given the absence of MIS11c-specific AIS model simulations, a dearth of information, As detailed, many modelling studies have investigated AIS responses over time periods that include MIS11. However, so far none has focused specifically on this period. Given the scarce information for MIS11 and conflicting constraints on how Antarctica responded to this exceptionally long interglacial (Milker et al., 2013; Dutton et al., 2015), we here present the first AIS model reconstructions zooming in on focus on MIS11c, the peak warming period between 420 and 394 ka. We aim Our aim is to reduce the current uncertainties in the AIS behaviour during MIS11c, specifically addressing the following questions:

1. How did the AIS respond to the warming of MIS11c? What More specifically, what are the uncertainties in the AIS minimum configuration, timing and potential sea level contribution?
2. What was the main driver of the changes in the AIS volume? Was it warming duration, peak temperature, or changes in precipitation? Are these drivers relevant to future ice sheet, or changes in the southern high latitudes oceanic forcing?

For this purpose, we perform five ensembles of numerical simulations of the AIS to evaluate the importance for evolution and focus on aspects that remain unaddressed by previous studies. We evaluate the impact on resulting ice volume and extent of the differences in the choice of proxy records (including their differences in signal intensity and structure of ice-core records, comparing to a reconstruction based on the LR04 stack of deep-sea sediment cores, uncertainties in sea level reconstructions, and uncertainties in), the choice of sea level reconstruction, and of uncertainties in assumptions regarding the geometry of the AIS at the start of MIS11c.

## 2 Methods

### 2.1 Ice-sheet model

For our experiments we employ the 3D thermomechanical polythermal ice-sheet model SICOPOLIS (Greve, 1997; Sato and Greve, 2012; Greve, 1997; Sato and Greve, 2012) with a 20 km horizontal grid resolution and 81 terrain-following layers in the vertical. It uses a the one-layer enthalpy scheme that of Greve and Blatter (2016), which is able to correctly track the position of the cold-temperate transition in the thermal structure of a polythermal ice body (Greve and Blatter, 2016).

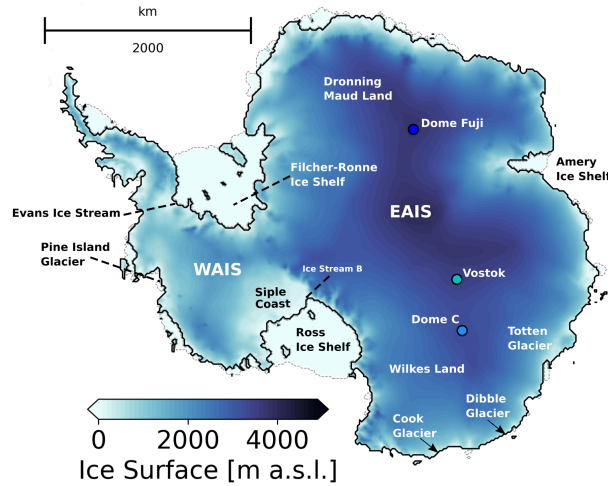


**Figure 1.** Surface topography of the AIS at the start of our [core](#) experiments (420–425 ka, see Fig. 3d), based on a calibration against [Bedmap2](#) (Fretwell et al., 2013, see Sect. 2.1). The locations mentioned in the text are showcased, including the drilling sites of the ice (circles) and sediment (red diamonds) cores on and around Antarctica, are showcased. Also shown are the GI reconstructions for the adopted records (cf. Sect. 2.2, Table 2) respectively.

The model combines the Shallow Ice Approximation (SIA) and Shelfy Stream Approximation (SSa) using (c.f. Bernales et al., 2017a, b).

$$\mathbf{U} = (1 - w) \cdot \mathbf{u}_{\text{sia}} + \mathbf{u}_{\text{ssta}}, \quad (1)$$

125 where  $\mathbf{U}$  is the resulting hybrid velocity,  $\mathbf{u}_{\text{sia}}$  and  $\mathbf{u}_{\text{ssta}}$  are the SIA and SSa horizontal velocities, respectively, and  $w$  is a weight computed as

$$w(|\mathbf{u}_{\text{ssta}}|) = \frac{2}{\pi} \arctan \left( \frac{|\mathbf{u}_{\text{ssta}}|^2}{u_{\text{ref}}^2} \right), \quad (2)$$

130 where the reference velocity  $u_{\text{ref}}$  is set to  $30 \text{ ma}^{-1}$ , marking the transition between slow and fast ice. This hybrid scheme reduces the contribution from SIA velocities mostly in coastal areas of fast ice flow and heterogeneous topography, where this approximation becomes invalid. Basal sliding is implemented within the computation of SSa velocities as a Weertman-type law (cf. Bernales et al., 2017a, Eqs. 2–6). The amount of sliding is controlled by a fixed, spatially varying map of friction coefficients that was iteratively adjusted during an initial present-day equilibrium run (cf. Pollard and DeConto, 2012b), such that the grounded ice thickness matches the present-day observations from [Bedmap2](#) (Fretwell et al., 2013) as close as possible. Sliding coefficients in sub-ice shelf and ocean areas are set to  $10^5 \text{ ma}^{-1} \text{ Pa}^{-1}$ , representing soft, deformable sediment, in case the grounded ice advances over this region. The initial bedrock, ice base, and ocean floor elevations are also taken from [Bedmap2](#). Enhancement factors for both grounded and floating ice are set to 1, based on sensitivity tests in Bernales et al. (2017b).

. This choice provides the best match between observed and modelled ice thickness for this hybrid scheme, similar to the findings in Pollard and DeConto (2012a).

140 Surface mass balance is calculated as the difference between accumulation and surface melting. The latter is computed using a semi-analytical solution of the positive degree day (PDD) model following Calov and Greve (2005). Near-surface air temperatures entering the PDD scheme are adjusted through a lapse rate correction of  $8.0\text{ }^{\circ}\text{C km}^{-1}$  to account for differences between the modelled ice sheet topography and that used in the climate model from which the air temperatures are taken. For the basal melting mass balance of ice shelves, ~~it adopts a calibration developed by~~ we use a calibration scheme of basal melting rates developed in Bernales et al. (2017b) to optimise a parameterisation based on Beckmann and Goosse (2003) and Martin et al. (2011), ~~but with that assumes~~ a quadratic dependence on ~~temperature (as in Holland et al., 2008; Pollard and DeConto, 2012a)~~ ~~which ocean thermal forcing (Holland et al., 2008; Pollard and DeConto, 2012a; Favier et al., 2019). This optimised parameterisation is able to respond to the variations in the applied~~ Glacial Index (GI, Sect. ~~2.2; a description of our 2.2~~) forcing. A more detailed description of this parameterisation is given in Sect. 1 of the supplementary material). ~~The quadratic dependence on thermal forcing is inspired by Favier et al. (2019), who found that a parameter yields results in good agreement with coupled ocean-ice shelf simulations. For glacial isostatic adjustment, we use.~~ In our experiments, we prescribe a time lag of 300 years for the ocean response to GI variations, which is considered the most likely lag in response time of the ocean compared to the atmosphere in the Southern Ocean (Yang and Zhu, 2011). At the grounding line, the basal mass balance of partially floating grid cells is computed as the average melting of the surrounding, fully floating cells, multiplied by a factor between 0 and 1 that depends on the fraction of the cell that is floating. This fraction is computed using an estimate of the sub-grid grounding line position based on an interpolation of the current, modelled bedrock and ice-shelf basal topographies. At the ice shelf fronts, calving events are parameterised through a simple thickness threshold, where ice thinner than 50 m is instantly calved away.

150 Glacial isostatic adjustment is implemented using a simple elastic lithosphere, relaxing asthenosphere (ELRA) model. We also use constant salinity since initial sensitivity tests using spatially variable salinity showed a negligibly small effect on the parameterised basal melting rates. The, with a time lag of 1 kyr and flexural rigidity of  $2.0 \times 10^{25}$  Nm, which Konrad et al. (2014) found to best reproduce the results of a fully-coupled ice sheet-self-gravitating viscoelastic solid Earth model. The geothermal heat flux applied at the base of the lithosphere is taken from Maule et al. (2005) and is kept constant. All relevant parameters used in the modelling experiments are listed in Table 1.

160 All ensembles cover a period from 420 to 394 ka. ~~To initialise the AIS, we first perform~~ After the calibration for basal sliding mentioned above, we initialise the AIS by performing a thermal spin-up over a period of 195 kyr from 620 to 425 ka, i.e., apply a transient surface temperature signal from the EDC ice core (Jouzel et al., 2007) as an anomaly to our PI climate (described in the next section) while keeping the ice sheet geometry constant at ~~PD~~our previously calibrated Bedmap2-based configuration. We then let the AIS freely adjust evolve for 5 kyr, between 425 and 420 ka, applying transient EDC forcing as a relaxation period. This is GI forcing during the relaxation period (Fig. S12). We chose 425 ka as the starting point for relaxation because it is when the MIS11c oxygen isotope values in the EDC ice core are closest to PI. In summary, we ignore the first 5 kyr (425–420 ka) to avoid a shock in from suddenly letting the ice-sheet topography freely evolve at the start of our

170

**Table 1.** Main ~~Parameters~~-parameters used in the experiments.

Parameter	Name	Value	Units
<del><math>E_{\text{grounded}}</math></del>	Enhancement <del>Factor</del> - <u>factor (grounded ice)</u>	1	~
<del><math>E_{\text{floating}}</math></del>	<u>Enhancement factor (ice shelves)</u>	1	
$n$	Glen's Flow Law <del>Exponent</del> - <u>exponent</u>	3	
$p$	Weertman's Law $p$ exponent	3	
$q$	Weertman's Law $q$ exponent	2	
$\tau$	ELRA model time lag	1	kyr
$D$	ELRA model flexural rigidity	$2.0 \times 10^{25}$	Nm
$\gamma_{lr}$	Lapse <del>Rate Correction</del> - <u>rate correction</u>	8.0	<del><math>^{\circ}\text{C km}^{-1}</math></del> - <u><math>^{\circ}\text{C km}^{-1}</math></u>
$S_0$	Sea water salinity	35	
$\rho_{sw}$	Sea water density	1028	$\text{kg m}^{-3}$
$\rho_{ice}$	Ice density	910	$\text{kg m}^{-3}$
$c_{p0}$	Ocean mixed layer specific heat capacity	3974	$\text{J kg}^{-1} \text{K}^{-1}$
$\gamma_T$	Thermal change velocity	$10^{-4}$	$\text{ms}^{-1}$
$L_i$	<del>Ice heat capacity</del> - <u>Latent heat of fusion</u>	$3.35 \times 10^5$	$\text{J kg}^{-1} \text{K}^{-1}$

~~simulations~~period of interest. Figure 1 shows the thermally spun-up ice sheet configuration at 425 ka, from which the relaxation simulations start.

## 2.2 Climate forcing and core experiments

In ~~our~~-an effort to assess similarities and differences in existing paleoclimate reconstructions, and regional differences in the  
175 ice-core records, we perform an ensemble of simulations where each member is forced by a GI (~~see~~-Eq. 3) derived from  $\delta D$   
from ice cores, ~~and~~-or  $\delta^{18}\text{O}$  from the LR04 stack of deep-sea sediment cores (Fig. 2a; Petit et al., 2001; EPICA Community  
Members, 2004; Lisiecki and Raymo, 2005; Uemura et al., 2018). Since ~~a~~-an ensemble of fully coupled climate-ice sheet model  
~~run~~-runs over 26 kyr is at present computationally challenging, an evaluation of possible scenarios for the peak-temperature  
response during MIS11c based on the paleoclimate signals from different ice sheet sectors can be a ~~simpler~~-cheaper, yet effective  
180 approach. The GI method is a way of weighting the contributions from interglacial (PI) and full glacial (Last Glacial Maximum;  
LGM) average states. It does so by rescaling a variable curve (usually temperature or isotope reconstructions from an ice or  
sediment record) based on reference PI and LGM values, which consider PI climate as  $GI = 0$  and LGM climate as  $GI = 1$   
(Eq. 3):

$$GI(t) = \frac{\delta X(t) - \delta X_{\text{PI}}}{\delta X_{\text{LGM}} - \delta X_{\text{PI}}} \quad (3)$$

**Table 2.** Ice and sediment cores reference values used in Eq. (3), together with the age (in thousand years before present; ka) from which the reference values were obtained. The respective age models of each core, and their references, are listed.

Record	Type (isotope)	$\delta X_{PI}$ [‰]	$\delta X_{LGM}$ [‰]	Age (ka)	Age <u>scale-model</u>	Reference
EDC	<u>Ice (<math>\delta D</math>)</u>	-397.4	-449.3	24.0	EDC3	EPICA Community Members (2004)
DF	<u>Ice (<math>\delta D</math>)</u>	-425.3	-469.5	22.8	AICC2012	Uemura et al. (2018)
Vostok	<u>Ice (<math>\delta D</math>)</u>	-440.9	-488.3	24.4	GT4	Petit et al. (2001)
LR04	<u>Sediment (<math>\delta^{18}O</math>)</u>	3.23	4.99	20.0	LR04	Lisiecki and Raymo (2005)

185 Where  $t$  is time, and  $X$  is Deuterium-deuterium for the ice cores or  $^{18}O$  for sediment cores. The value for  $\delta X_{PI}$  was obtained as the average of the last 1000 years before 1850 CE, while  $\delta X_{LGM}$  was taken as the minimum and maximum value for  $\delta D$  and  $\delta^{18}O$ , respectively, between 19 and 26.5 ka (cf. Clark et al., 2009; Clason et al., 2014). For our two reference climate states (i.e., PI and LGM), we use the Community Climate System Model version 3 (CCSM3) PI time slice in Rachmayani et al. (2016), and the LGM time slice in Handiani et al. (2013), which used identical model versions and were run on the same  
190 platform. A brief assessment of the model biases against PD data is provided in (Sects. 2 and 3 of the supplementary material: For further details the reader is referred to the respective original papers). The atmospheric and ocean temperature ( $T$ ) fields at time  $t$  are reconstructed using based on their respective PI and LGM reference fields ( $T_{PI}$  and  $T_{LGM}$  respectively) using (see also Fig. S13):

$$T(t) = T_{PI} + GI(t) \cdot (T_{LGM} - T_{PI}) \quad (4)$$

195 while precipitation is reconstructed given by an exponential function  $\tau$  to prevent negative values and also to ensure a smooth transition between the PI and LGM states, using:

$$P(t) = P_{PI}^{1-GI(t)} \cdot P_{LGM}^{GI(t)} \quad (5)$$

The PI and LGM reference values (including the reference ages for the latter) for the three ice cores and the LR04 stack are summarised in Table 2, together with the respective age scales their respective age models. The ensemble of simulations forced  
200 by different GI curves constitutes our core experiments and is termed CFEN (Climate Forcing Ensemble) ENsemble, CFEN) constitutes our core experiments.

## 2.3 Sensitivity experiments

### 2.3.1 Uncertainties due Sensitivity to the GI scaling

Given the fact that Because different approaches have been used to transform the isotope curves into a GI, we assess the impact  
205 of such scaling by comparing the effect of changing the reference values for  $\delta X_{PI}$  and sensitivity to the choice of the scaling

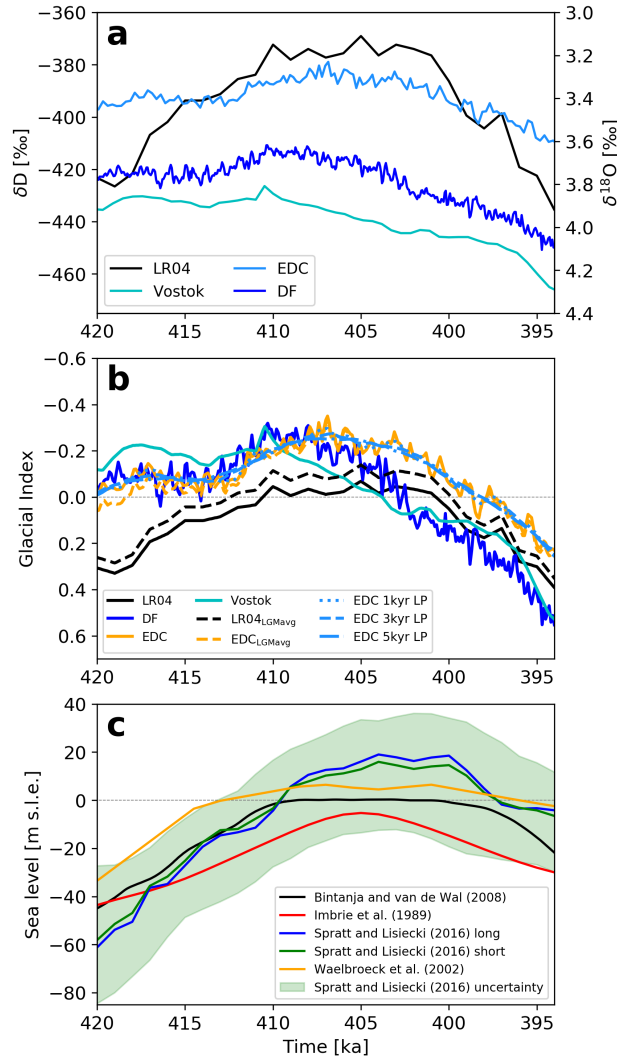


**Figure 2.** Reconstructions used in this study: (a) LR04  $\delta^{18}\text{O}$  (black) and Vostok, Dome C (EDC), and Dome Fuji (DF) ice-core  $\delta\text{D}$  [‰]; and; (b) resulting Glacial Indices from the reconstructions in (a) (cf. Sect. 2 and Table 3 for the legends); (c) global mean sea level anomaly relative to PI (meter sea level equivalent, m s.l.e.).

procedure by performing an additional scaling using another reference value for  $\delta X_{\text{LGM}}$ . For the former, we tested using as reference the average of the last 10 kyr (rather than the 1000 years before 1850 CE), due to the fact that the temperature increase throughout the Holocene is inconsistent between ice and sediment cores (Fig. 2a). For the latter, we also treat  
In the new scaling procedure,  $\delta X_{\text{LGM}}$  as is the average (between 19 ka and 26.5 ka) instead of rather than the peak value. We apply the different combinations of these references and their values compare the effects of using these two procedures when applied to the EDC ice core  $\delta\text{D}$  and the LR04 stack  $\delta^{18}\text{O}$  curves. For LR04 we only present the results for the sensitivity to the rescaling of  $\delta^{18}\text{O}_{\text{PI}}$

210

~~since there was virtually no difference when changing the treatment for  $\delta^{18}\text{O}_{\text{LGM}}$  (Supplementary Fig. S3) records.~~ We call this ensemble the Scaling Sensitivity ~~Ensemble~~ ENSEMBLE (SSEN).”

### 2.3.2 ~~Impacts of multi-centennial~~ Sensitivity to millennial-scale variability

215 Given the different temporal resolutions of climate records, lower-resolution reconstructions such as LR04 and Vostok might not capture the impact of ~~multi-centennial~~ millennial variability or shorter events, as do EDC and DF (Fig. 2a). Thus, we assess the potential effects of record data resolution and ~~centennial~~ millennial (or shorter) time scale variability by applying 1, 3, and 5 kyr low-pass filters to the EDC ice core GI and forcing our model with the resulting smoothed GI curves (light blue lines in Fig. 2b). We then compare these three simulations to the ~~unaltered~~ original EDC-derived ice sheet history, and call this  
220 ensemble the Resolution Sensitivity Ensemble (RSEN).

### 2.3.3 ~~Uncertainties in~~ Sensitivity to sea level

Sea-Mean sea level plays an important role in determining the flotation of ~~ice~~ the ice sheet and the stresses at its marine margins. Uncertainties in global mean sea ~~Level~~ level reconstructions are therefore a significant concern, and several studies have indeed focused on improving ~~its estimates for the past millions of years (e.g., Imbrie et al., 1989; Bintanja and van de Wal, 2008; Spratt and Lisiecki~~  
225 their estimates (e.g., Imbrie et al., 1989; Waelbroeck et al., 2002; Bintanja and van de Wal, 2008; Spratt and Lisiecki, 2016, Fig. 2c). We evaluate the effect of using a particular sea level reconstruction on the evolution of the AIS by running an ensemble of simulations with ~~EDC-based~~ EDC-derived GI, where each member uses a different sea level reconstruction. Sea level curves included in this ensemble are three of the reconstructions presented by Spratt and Lisiecki (2016), termed "long" (i.e., uses records that extend as far back as 798 ka), "short" (uses records that extend at least until 430 ka), and the "upper uncertainty  
230 boundary" from their records, because we consider their lower uncertainty boundary to be satisfactorily covered by SPECMAP (Imbrie et al., 1989), which we include, ~~and finally the reconstruction from Bintanja and van de Wal (2008).~~ We also include in the analysis the reconstructions from Bintanja and van de Wal (2008) and from Waelbroeck et al. (2002). All these records are presented in Fig. 2bc, and we call this ensemble, where we test ~~for~~ different sea level reconstructions, the Sea Level Sensitivity Ensemble (SLSSEN).

### 235 2.3.4 ~~Uncertainties in~~ Sensitivity to the choice of initial ice sheet geometry

Similar studies that ~~aim to~~ assess AIS changes over (~~one or more~~) glacial and interglacial cycles often ~~assume the PD geometry as a starting condition~~ adopt a PI or PD starting geometry (e.g., Sutter et al., 2019; Tigchelaar et al., 2019; Albrecht et al., 2020), ~~as has been done.~~ We have followed the same approach in our CFEN experiments (see Sect. 2.2). Although this has been loosely inferred from sedimentary (Capron et al., 2019) and ice-core (EPICA Community Members, 2004) proxy records,  
240 to our knowledge there is no direct evidence to support this (e.g., Swanger et al., 2017). Hence, we also perform an ensemble of simulations starting from ~~distinct~~ different ice sheet geometries ~~that are larger than PD, given the fact that at 420 ka the climate was transitioning to the interglacial.~~ This allows for an evaluation of the influence of an initial AIS configuration at 420 ka

on ~~the-its~~ modelled retreat and advance ~~of-the-AIS~~ (including possible thresholds), and provides an uncertainty envelope in its potential sea level contribution based on this criterion. We call this the Starting Geometry Sensitivity ~~Ensemble~~ ENSEMBLE (SGSEN), and ~~all-its-its three~~ unique geometries are forced with the ice-core reconstructed climate forcings tested in CFEN.

In order to create a representative range of initial geometries at 420 ka, we use a common starting geometry, but vary the relaxation time. For this purpose, we first create an ancillary geometry by perturbing the thermally spun-up AIS with a constant LGM climate (air temperature and precipitation rates) and no sub ice-shelf melting over a 5 kyr period. The resulting ancillary ice sheet (which has an extent that sits between PI and LGM configurations) is then placed at 420, we vary the forcing conditions relative to the control run (i.e., temperature, precipitation, calving, and sub-ice-shelf melting) during the 425–420 ka relaxation. ~~We use constant LGM temperature 425 and LGM or PI precipitation fields during this period, as opposed to the transient GI approach of the control run. Table ?? summarises the different combinations used in creating each initial ice sheet geometry 430 ka and runs transiently (following the respective GIs) until 394 ka. This creates a representative range of starting geometries~~ at 420 ka (labelled gmt1 to gmt3; Fig. 3). ~~These different combinations allow the ice sheet to advance towards its intermediate-to-full glacial extent during a relatively short time, and their numbering (1 to 3) reflects an increasing areal extent relative to the 'control' run, and each initial ice sheet geometry is labelled gmt1 to gmt3 (Fig. 3d). Geometry 1 a-c; shortest relaxation is gmt1, longest is gmt3). The gmt1 initial topography is generally more extensive and thinner than the control. Its grounding line advanced at the southern margin of the Filcher-Ronne Ice Shelf and at Siple Coast, but the ice sheet interior is on average 200 m thinner than the control and indeed up to 400 up to 500 m thinner across particular regions such as the dome areas of the WAIS and Wilkes Land (Dome C). It is, however, about 200 m thicker at its fringes, which results in a gentler surface gradient towards the ice sheet margins. Geometries 2 and 3 show a more pronounced height difference and larger extent than the control run. They yield a slightly thinner ice sheet interior along its ice divides (The gmt2 initial topography is less than 100 m ), but thicker at the main drainage outlets (between 200 m in the interior and 400 m close to the former grounding lines). The gmt2 ice sheet is almost completely grounded across the Filchner-Ronne and Amery basins, with a reduced Ross Ice Shelf compared to gmt1 thinner than control over the EAIS interior, and about 100 m thicker over the WAIS interior and at the EAIS margins. Finally, the gmt3 has no prominent ice shelves, because the ice sheet becomes grounded across most of the domain initial topography is overall thicker than control, though not by more than 100 m except at the western side of the Antarctic Peninsula and the WAIS margins, where some regions are up to 300 m thicker (Fig. 3c). Table 3 summarises all experiments described in this section.~~

270 Different starting ice sheet geometries at 420 ka. (a-c) the different starting geometries corresponding to gmt1-gmt3 after 5kyr of relaxation following climate parameters given in Table ??; (d) original "control" conditions used for CFEN and SLSEN sensitivity analyses (Table ??). (e-g) difference maps between control (panel d) and the three alternative ice sheet geometries (respectively panels a-c). Differences are only shown where the ice is grounded in both geometries, and grey lines show the grounding lines in gmt1-3.

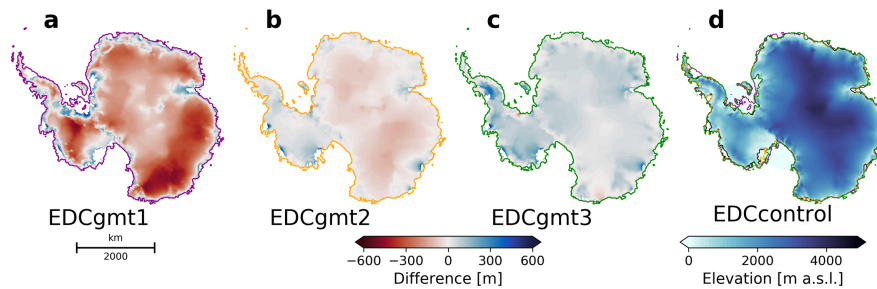


**Figure 3.** (a-c) Three different starting ice sheet geometries at 420 ka for gmt1–3 using EDC forcing, the EDC CFEN member is used as "control". Color scheme shows differences in surface elevation between each geometry and the control for 420 ka (d). Differences are only shown where the ice is grounded in both geometries, and coloured lines show the respective grounding lines in gmt1-3, also overlain in (d)

## 275 3 Results

### 3.1 Climate forcing reconstructions

Considering the four adopted isotope curves (Fig. ??2a,b), although similar at first sight, the GI reconstructions are different from one another, and therefore offer a range of modelled ice-sheet responses. The LR04 GI reconstruction ~~shows conditions close to PI is generally colder, showing conditions warmer than PI only~~ for the warmest period of MIS11c (~~and colder than PI before and after~~), thus not showing i.e., between ca. 410 ka and 400 ka. Consequently, it does not show a peak warming ; or at least one that is warmer than PI as strong as the other reconstructions (Fig. ??2b). Although the ice cores have similar ranges in GI values and similar overall aspects of the curves (and good covariance between EDC and DF; Uemura et al., 2018), they differ in key aspects (Fig. ??). The Vostok reconstruction starts at a warmer state than the others at 420 ka, has a modest peak warming at 410 ka, and then consistently declines towards a colder state (crossing the GI = 0 line at about 404 ka). The EDC reconstruction shows a mildly warmer-than-PI state at 420 ka, which persists until about 412 ka. Subsequently, the peak warming starts and persists (in a slightly warmer state than reconstructed with Vostok ) until ca. after 410 ka) until 397 ka. Its rate of decline after about 404 ka is very similar to the Vostok and LR04 curves, although it is in a warmer state than the previous two. Finally, the DF reconstruction is somewhere in-between the other two ice cores (Fig. ??2b). It shows more quite stable conditions at the start (i.e., no pronounced warming), rising to a rather prolonged warming period pronounced warming peak similar in structure to the EDC reconstruction, but peaks at 410 ka, similar to the Vostok curve. Finally, its rate of decline is similar to the other cores and so it crosses PI values (GI = 0) later than the Vostok but earlier than the EDC curves, between 404 ka and 403 ka.

The ice sheet history for MIS11c using the LR04 forcing is clearly different from the others, ~~because the ice sheet only. The ice sheet loses less than a third of its volume compared to the other CFEN members, and becomes smaller than its initial state for a brief period of 1–2 kyr before 400 ka PD for a duration of 9 kyr, while the others are consistently below PD levels~~ (Fig. ??4a). It is worth reminding that, in contrast to other members of CFEN, the LR04 curve starts with colder-than-PI conditions and

**Table 3.** Experiments performed to create alternative experiments grouped by ensemble, listing their respective GI forcings, applied sea level reconstruction, and choice of initial geometries during geometry. LGMavg denotes that the relaxation period between 425 ka-GI was rescaled using the average LGM value as opposed to the peak value (cf. Sect. 2.3.1 and 420 ka Table 4). The SGSEN experiments were designed to create increasingly larger ice sheet geometries, i.e. grouped for better visualisation, gmt1 larger than control but smaller and much smaller than gmt2 and gmt3 each SGSEN row corresponds to 3 experiments, respectively one starting from each geometry (cf. Fig. 3gmt1-3).

Experiment Ensemble	Temperature (atm/ocn) Experiment	GI forcing	Sea level reconstruction	Initial
CFEN	lr04	LR04	Bintanja and van de Wal (2008)	
CFEN	edc	EDC	Bintanja and van de Wal (2008)	
CFEN	df	DF	Bintanja and van de Wal (2008)	
CFEN	vos	Vostok	Bintanja and van de Wal (2008)	
SSEN	lr04lgmavg	LR04LGMavg	Bintanja and van de Wal (2008)	
SSEN	edclgmavg	EDCLGMavg	Bintanja and van de Wal (2008)	
RSEN	lp1bx	EDC (1 kyr low pass, LP)	Precipitation-Bintanja and van de Wal (2008)	Calv
RSEN	Sub-ice-shelf melting-lp3bx	EDC (3 kyr low pass, LP)	Bintanja and van de Wal (2008)	
RSEN	lp5bx	EDC (5 kyr low pass, LP)	Bintanja and van de Wal (2008)	
SLSSEN	s16l	EDC	Spratt and Lisiecki (2016) long	
SLSSEN	s16s	EDC	Spratt and Lisiecki (2016) short	
SLSSEN	transient-s16u	transient-EDC	On-Spratt and Lisiecki (2016) upper uncertainty	On
gmt1-SLSSEN	LGM-spm	LGM-EDC	On-Imbrie et al. (1989)	On
gmt2-SLSSEN	LGM-wae	PI-EDC	On-Waelbroeck et al. (2002)	On
gmt3-heightSGSEN	LGM-edcgmt[1-3]	PI-EDC	Off-Bintanja and van de Wal (2008)	On
SGSEN	dfgmt[1-3]	DF	Bintanja and van de Wal (2008)	
SGSEN	vosgmt[1-3]	Vostok	Bintanja and van de Wal (2008)	

does not become significantly warmer afterwards produce a peak warming as strong as the others. It only shows a brief period of warmer-warmer-than-PI conditions between 410 and 400-401 ka (Fig. ??a2b), resulting in the observed an overall larger AIS (Fig. ??b5). The ice core CFEN members yield lower ice volumes throughout all-the-entire MIS1c (Fig. ??b4a), but with important variations. The Vostok-forced experiment, for example, introduces a faster ice loss at the beginning of the simulation period, when it shows a sudden warming (Fig. ??a). However, it recovers more quickly than the EDC and DF experiments as soon as the peak warming is over and the climate starts to shift back to PI conditions, without a WAIS collapse (Supplementary Fig. S45).

The members that result in a collapse of the WAIS (forced with the DF and EDC reconstructions) reveal slightly different responses. For example, the (Fig. 4a). The experiment forced by the EDC reconstruction shows an AIS volume reduction after

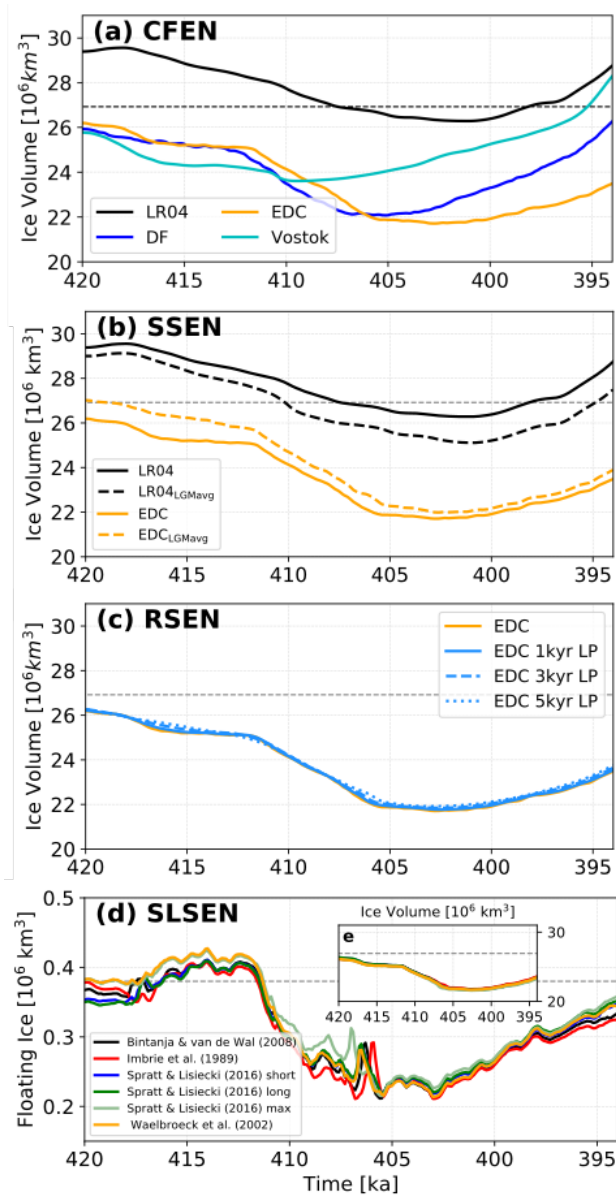


**Figure 4.** Sensitivity of AIS response to CFEN GI reconstructions during the peak warming (in total ice volume,  $10^6 \text{ km}^3$ ) between 420 ka and 394 ka to (a) CFEN GI reconstructions; (b) SSEN rescaled GI reconstructions; (c) RSEN low-pass filtered GI reconstructions; (d) SLEN sea level reconstructions forced by EDC GI (cf. Fig. 2a Table 3). (b) Total Dashed line shows PD ice volume  $10^3 \text{ km}^3$ . (Fretwell et al., 2013)

a sudden warming at ca. 417 ka (Fig. ??) around 418 ka, but the WAIS collapse is delayed until 410 ka, after 407–406 ka (Fig. 5), following a second short period with an increased warming rate after 412 ka, that leads up to the peak-warming of MIS11c. The DF experiment on the other hand is rather stable until ca. 412 ka, when the climate starts warming towards its peak. Most

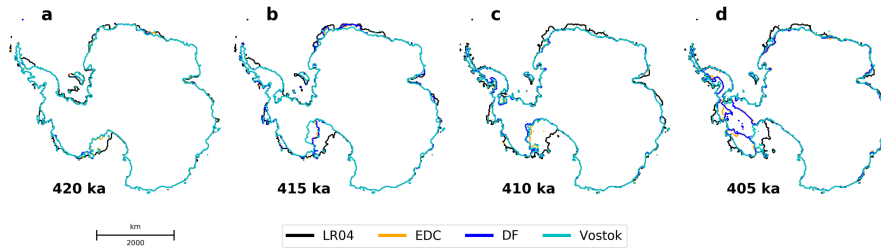


**Figure 5.** Total Mass-Balance (i.e. Grounding lines at 420, ice-shelf basal melting and surface mass-balance combined 415, in  $\text{ma}^{-1}$ ) at 416, 410, and 405 ka for the CFEN simulations. Hatched areas show where basal melting dominates over surface mass-balance.

of the retreat seems to be triggered at times when the warming rate is strongest is triggered after the sudden temperature rise at 412 ka, as opposed to when the peak warming occurs.

For all ice-core ensemble members, contraction of the AIS is already ongoing by 416 ka, and by 405 ka they are at, or close to, their minimum extents. In all CFEN simulations, ice-sheet contraction is associated with strong basal melting close to ice-shelf grounding lines, especially at Siple Coast at the Ross Ice Shelf and underneath the Evans Ice Stream at the Filchner-Ronne Ice Shelf (Fig. ??). These are caused by the combination of an increased warming of the ocean upper layer in these regions (Supplementary Fig. S5) and higher melt rates at the ice-stream flux-gates (Supplementary Fig. S2d). The same does not happen for the marine-based margin of western Dronning Maud Land, which shows more limited retreat during MIS11c than their western counterparts in the Weddell Sea region. Around most of the EAIS (except for the Amery Ice Shelf), either upper-layer ocean temperatures or ice-shelf melt rates are not high enough to force grounding-line retreat as strongly as in the aforementioned regions, and the relatively lower ice-loss is dominated by surface ablation (Fig. ??).

### 3.2 Sensitivity to rescaling of the climate forcings

The different  $\delta$  isotope reference values used for the SSEN experiments are shown in Table 4 (cf. Table 2). Using an LGM-averaged value results in a smaller ice sheet for the LR04 GI, while for the EDC GI it results in a slightly larger AIS than their correspondent CFEN experiments throughout the entire MIS11c (Fig. ??). This LR04-rescaled 4b). The LR04-LGM-averaged run, however, still does not produce significant AIS-contraction compared to AIS retreat as significant as the other experiments, with an ice-volume at 405 ka of ca.  $10^6 \text{ km}^3$  less than its initial state (Fig. ??b) 3.4% less volume ( $1 \cdot 10^6 \text{ km}^3$ ) at 402 ka when compared to its original rescaling. The warmer conditions resulting from the GI rescaling are still not enough to compensate for the initial growth caused by significantly colder-colder-than-PI conditions at 420 ka, and during the preceding relaxation stage. Although differences in ice-sheet volumes exist between the different scaling strategies in the EDC-forced experiments, the resulting ice sheet histories are quite similar. Despite ice-sheet volume at 402 ka being smaller in the run where the LGM reference is taken as the peak value, the differently scaled ice sheet is only 2.3% larger in volume than the CFEN ice-sheet ( $0.5 \cdot 10^6 \text{ km}^3$ ).

**Table 4.** Different isotope values adopted for the GI rescaling procedure. *Hol* is the reference value produced by the average over the last 10 kyr (which replaces PI in Eq. 3 for the respective experiments), while *LGM<sub>avg</sub>* is the reference value obtained from the average between 26 and 19.5 ka (see Sect. 2.3.1).

Record	$\delta X_{PI}$ [‰]	$\delta X_{Hol}$ [‰]	$\delta X_{LGM}$ [‰]	$\delta X_{LGM_{avg}}$ [‰]
EDC	-397.4	-394.6	-449.3	-442.3
LR04	3.23	3.33	4.99	4.85

Although differences in ice sheet volumes exist between the different scaling strategies in the EDC-forced experiments, the resulting ice sheet histories are quite similar.

### 3.3 Sensitivity to millennial variability

335 The trajectories of each ensemble member in RSEN agree with one another (Fig. ??b). Despite the ice sheet volume at 405  
 ka being smaller in the run where both LGM and PI isotope values were applied differently to scale the EDC record (i.e.,  
 multi-millennial averages, see Sect. 2.3.1) than in the CFEN EDC-forced experiment, this difference amounts to ca. 0.6 m  
 s.l.e., with only 0.1 m s.l.e. coming from the WAIS and the remainder coming from the EAIS (AIS sea level contribution, as  
 well as separate contributions from EAIS and WAIS will be further discussed in Sect. 3.5 and thereafter). It is also important to  
 340 keep in mind that using the last 10 kyr as reference for  $GI = 0$  is problematic due to the fact that the resulting GI for PI itself,  
 which our reference fields are representative of, is much smaller than zero, which was the value it should have following the  
 established routine for the derivation of paleoclimate conditions using a combination of GI and climate model time slices  
 (e.g., Forsström et al., 2003; Forsström and Greve, 2004; Greve, 2005; Clason et al., 2014). Consequently, the PI field has a  
 stronger influence, producing an unrealistic forcing at time  $t$  that is warmer than expected.

345 Sensitivity of AIS response to SSEN GI reconstructions during peak warming between 420 ka and 394 ka. "Hol" denotes the  
 experiments where the last 10 kyr were used as opposed to the last 1 kyr, and "LGM<sub>avg</sub>" denotes the experiments where the  
 average over the LGM was taken as opposed to the peak value. (a) Differently scaled GI curves. (b) Total ice volume  $10^3 \text{km}^3$ .

### 3.4 Sensitivity to multi-centennial variability

Although the minimum volumes achieved by the filtered-GI experiments in RSEN are similar to the original ice sheet history  
 350 obtained from the CFEN EDC-forced experiment, their individual trajectories are slightly different (Fig. ??). Ice sheet contraction  
 and the timing at which each low-pass filter experiment reaches its minimum volume and starts its subsequent recovery are  
 delayed compared to the original EDC forcing. The lag between the ice sheet histories increases with an increased filtering  
 window. Whereas the 1 kyr low-pass experiment shows relatively small differences in the timing of the events compared to  
 the CFEN EDC-forced run, the 3 and 5 kyr low-pass experiments show a significant delay in the ice sheet contraction (this  
 355 is especially clear after 412 ka; Fig ??b). This effect seems to be non-physical, and a result of the delay introduced by the  
 low-pass filter. While such delay prevents these results from being discussed in terms of absolute time, it still has implications

for the impact of high-frequency variations. The 1 kyr low-pass GI is the only one that still preserves some higher-frequency variability, although its peaks are shifted or even in anti-phase with the original EDC GI series. This, however, appears to have little to no effect on the resulting ice sheet evolution, indicating that higher-frequency oscillations play a minor role in ice-sheet volume changes.

360 Sensitivity of AIS response to RSEN GI reconstructions during peak warming between 420 ka and 394 ka. (a) GI reconstructions. (b) Total ice volume  $10^3\text{km}^3$ . LP in the figure stands for "low-pass". 4c), showing increased delays in the ice sheet retreat in response to the filtering intensity. Also, although it is possible to see slight differences in ice sheet volumes between ensemble members (the volume is larger the more filtered the forcing is), it is negligible compared to the overall changes in volume  
365 experienced by the entire ensemble.

### 3.4 Sensitivity to sea level reconstructions

Although the range of global mean sea level reconstructions is wide (nearly reaching 60 m between 405 ka and 400 ka; Fig. ??a2c), the AIS response in terms of volume is remarkably similar for different sea level curves (Fig. ??b4e). The differences in sea level have their largest impacts on the volumes of floating ice (Fig. ??e), directly reflecting 4d). It directly  
370 reflects their effect on the flotation of ice close to, and consequently on the grounding line position. The SLEN member with the highest sea level rise (i.e., the upper uncertainty boundary of Spratt and Lisiecki, 2016) deviates the most from the other members, especially in the portion of grounded ice being brought to flotation (Fig. ??e4d). However, the differences are not significant enough to yield substantially distinct ice volume changes (Fig. ??b4e).

375 Sensitivity of AIS response to SLEN reconstructions during peak warming between 420 ka and 394 ka. (a) records of global mean sea level relative to today meter sea level equivalent, m s.l.e. (cf. Fig. 2b). (b) Total ice volume  $10^3\text{km}^3$ ; (c) Floating ice volume  $10^3\text{km}^3$ .

### 3.5 Sensitivity to the choice of initial ice sheet geometry

In order to evaluate the uncertainty arising from the assumption of a PD-like initial ice sheet configuration, we perform a sensitivity experiment by running simulations starting from three alternative ice sheet geometries (Table ??) for those GI reconstructions indicating a WAIS collapse in CFEN, i.e., those forced by DF and EDC. We also include SLEN member forced by  $\text{EDC}_{\text{Hol,LGM}_{\text{avg}}}$  (cf. Table 4) in this analysis, since it attained a lower ice volume at 405 ka than any other member of CFEN, and thus provides an interesting end member for this ensemble. Finally, we also apply the same set of experiments to the Vostok GI reconstruction, in order to test whether a choice of alternative ice sheet geometries at 420 ka might trigger a WAIS collapse or enhance the response of the EAIS.

385 Looking at how the four initial geometries (gmt1-3 and the control) evolve under the four three different climate forcings from the ice-core derived GI reconstructions (Fig. 6), it becomes clear that all members under the same climate forcing have a tendency to converge follow the same path despite differing initial ice sheet configurations. Thus, the uncertainties in the The spread in minimum ice-sheet volumes (and consequently implications for WAIS collapse) due to assumptions of starting geometry are becomes rather small, with a spread between 1 and 1.1 3 m s.l.e. at 405 ka among the four different members three

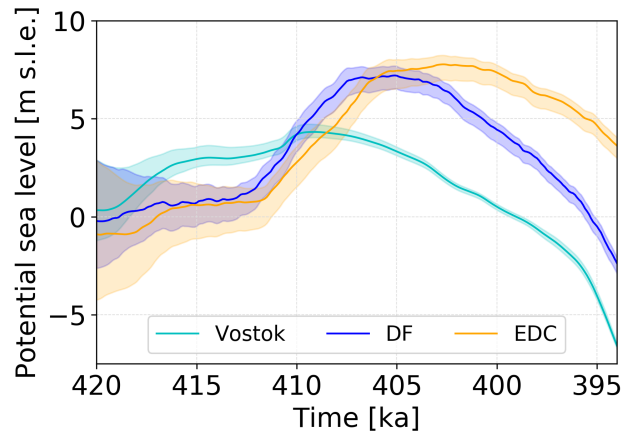


**Figure 6.** Sensitivity of the AIS response to CFEN GI reconstructions (Vostok, DF, EDC) and SSEN-EDC<sub>Hot,LGMavg</sub> between 420 and 394 ka with uncertainty bands from four distinct initial ice sheet starting geometries (Table ??gmt1-3 and respective CFEN member)- Contribution, expressed in contribution to (a)-global mean sea level [m s.l.e.]-and (b)-total ice volume  $10^3\text{km}^3$ . Solid lines show the mean of each common-forcing ensemble member, while the color filling shows the spread given by the different starting geometries (cf. Fig. 3).

390 different forcings in SGSEN. The different ice sheet configurations also show similar rates of retreat a similar pacing of retreat after 412 ka, indicating that the ice sheet size does their corresponding volume by that time did not affect its rate of contraction retreat due to climate warming. In our SGSEN simulations, it appears that the main source of variability between ice sheets with different geometries comes from the interior of the EAIS and the drainage basins of Ninnis and Totten specific EAIS drainage basins, such as those of Totten, Dibble, and Cook glaciers (Fig. 7 showcases the EDC ensemble; cf. Fig. 1 for geographical locations). The latter remains two remain thicker in the alternative geometry experiments than in the correspondent CFEN /SSEN correspondent experiment (Figs. 7e-g) experiment, whereas the former is thinner in gmt3 (Fig. 7gc). Some variability can also be observed in the WAIS domain. Parts of Pine Island Glacier appear to resist ice sheet collapse in the thicker-ice-geometry experiments (i.e., gmt2 and gmt3) when compared to the CFEN /SSEN correspondent run (Figs. 7f,gc,d). Given the observed spread, the three ensemble members constrain the range of potential sea level contributions from Antarctica during the MIS11c highstand at 405 ka to 2.33.2–8.8.2 m (minimum from Vostok, maximum from EDC<sub>Hot,LGMavg</sub>). This range can be essentially linked to whether the WAIS has collapsed or not during this period.

395

400

#### 4 Discussion

Offshore and far-field studies show results similar to our model-based inferences regarding the loss of the WAIS during MIS11c and minor losses of ice from the EAIS (thinning and margin retreat). Sediment cores in the WAIS sector of the Southern Ocean revealed evidence for a strong ice retreat during MIS11 (e.g., Scherer et al., 1998), whereas evidence for the EAIS retreat over past Quaternary interglacials has only recently been provided (Wilson et al., 2018, core U1361 in Fig. ??)

405

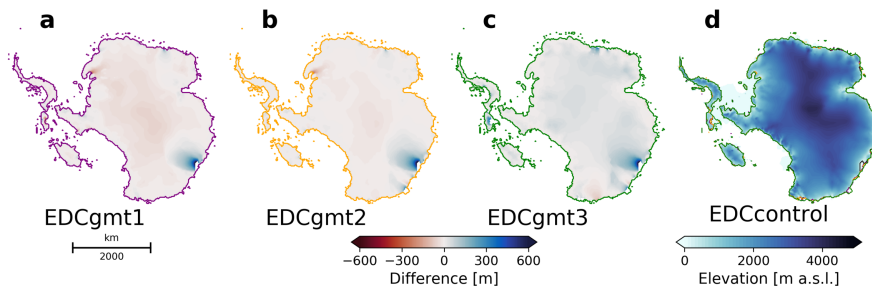


**Figure 7.** EDC-forced SGSEN members at 405 ka. (a-c) Ice sheet geometries at 405 ka for the EDC CFEN member using three different starting geometries corresponding to gmt1-3; at 420 ka (d) their reference run. i.e., CFEN member forced by the EDC-derived GI (Fig. e-g 3) difference-maps. Color scheme shows differences in surface elevation between their reference each geometry and the control for 405 ka (panel-d) and. Differences are only shown where the three resulting ice sheet is grounded in both geometries, and coloured lines show the respective grounding lines in gmt1-3, also overlain in (respectively panels a-ed).

Hillenbrand et al. (2009) compared sediment cores PS2547 and PS58/254 from the WAIS sector, and PS1506 offshore of Dronning Maud Land (Fig. ??) and found them to be inconclusive regarding the evidence for a WAIS collapse during MIS11, suggesting MIS13 or MIS15 as more likely candidates. They postulated, however, that the duration is more important than the magnitude of warming for a WAIS drawdown. Scherer et al. (1998) argue, based on samples from sediment cores drilled below Ice Stream B, that open ocean conditions existed for the Ross Ice Shelf Basin during MIS11. This is consistent with the open ocean conditions required to explain a closer source of moisture fuelling an advance of Dry Valley glaciers during the same period (Swanger et al., 2017). Finally, Raymo and Mitrovica (2012) estimated a MIS11 sea level rise of 6 to 13 m above PD, which they postulate that, considering the upper bound, could only be obtained if, in addition to Greenland's contribution, the WAIS had collapsed and the EAIS also provided its share.

Numerical modelling studies in which the WAIS did not collapse during MIS11 were acknowledged to be less sensitive to the ability of ocean temperatures to drive basal melting (e.g., Pollard and DeConto, 2009; Tigheelaar et al., 2019). Despite differences in the sensitivity to ocean temperature, our results support those of Tigheelaar et al. (2019) and Albrecht et al. (2020) regarding the minor role that variations in sea level alone play in driving ice sheet retreat. Instead, changes in sea level most likely act to boost the effect of air and ocean temperatures to drive the ice loss, as stipulated by Tigheelaar et al. (2019). In their study, Pollard and DeConto (2009) use the LR04 stack as forcing, which lacks significant warming above PI during MIS11e, and for which we did not obtain a WAIS collapse either, despite the very different approaches in reconstructing the transient signal between the two studies.

We found that the relatively low temporal resolution of LR04 is not the reason why it cannot produce a WAIS collapse as do the ice core records (i.e., it would have missed a short period where a pronounced peak would be present). Our RSEN low-pass-filter-forcing experiments with the EDC GI reconstruction show a WAIS collapse and significant ice sheet contraction, regardless of how much high-frequency variability is removed. It is worth reminding that Our simulations show that during the

LR04 stack contains no regional signal from the Southern Ocean at all, with its southernmost oxygen isotope records being taken from cores drilled in the Agulhas region (south of Africa in the Atlantic Ocean), at about 45S (see Fig. 1 in Lisiecki and Raymo, 2005). This could explain why LR04 does not capture the Antarctic warming event during MIS11, and consequently fails to provoke ice sheet contraction. The different criteria attempted for its scaling also had little effect (Fig. ??), further strengthening our argument that LR04 shows the global signature height of MIS11c, which is not representative of the peak warming in Antarctica. A possible way of circumventing this problem could be by using a similar approach to Sutter et al. (2019), who combined the LR04 stack and EDC ice core temperature records, that led to a WAIS collapse during MIS11.

From our experiments with different initial ice sheet geometries it seems that ice-shelf calving plays a role just as big as, if not larger, than basal ice-shelf melting in terms of regulating the grounding-line advance, since in gmt3 the grounding lines advanced more than in gmt2. The simplified treatment of the grounding lines could also have had an influence on the seeming insensitivity of our experiments to sea level uncertainties, although models which apply more refined treatments yield similar results for a similar spatial resolution (e.g., Tigheelaar et al., 2019). Thus, while these caveats must be taken into consideration, they do not appear to have influenced our results dramatically, since they can be directly compared to what other studies have obtained using similar forcings.

To construct our climate forcings, we used four the WAIS probably collapsed. We base this statement on different proxy records which show with significant differences in their structure during the MIS11c peak warming. They either consist One consisted of a short single peak (Vostok), or while others showed a prolonged period of (relatively) warmer conditions ; including a peak (LR04, DF, and EDC). Although the extensive warming signal is seen in most records, they too show differences from one another Despite having a warming peak of a similar GI magnitude at 410 ka, the Vostok-forced CFEN member is the only ice core-forced ensemble member that shows no collapse of the WAIS. Although the remaining climate reconstructions all show a longer peak, differences still exist among them. For example, EDC and DF, which are the most similar among the four records to each other, start shifting to their warmest conditions at about the same time (ea around 414 ka), but peak at different times. DF peaks at 410 ka, which is 3 kyr earlier than EDC. However, the Regardless of this difference, the simulated WAIS collapse occurs at 407 ka for using the DF and at 406 ka for using the EDC core experiments forcing, which is closer than the timing of their their timing of peak warming. Both records also produce Experiments forced by both records also yielded similar ice volumes (Fig. 64a) and extents (Supplementary Fig. S4). In contrast, the Vostok-forced ensemble member, which has a short warming peak, shows no collapse of the WAIS despite having a short warming peak of a similar GI magnitude at 410 ka5). It should be mentioned that the combination of GI and climate-model forcing results in a warmer signal in the surface temperatures at the DF, EDC, and Vostok core sites than obtained directly from their  $\delta D$  records (Supplementary Fig. S14). Vostok's GI-reconstructed temperature peak, however, matches the peak observed in DF for its  $\delta D$ -derived curve, and is also close to the warmest temperature reconstructed with the EDC isotopes. Finally, LR04 stands out when compared to the ice cores, and will be discussed in more detail separately.

It is important to remember that the Although sensitivity experiments show WAIS-collapse results using DF and EDC to be robust, the timing of the events discussed above should be taken with caution for two main reasons. First, we are forcing the entire AIS model with a climate signal from the EAIS, while previous studies have shown that the WAIS could have responded

over 2 kyr earlier to changes in climate (WAIS Divide Project Members, 2013). Second, all discrepancies in the timing of the events discussed so far recorded by the ice-core records, especially the peak warming and ice sheet collapse, are within the uncertainty in the age models of the ice cores (Parrenin et al., 2007; Bazin et al., 2013), preventing their respective age models (Parrenin et al., 2007; Bazin et al., 2013). Consequently, these two factors prevent us from establishing an exact point-in-time for these events. It should also be mentioned that the combination of GI and climate-model forcing to reconstruct the surface temperature results in a warmer temperature signal than the one obtained directly from the  $\delta D$  of the EDC and DF ice cores. This happens both to the average over the entire domain and at their drilling sites timing of these events, which means that the lags in AIS response are the most important to be considered.

In all our CFEN simulations, ice sheet retreat is associated with stronger basal melting close to ice shelf grounding lines, especially at Siple Coast, and in the Ross and Filchner-Ronne ice shelves (Fig. 8). Surface ablation seems to be significant only over the fringes of the EAIS, notably at Dronning Maud Land (DML) and the Amery ice shelf, where surface temperatures reach positive values during summer (Fig. ??), highlighting the fact that a linear interpolation between two fields does not fully capture the spatial pattern of the temperature anomalies. The EDC and DF  $\delta D$ -derived temperatures peak at 3.1 and 2.7°C respectively, while the temperature obtained by the GI reconstruction (Eq 9a). Nevertheless, they show limited retreat compared to the former two in the WAIS regions. The strong WAIS retreat seen in the EDC and DF-forced runs starting from 412 ka is triggered by an increase in ocean temperatures at intermediate depths (hereafter defined as the average between 400 and 1000 m depth) under the Ross and Filchner-Ronne ice shelves (Fig. 9b). Although this increase is progressive, it triggers a faster loss of volume by the WAIS compared to the EAIS after 412 ka (Fig. 4) ranges from 3.3 to 3.7°C. The same does not hold for Vostok: the  $\delta D$ -derived temperature peaks at 2.1°C, compared to 9c), in contrast with a similar evolution between the ice sheets before then. This observed tipping point at 412 ka also explains why the different ice-sheet configurations all follow the same trend from that moment onwards (Fig. 6), as ocean forcing becomes the main driver of ice-sheet retreat. Around most of the EAIS (except for the GI reconstruction that peaks at 1.6°C at the Vostok drilling site, and 2.5°C Amery Ice Shelf), neither ocean temperatures nor ice-shelf melt rates are high enough to force grounding line retreat as strongly as in the aforementioned regions, and ice loss is dominated by surface ablation at the ice-sheet fringes (cf. hatched patterns in Fig. 8).

The average intermediate-depth ocean temperatures under the Filchner-Ronne and Ross ice shelves peak between 0.4 and 0.85°C averaged over the entire domain. This mismatch between isotope-derived and GI-derived temperatures does not make our results less relevant: a set of simulations where the GI was for the three ice core-forced CFEN members (Fig. 9b). This happens at 410 ka for Vostok, 408 ka for DF, and 407 ka for EDC. Strong WAIS retreat, however, starts before the peak in forcing, supporting the presence of a tipping point at 412 ka. To further test whether this tipping point is the trigger of WAIS collapse, we have performed four additional experiments: (i) forced by EDC GI, but keeping the GI constant after 416 ka (i.e., before the threshold found in ocean temperatures), (ii) forced by EDC GI, but keeping the GI constant after 410 ka (i.e., just after the sudden increase in ocean temperatures, cf. Fig. 9b), (iii) forced by Vostok GI, where climate forcing is kept constant at its peak condition at 410 ka, and (iv) forced by Vostok GI where, after the 410 ka peak value (at 2.1°C above PI-, GI is brought back to its 411 ka value (i.e., the peak warming of Vostok) from between the peak and the observed tipping point) and kept constant. Figures 10a,b show that keeping the EDC-derived climate constant at 416 ka conditions prevents the WAIS

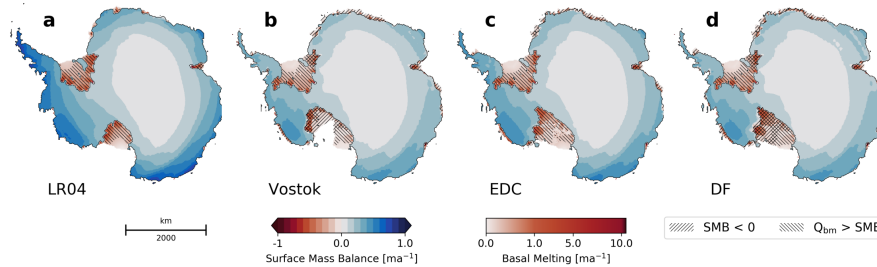


**Figure 8.** Surface Mass Balance ( $SMB, \text{ma}^{-1}$ ) for the grounded ice and basal melting ( $Q_{bm}, \text{ma}^{-1}$ ) for the ice shelves for the CFEN simulations at 415 ka. Hatched areas show where basal melting dominates over surface mass balance and where surface mass balance is negative (i.e., where surface ablation occurs). Everywhere where  $Q_{bm} > SMB$ , ice shelves are thinning.

from collapsing, while keeping it constant at 410 ka onward resulted in a WAIS collapse for all starting geometries after ca. 4 kyr (with a total sea-level contribution of 6.5–8.0 m at 405 ka; Fig conditions delays its collapse by almost 5 kyr compared to the core CFEN run. The Vostok-based simulations (Figs. ??), coinciding with what is observed for the EDC and DF-forced experiments. Thus, a more prolonged warming as seen in DF (which has a GI peak of similar magnitude as Vostok) and EDC seems to be crucial for the collapse of the WAIS, as opposed to the intensity of such peak, similar to what was suggested by Robinson et al. (2017) for the GIS.

Sensitivity of the AIS ice volume ( $10^3 \text{km}^3$ ) to "post 410 ka constant conditions". Solid line shows ice-sheet volume for the Vostok-forced CFEN member (c.f. Fig. 4), dotted and dashed lines show ice-sheet volume history when conditions are kept constant using a GI correspondent to 1.6C and 2.1C above PI, respectively.

Considering that EDC, Vostok, and DF reach similar GI values at 411 ka (10e-h) show that there is indeed a threshold, which is of approximately  $0.45^\circ\text{C}$  for the Filchner-Ronne ice shelf, and  $0.54^\circ\text{C}$  for the Ross ice shelf. However, our results also imply that this threshold must be sustained for at least 4 kyr to cause a collapse (compare red and blue dashed lines in Figs. 10f-h). A short peak at this threshold and subsequent cooling prevents the WAIS from collapsing, compared to keeping it constant at the same peak value (Fig. ??a); the value at this point seems to be the threshold for which a WAIS collapse is possible if such conditions are sustained for at least 4–5 kyr. This happens before the peak warming in these records, and corresponds to a 1.6–2.1 (10e,f). Comparing these values to PI temperatures averaged over the same extent of the water column, the magnitude of warming necessary to cross this threshold is  $0.4^\circ\text{C}$ . In other words, a warming of this magnitude can be understood as the condition necessary for WAIS collapse (Figs. 10c,d,g,h). Additional experiments where we test for a weakened ocean forcing further confirm this threshold, as a complete collapse of the WAIS is prevented when the temperatures at intermediate depths fail to reach a  $0.4^\circ\text{C}$  mean-annual-atmospheric warming across the Antarctic continent (i.e., the range of resulting temperature values between the three GI reconstructions cited above; warming relative to PI under the Filchner-Ronne and Ross ice shelves (Sect. 4 of the supplementary material). Considering that the temperature peak reconstructed by the Vostok GI is the closest to the  $\delta\text{D}$ -derived temperature peaks in DF and EDC (Fig. S6), which, considering our ocean forcing, translates to a 1.5–1.9C warming of the ocean surface averaged around Antarctica (i.e., south of 65S). S14), a more prolonged warming

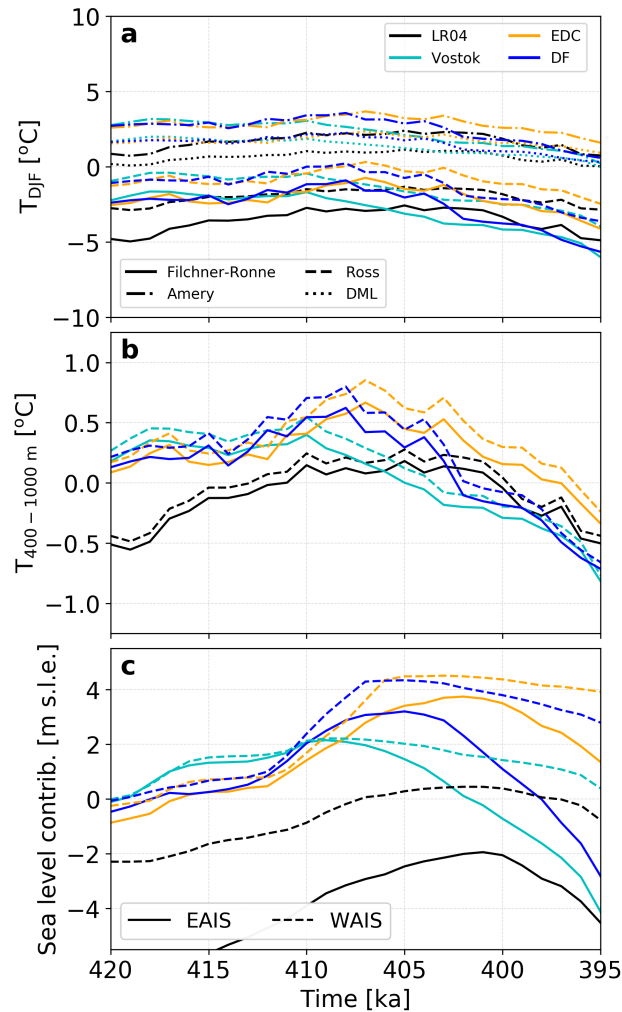


**Figure 9.** Evolution throughout MIS11 for each CFEN member for (a) Summer surface air temperature [°C] averaged over the main Antarctic ice shelves; (b) ocean temperatures averaged between 400 and 1000 m [°C] for the Filchner-Ronne and Ross ice shelves; (c) sea level contribution by EAIS and WAIS. Colours denote the respective CFEN member, while line styles in panels (a,b) denote each ice shelf, and each ice sheet in panel (c). DML refers to all smaller ice shelves along the Dronning Maud Land margin.

as seen in the DF and EDC ice core seems to be the crucial condition for the WAIS drawdown, similar to what was suggested by Robinson et al. (2017) for the GIS, while the peak's intensity could have accelerated or delayed the timing of collapse.

This threshold is much lower than the 4°C stipulated by Tigheelaar et al. (2018), but is in line with model close to the equilibrium model results in Garbe et al. (2020), but lower than the results from Turney et al. (2020) for the LIG. Our surface ocean temperature threshold should be considered with caution, because it is derived using an interpolation of ocean temperatures to compute our anomalies instead of a coupled ice-ocean setup (a full description is available in the supplementary material). A

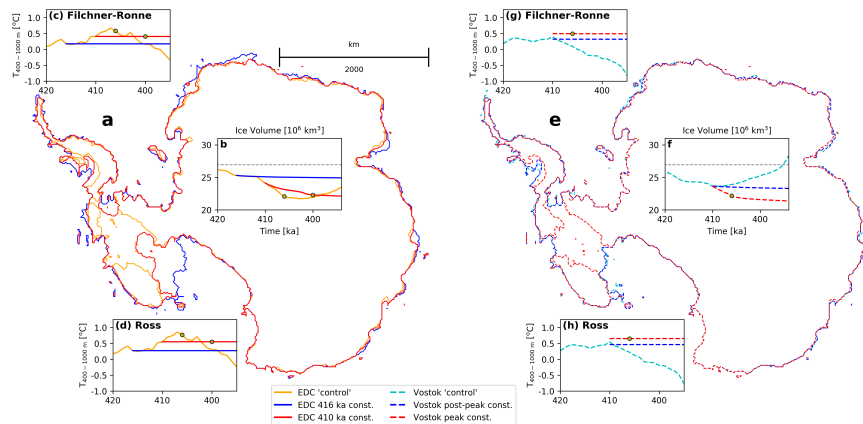


**Figure 10.** Thresholds for WAIS collapse. (a,e) grounding lines at 405 ka for three EDC-based (solid lines) and three Vostok-based (dashed lines) experiments, respectively (see below for explanation); (b,e) ice volume ( $10^6 \text{ km}^3$ ), (c,d; g,h) intermediate-depth (400–1000 m) ocean temperatures [ $^{\circ}\text{C}$ ] for the Filchner-Ronne and Ross ice shelves, respectively. Time series cover the period between 420 and 395 ka for both EDC (solid lines) and Vostok-based (dashed lines) experiments. Orange line shows the EDC control run, while cyan line shows the Vostok control run. Blue lines show EDC and Vostok simulations where climate was kept constant and the WAIS did not collapse, while the red lines show EDC and Vostok simulations where climate was kept constant and the WAIS collapsed. Yellow circles show the moment when the WAIS breaks down and an open-water connection between the Ross, Weddell and Amundsen seas is established.

simulation analogous to the one where the GI was kept fixed at conditions equivalent to the peak warming of Vostok, but using the GI value that corresponds to a 1.6 AIS retreat during the LIG. While the former shows a strong WAIS retreat is already possible for an ocean warming of  $0.7^{\circ}\text{C}$  warming across Antarctica for the Vostok ice core, was performed (Fig. C, the latter identify a tipping point at 2 ??). This time, a WAIS collapse has not been observed, corroborating the lower end of the inferred temperature interval  $^{\circ}\text{C}$  in ocean temperatures. It should be noted that the a minimum duration of the warming as the period as a key factor for the WAIS collapse is specific to MIS11c. In other words, a A more intense albeit shorter peak warming could also trigger WAIS collapse, since a strong rate of warming can drive ice retreat at a much faster pace , which was most likely the case for the LIG (Dutton et al., 2015; Turney et al., 2020)(Dutton et al., 2015; Turney et al., 2020). Numerical modelling studies in which the WAIS did not collapse during MIS11 were acknowledged to be less sensitive to the ability of ocean temperatures to drive basal melting (e.g., Pollard and DeConto, 2009; Tigchelaar et al., 2019).

The EDC and DF GI reconstructions yield results that mirror expectations from the paleorecord, including the estimations of the sea level contribution from Antarctica. Despite differences in the model sensitivity to ocean temperature, our results support those of Tigchelaar et al. (2019) and Albrecht et al. (2020) regarding the minor role that variations in sea level play in driving ice-sheet retreat. Although the coarse treatment of the grounding lines could have had an influence on the seeming insensitivity of our experiments to sea level uncertainties, other models of similar resolution which apply different sub-grid parameterisations to the grounding lines yield similar results. Hence, while this caveat must be taken into consideration, it does

not appear to have influenced our results dramatically. Moreover, AIS extent, the timing of WAIS collapse, and its contribution to sea level are robust regardless of model resolution (Fig. S15). Finally, we note that, despite very different approaches in reconstructing transient signals, neither Pollard and DeConto (2009) nor we were able to simulate a collapse of the WAIS using the LR04 stack as climate forcing.

We find that the relatively low temporal resolution of LR04 is not the reason why it did not produce a strong WAIS ice retreat. All RSEN experiments using low-pass-filter-forcing on the EDC GI reconstruction show a similar trajectory compared to the unfiltered forcing. The fact that MIS11c marine records in LR04 show oxygen isotopic values similar to the Holocene (Lisiecki and Raymo, 2005) despite geological evidence showing that there was a contribution to higher-than-Holocene sea levels from both Greenland and Antarctica (Scherer et al., 1998; Raymo and Mitrovica, 2012) implies that, if true, the ocean must have been colder. Indeed, paleoceanographic records from the Nordic Seas, for example, indicate that they were colder than present during MIS11 (Bauch et al., 2000; Kandiano et al., 2016; Doherty and Thibodeau, 2018). Southern Ocean records remain equivocal about a warming during MIS11 relative to the Holocene (e.g., Droxler et al., 2003). Hence, the inclusion of many Northern Hemisphere records in the LR04 stack could explain why it fails to capture Antarctic warming during MIS11c seen in the ice cores. This also helps explain why the different criteria adopted for changing its scaling procedure had little effect on the results (Fig. 4b). A possible way of circumventing this problem could be to adopt a similar scaling approach to Sutter et al. (2019), who combined the LR04 stack and EDC ice-core temperature records, which, in their study, also led to WAIS collapse during MIS11c.

In East Antarctica, our simulations do not capture the ice sheet retreat into the Wilkes Subglacial Basin recently proposed by Wilson et al. (2018) and Blackburn et al. (2020) for MIS11. Blackburn et al. (2020) suggest this retreat to have been caused by ocean warming, with little to no atmospheric influence. However, further paleoceanographic data are needed to fully understand this retreat (Noble et al., 2020), which so far has not been captured by other model experiments (cf. Wilson et al., 2018, Fig. 2b). As for West Antarctica, far-field sea level reconstructions suggest that a WAIS collapse was the most probable scenario (Raymo and Mitrovica, 2012; Chen et al., 2014) when comparing their results with estimates for the contribution from the GIS. While Robinson et al. (2017) found that Greenland contributed between 3.9 and 7.0 m to sea level rise (having 6.1 m s.l.e. as the most likely value), the ~~time at which their sea level contribution curve peaks, AIS contribution cannot be constrained by simply subtracting the GIS's contribution from the global sea level highstand. The suggested asynchronicity between the GIS and AIS minimum extents (Steig and Alley, 2002) and~~ the uncertainties in the age models of the different analysed ice cores (Petit et al., 1999; Parrenin et al., 2007; Bazin et al., 2013) ~~, and the suggested asynchronicity between the GIS and AIS minimum extents (Steig and Alley, 2002), do not allow us to simply constrain Antarctica's contribution by subtracting Greenland's contribution from the global sea level highstand. Based on EDC and DF (i. e., the scenarios prevent a simple relationship between both ice-sheet records to be established. Based on the ice-core experiments, our interval for the potential sea level contribution of the AIS is 3.2–8.2 m. This wide range is mainly related to whether the WAIS collapses or not. Considering the cases where the WAIS collapsed (i.e., EDC and DF core experiments) as the most probable scenario, our interval for the potential sea level contribution of the AIS is 6.4–8.8 m, with .2 m. In this case, the EAIS contribution is the largest source of uncertainty being the contribution of the EAIS (Fig. 11). Contrary to the WAIS (4.3–4.6 m s.l.e.), the EAIS reacted sensitively, being most~~

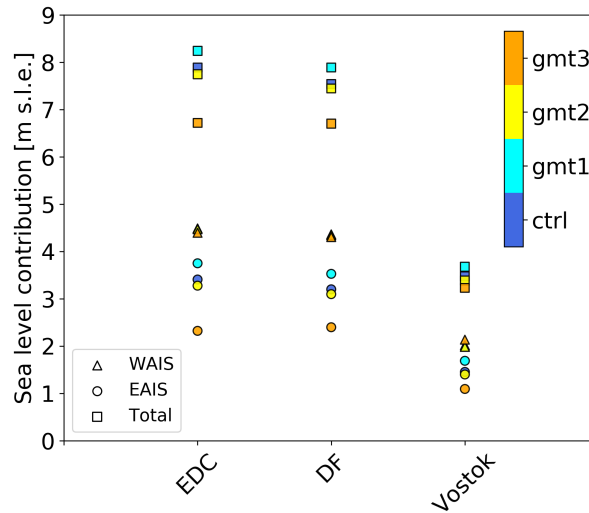


**Figure 11.** Sea level contribution (in m s.l.e.) of each SGSEN member during the global sea level highstand at 405 ka. LR04 member from CFEN is included for reference.

580 sensitive to the choice of starting ice geometry—especially—. This effect is strongest over Wilkes Land, which remains stable given a more extensive ice sheet. Conversely, a more extensive yet thinner ice sheet than the reference control run (i.e., gmt1; Fig where the spread in position of the grounding line is wider, and ice thickness is more variable than for other basins (Fig. 7). While nearby drainage basins, such as those of Totten and Dibble glaciers, become more stable given the larger ice sheet configurations of the alternative geometries (Figs. 3, Table ??) proved to be more prone to ice loss over the rest of the AIS than the relatively "bulkier" ice sheet of the control run b,c), Cook glacier, emanating from Wilkes Subglacial basin, appears to thin 585 regardless of the choice of initial geometry (Figs. 3a-c). Overall, the EAIS contributes 1.1 to 3.7 m s.l.e. at 405 ka (Fig. 11). This yields a range of 2.4 to 4.2 Conversely, the WAIS was rather insensitive to the choice of starting geometry (yielding 4.3–4.5 m s.l.e. contribution of the EAIS at 405 ka in the case of a collapse, and 2.0–2.1 otherwise) due to the stronger role played by the sub-shelf ocean forcing after 412 ka. There are, however, two stabilising feedbacks which are not incorporated in our model: 590 (i) a local sea-level drop caused by a reduced gravitational attraction of a shrinking ice sheet (e.g., Mitrovica et al., 2009), and (ii) the observed faster rebound of the crust due to a lower mantle viscosity in some WAIS locations (Barletta et al., 2018). The first effect is probably small based on our model's insensitivity to sea-level changes over these time scales, but we have been unable to robustly test the effect of a faster rebound on AIS response during MIS11c. However, we note that our ELRA model is set up with a relatively short response time of 1 kyr, for which the resulting bedrock uplift is still not able to trigger a stabilizing effect large enough to prevent WAIS collapse.

Several studies have been carried out ~~trying in order~~ to reconstruct past ice changes over the Antarctic continent, but to our knowledge no special focus has been given to Antarctica's response to the peak warming during MIS11c and the driving mechanisms behind it. To fill this gap we evaluated the deglaciation of Antarctica using a numerical ice-sheet model forced by a combination of climate model time-slice-forcing and various transient ~~signals. These signals records through a Glacial~~ Index (GI). The records were obtained from ice cores ~~taken at of~~ the EAIS interior and a stacked record of deep-sea sediment cores taken from far-field regions. We evaluated ~~possible sources of uncertainty due to (i) the sensitivity of our results to (i) the scaling of the GI, (ii) multi-centennial (ii) millennial~~ variability and temporal record resolution, ~~(iii) (iii) different sea level reconstructions, and (iv) initial ice-sheet conditions (iv) initial ice sheet configurations~~. While sea level, higher-frequency variability, and the GI scaling of the records seemed to play a small role, different responses were seen for both East and West Antarctic Ice Sheets regarding the different applied transient signals, and for the initial ice sheet configurations. Among the applied ice-core reconstructions, the warming captured by the Vostok ice core during MIS11c was not strong enough to cause a collapse of the WAIS, which was attributed to the short duration of its peak. Our results indicate that our modelled WAIS collapse was caused by the duration rather than the intensity of warming, and that it was insensitive to the choice of the starting geometry. The latter proved to be a larger source of uncertainty for the EAIS. Regarding the initial questions posed in the beginning of this study, we now provide ~~objective~~, short answers to them:

1. **How did the AIS respond to the peak warming of MIS11c? What are the uncertainties in the AIS minimum configuration, its timing and potential sea level contribution?**

~~We found the WAIS to collapse about 5 kyr after the mean annual atmospheric temperature exceeded 1.6–2.1°C above Pre-Industrial across Antarctica~~ Using transient signals from EAIS ice cores, we found a range in sea level contribution of 3.2 to 8.2 m s.l.e., which mainly reflects whether the WAIS has collapsed or not in our experiments. For the former scenario –which is supported by far-field sea level reconstructions– we find that a WAIS collapse during MIS11c is attained after a prolonged warming period of the ocean of ca. 4 kyr. The resulting AIS contribution in this case is 6.7–8.2 m s.l.e. at 405–402 ka. Uncertainties in these values are primarily due to the choice of climate forcing and ice sheet starting configuration (at 420 ka). While the contribution to sea level rise by the WAIS was consistent among the experiments for which we observe strong WAIS retreat those experiments that yielded its collapse (4.3–4.6 m), varying mostly due to the choice of climate forcing, 5 m s.l.e., the EAIS contribution was less constrained (2.4–4.2 m) remained more uncertain because of its sensitivity to the initial geometry of the ice sheet (2.4–3.7 m s.l.e.).

2. **What was the main driver for AIS of the changes in size the AIS volume? Was it warming length duration, peak temperature, or changes in precipitation? Are any of these processes relevant to future, or changes in the southern high latitudes oceanic forcing?**

~~Ice retreat was found to be~~ We identify a tipping point at ca. 412 ka, beyond which strong WAIS retreat occurred in response to the ocean warming. Past this point, retreat leading to WAIS collapse was mostly sensitive to the length of

630 ~~warming rather than its intensity. We found a threshold of 1.6–2.1~~warming duration more than intensity, provided ocean  
temperatures at intermediate depths become 0.4 °C above PI mean-annual average atmospheric temperatures at which  
~~strong WAIS ice retreat is triggered given a 4–5 kyr duration of the warming. This indicates that an onset of massive~~  
~~WAIS retreat in the near future is possible, although aiming at a reduction in global/Antarctic average temperatures~~  
~~could still prevent its collapse~~warmer than PI under the Filchner-Ronne and Ross ice shelves. This threshold should be  
sustained for at least 4 kyr so that strong WAIS ice retreat is triggered.

635 *Code and data availability.* The numerical code for the ice-sheet model SICOPOLIS can be obtained in <http://sicopolis.net/>. All settings files used for the model runs are available in [https://github.com/martimmas/MIS11c\\_exps](https://github.com/martimmas/MIS11c_exps). The full model outputs are available upon request to the corresponding author.

*Author contributions.* MMB, IR and JB designed the study. Experiments were carried out and analyzed by MMB and JB. MMB wrote the manuscript with contributions from all co-authors

640 *Competing interests.* The authors declare that they have no conflict of interest.

*Acknowledgements.* This work is funded by the MAGIC-DML project. MAGIC-DML is a consortium supported by Stockholm University (Arjen Stroeven), Norwegian Polar Institute/NARE under Grant "MAGIC-DML" (Ola Fredin), the US National Science Foundation under Grant No. PLR-1542930 (Jonathan Harbor & Nathaniel Lifton), Swedish Research Council under Grant No. 2016-04422 (Jonathan Harbor & Arjen Stroeven), and the German Research Foundation (DFG) Priority Programme 1158 "Antarctic Research" under Grant No. 365737614  
645 (Irina Rogozhina & Matthias Prange). Jorge Bernales has been supported by the MAGIC-DML project through DFG SPP 1158 (RO 4262/1-6). We would also like to acknowledge support from the Carl Mannerfelts fond and the Bolin Centre Climate Research School (Martim Mas e Braga). The ice-sheet model simulations were performed on the GeoMod cluster at MARUM, Bremen University. We thank Andreas Manschke ~~and the GeoMod team at MARUM, Bremen University, for providing us with~~for technical support and continuous access to ~~their computer cluster where the model simulations were performed~~the computer cluster.

## 650 **References**

- Albrecht, T., Winkelmann, R., and Levermann, A.: Glacial-cycle simulations of the Antarctic Ice Sheet with the Parallel Ice Sheet Model (PISM) – Part 1: Boundary conditions and climatic forcing, *The Cryosphere*, 14, 599–632, <https://doi.org/10.5194/tc-14-599-2020>, 2020.
- Barletta, V. R., Bevis, M., Smith, B. E., Wilson, T., Brown, A., Bordononi, A., Willis, M., Khan, S. A., Rovira-Navarro, M., Dalziel, I., et al.: Observed rapid bedrock uplift in Amundsen Sea Embayment promotes ice-sheet stability, *Science*, 360, 1335–1339, 2018.
- 655 Bauch, H. A., Erlenkeuser, H., Helmke, J. P., and Struck, U.: A paleoclimatic evaluation of marine oxygen isotope stage 11 in the high-northern Atlantic (Nordic seas), *Global and Planetary Change*, 24, 27–39, [https://doi.org/https://doi.org/10.1016/S0921-8181\(99\)00067-3](https://doi.org/https://doi.org/10.1016/S0921-8181(99)00067-3), 2000.
- Bazin, L., Landais, A., Lemieux-Dudon, B., Kele, H. T. M., Veres, D., Parrenin, F., Martinerie, P., Ritz, C., Capron, E., Lipenkov, V., et al.: An optimized multi-proxy, multi-site Antarctic ice and gas orbital chronology (AICC2012): 120-800 ka, *Climate of the Past*, 9, 1715–1731, 660 2013.
- Beckmann, A. and Goosse, H.: A parameterization of ice shelf–ocean interaction for climate models, *Ocean modelling*, 5, 157–170, 2003.
- Berger, A. and Loutre, M.-F.: *Climate 400,000 years ago, a key to the future?*, Washington DC American Geophysical Union Geophysical Monograph Series, 137, 17–26, 2003.
- Bernales, J., Rogozhina, I., Greve, R., and Thomas, M.: Comparison of hybrid schemes for the combination of shallow approximations in 665 numerical simulations of the Antarctic Ice Sheet, *The Cryosphere*, 11, 247–265, <https://doi.org/10.5194/tc-11-247-2017>, 2017a.
- Bernales, J., Rogozhina, I., and Thomas, M.: Melting and freezing under Antarctic ice shelves from a combination of ice-sheet modelling and observations, *Journal of Glaciology*, 63, 731–744, 2017b.
- Bintanja, R. and van de Wal, R.: North American ice-sheet dynamics and the onset of 100,000-year glacial cycles, *Nature*, 454, 869–872, 2008.
- 670 Blackburn, T., Edwards, G., Tulaczyk, S., Scudder, M., Piccione, G., Hallet, B., McLean, N., Zachos, J., Cheney, B., and Babbe, J.: Ice retreat in Wilkes Basin of East Antarctica during a warm interglacial, *Nature*, 583, 554–559, 2020.
- Calov, R. and Greve, R.: A semi-analytical solution for the positive degree-day model with stochastic temperature variations, *Journal of Glaciology*, 51, 173–175, 2005.
- Capron, E., Rovere, A., Austermann, J., Axford, Y., Barlow, N. L., Carlson, A. E., de Vernal, A., Dutton, A., Kopp, R. E., McManus, J. F., 675 et al.: Challenges and research priorities to understand interactions between climate, ice sheets and global mean sea level during past interglacials, *Quaternary Science Reviews*, 219, 308–311, 2019.
- Chen, F., Friedman, S., Gertler, C. G., Looney, J., O’Connell, N., Sierks, K., and Mitrovica, J. X.: Refining estimates of polar ice volumes during the MIS11 Interglacial using sea level records from South Africa, *Journal of Climate*, 27, 8740–8746, 2014.
- Clark, P. U., Dyke, A. S., Shakun, J. D., Carlson, A. E., Clark, J., Wohlfarth, B., Mitrovica, J. X., Hostetler, S. W., and McCabe, A. M.: The 680 Last Glacial Maximum, *Science*, 325, 710–714, <https://doi.org/10.1126/science.1172873>, 2009.
- Clason, C. C., Applegate, P., and Holmlund, P.: Modelling Late Weichselian evolution of the Eurasian ice sheets forced by surface meltwater-enhanced basal sliding, *Journal of Glaciology*, 60, 29–40, 2014.
- de Boer, B., van de Wal, R. S. W., Lourens, L. J., Bintanja, R., and Reerink, T. J.: A continuous simulation of global ice volume over the past 1 million years with 3-D ice-sheet models, *Climate Dynamics*, 41, 1365–1384, <https://doi.org/10.1007/s00382-012-1562-2>, 2013.

- 685 de Boer, B., Dolan, A., Bernales, J., Gasson, E., Gollidge, N., Sutter, J., Huybrechts, P., Lohmann, G., Rogozhina, I., Abe-Ouchi, A., et al.:  
Simulating the Antarctic Ice Sheet in the late-Pliocene warm period: PLISMIP-ANT, an ice-sheet model intercomparison project, *The Cryosphere*, 9, 881–903, 2015.
- Doherty, J. M. and Thibodeau, B.: Cold Water in a Warm World: Investigating the Origin of the Nordic Seas’ Unique Surface Properties  
During MIS 11, *Frontiers in Marine Science*, 5, 251, <https://doi.org/10.3389/fmars.2018.00251>, 2018.
- 690 Dolan, A. M., De Boer, B., Bernales, J., Hill, D. J., and Haywood, A. M.: High climate model dependency of Pliocene Antarctic ice-sheet  
predictions, *Nature communications*, 9, 2799, 2018.
- Droxler, A. W., Alley, R. B., Howard, W. R., Poore, R. Z., and Burckle, L. H.: Unique and Exceptionally Long Interglacial Marine Isotope  
Stage 11: Window Into Earth Warm Future Climate, pp. 1–14, *American Geophysical Union (AGU)*, <https://doi.org/10.1029/137GM01>,  
2003.
- 695 Dutton, A., Carlson, A. E., Long, A. J., Milne, G. A., Clark, P. U., DeConto, R., Horton, B. P., Rahmstorf, S., and Raymo, M. E.: Sea-level  
rise due to polar ice-sheet mass loss during past warm periods, *Science*, 349, aaa4019, <https://doi.org/10.1126/science.aaa4019>, 2015.
- EPICA Community Members: Eight glacial cycles from an Antarctic ice core, *Nature*, 429, 623–628, <https://doi.org/10.1038/nature02599>,  
2004.
- Favier, L., Jourdain, N. C., Jenkins, A., Merino, N., Durand, G., Gagliardini, O., Gillet-Chaulet, F., and Mathiot, P.: Assessment of sub-shelf  
700 melting parameterisations using the ocean–ice-sheet coupled model NEMO (v3. 6)–Elmer/Ice (v8. 3), *Geoscientific Model Development*,  
12, 2255–2283, 2019.
- Forsström, P.-L. and Greve, R.: Simulation of the Eurasian ice sheet dynamics during the last glaciation, *Global and Planetary Change*, 42,  
59–81, 2004.
- Forsström, P.-L., Sallasmaa, O., Greve, R., and Zwinger, T.: Simulation of fast-flow features of the Fennoscandian ice sheet during the Last  
705 Glacial Maximum, *Annals of Glaciology*, 37, 383–389, 2003.
- Fretwell, P., Pritchard, H. D., Vaughan, D. G., Bamber, J. L., Barrand, N., Bell, R., Bianchi, C., Bingham, R., Blankenship, D. D., Casassa,  
G., et al.: Bedmap2: improved ice bed, surface and thickness datasets for Antarctica, *The Cryosphere*, 7, 375–393, 2013.
- Garbe, J., Albrecht, T., Levermann, A., Donges, J. F., and Winkelmann, R.: Hysteresis of the Antarctic Ice Sheet, *Nature*, 585, 538–544,  
2020.
- 710 Greve, R.: Application of a polythermal three-dimensional ice sheet model to the Greenland ice sheet: response to steady-state and transient  
climate scenarios, *Journal of Climate*, 10, 901–918, 1997.
- Greve, R.: Relation of measured basal temperatures and the spatial distribution of the geothermal heat flux for the Greenland Ice Sheet,  
*Annals of Glaciology*, 42, 424–432, 2005.
- Greve, R. and Blatter, H.: Comparison of thermodynamics solvers in the polythermal ice sheet model SICOPOLIS, *Polar Science*, 10, 11–23,  
715 2016.
- Handiani, D., Paul, A., Prange, M., Merkel, U., Dupont, L., and Zhang, X.: Tropical vegetation response to Heinrich Event 1 as simulated  
with the UVic ESCM and CCSM3, *Climate of the Past*, 9, 1683–1696, 2013.
- Hearty, P. J., Hollin, J. T., Neumann, A. C., O’Leary, M. J., and McCulloch, M.: Global sea-level fluctuations during the Last Interglaciation  
(MIS 5e), *Quaternary Science Reviews*, 26, 2090–2112, 2007.
- 720 Hillenbrand, C.-D., Fütterer, D., Grobe, H., and Frederichs, T.: No evidence for a Pleistocene collapse of the West Antarctic Ice Sheet from  
continental margin sediments recovered in the Amundsen Sea, *Geo-Marine Letters*, 22, 51–59, [https://doi.org/10.1007/s00367-002-0097-](https://doi.org/10.1007/s00367-002-0097-7)  
[7](http://link.springer.com/10.1007/s00367-002-0097-7), <http://link.springer.com/10.1007/s00367-002-0097-7>, 2002.

- Hillenbrand, C.-D., Kuhn, G., and Frederichs, T.: Record of a Mid-Pleistocene depositional anomaly in West Antarctic continental margin sediments: an indicator for ice-sheet collapse?, *Quaternary Science Reviews*, 28, 1147–1159, 725 <https://doi.org/10.1016/j.quascirev.2008.12.010>, 2009.
- Hodell, D. A., Charles, C. D., and Ninnemann, U. S.: Comparison of interglacial stages in the South Atlantic sector of the Southern Ocean for the past 450 kyr: implications for Marine Isotope Stage MIS11, *Global and Planetary Change*, 24, 7–26, 2000.
- Holden, P. B., Edwards, N. R., Wolff, E. W., Lang, N. J., Singarayer, J. S., Valdes, P. J., and Stocker, T. F.: Interhemispheric coupling, the West Antarctic Ice Sheet and warm Antarctic interglacials, *Climate of the Past*, 6, 431–443, <https://doi.org/10.5194/cp-6-431-2010>, 2010.
- 730 Holden, P. B., Edwards, N. R., Wolff, E. W., Valdes, P. J., and Singarayer, J. S.: The Mid-Brunhes Event and West Antarctic Ice Sheet stability, *Journal of Quaternary Science*, 26, 474–477, <https://doi.org/10.1002/jqs.1525>, <http://doi.wiley.com/10.1002/jqs.1525>, 2011.
- Holland, P. R., Jenkins, A., and Holland, D. M.: The response of ice shelf basal melting to variations in ocean temperature, *Journal of Climate*, 21, 2558–2572, 2008.
- Imbrie, J., McIntyre, A., and Mix, A.: Oceanic Response to Orbital Forcing in the Late Quaternary: Observational and Experimental Strategies, in: *Climate and Geo-Sciences*, edited by Berger, A., Schneider, S., and Duplessy, J. C., pp. 121–164, Springer Netherlands, Dordrecht, 735 [https://doi.org/10.1007/978-94-009-2446-8\\_7](https://doi.org/10.1007/978-94-009-2446-8_7), [http://link.springer.com/10.1007/978-94-009-2446-8\\_7](http://link.springer.com/10.1007/978-94-009-2446-8_7), 1989.
- Jouzel, J., Masson-Delmotte, V., Cattani, O., Dreyfus, G., Falourd, S., Hoffmann, G., Minster, B., Nouet, J., Barnola, J.-M., Chappellaz, J., et al.: Orbital and millennial Antarctic climate variability over the past 800,000 years, *Science*, 317, 793–796, 2007.
- Kandiano, E. S., van der Meer, M. T. J., Bauch, H. A., Helmke, J., Damsté, J. S. S., and Schouten, S.: A cold and fresh ocean 740 surface in the Nordic Seas during MIS 11: Significance for the future ocean, *Geophysical Research Letters*, 43, 10,929–10,937, <https://doi.org/10.1002/2016GL070294>, 2016.
- Kleinen, T., Hildebrandt, S., Prange, M., Rachmayani, R., Müller, S., Bezrukova, E., Brovkin, V., and Tarasov, P. E.: The climate and vegetation of Marine Isotope Stage 11—model results and proxy-based reconstructions at global and regional scale, *Quaternary International*, 348, 247–265, <https://doi.org/10.1016/j.quaint.2013.12.028>, 2014.
- 745 Konrad, H., Thoma, M., Sasgen, I., Klemann, V., Grosfeld, K., Barbi, D., and Martinec, Z.: The deformational response of a viscoelastic solid earth model coupled to a thermomechanical ice sheet model, *Surveys in Geophysics*, 35, 1441–1458, 2014.
- Kukla, G.: How long and how stable was the last interglacial?, *Quaternary Science Reviews*, 16, 605–612, [https://doi.org/10.1016/S0277-3791\(96\)00114-X](https://doi.org/10.1016/S0277-3791(96)00114-X), 1997.
- Lisiecki, L. E. and Raymo, M. E.: A Pliocene-Pleistocene stack of 57 globally distributed benthic  $\delta^{18}\text{O}$  records, *Paleoceanography*, 20, 750 PA1003, <https://doi.org/10.1029/2004PA001071>, 2005.
- Loutre, M. and Berger, A.: Marine Isotope Stage 11 as an analogue for the present interglacial, *Global and Planetary Change*, 36, 209–217, [https://doi.org/10.1016/S0921-8181\(02\)00186-8](https://doi.org/10.1016/S0921-8181(02)00186-8), 2003.
- Martin, M. A., Winkelmann, R., Haseloff, M., Albrecht, T., Bueler, E., Khroulev, C., and Levermann, A.: The Potsdam Parallel Ice Sheet Model (PISM-PIK)—Part 2: Dynamic equilibrium simulation of the Antarctic Ice Sheet, *The Cryosphere*, 5, 727–740, 2011.
- 755 Maule, C. F., Purucker, M. E., Olsen, N., and Mosegaard, K.: Heat Flux Anomalies in Antarctica Revealed by Satellite Magnetic Data, *Science*, 309, 464–467, <https://doi.org/10.1126/science.1106888>, 2005.
- Milker, Y., Rachmayani, R., Weinkauff, M. F. G., Prange, M., Raitzsch, M., Schulz, M., and Kučera, M.: Global and regional sea surface temperature trends during Marine Isotope Stage 11, *Climate of the Past*, 9, 2231–2252, <https://doi.org/10.5194/cp-9-2231-2013>, 2013.
- Mitrovica, J. X., Gomez, N., and Clark, P. U.: The sea-level fingerprint of West Antarctic collapse, *Science*, 323, 753–753, 2009.

- 760 Naish, T., Powell, R., Levy, R., Wilson, G., Scherer, R., Talarico, F., Krissek, L., Niessen, F., Pompilio, M., Wilson, T., et al.: Obliquity-paced Pliocene West Antarctic ice sheet oscillations, *Nature*, 458, 322–328, 2009.
- Noble, T., Rohling, E., Aitken, A., Bostock, H., Chase, Z., Gomez, N., Jong, L., King, M., Mackintosh, A., McCormack, F., et al.: The sensitivity of the Antarctic Ice Sheet to a changing climate: Past, present and future, *Reviews of Geophysics*, p. e2019RG000663, <https://doi.org/10.1029/2019RG000663>, 2020.
- 765 Parrenin, F., Barnola, J.-M., Beer, J., Blunier, T., Castellano, E., Chappellaz, J., Dreyfus, G., Fischer, H., Fujita, S., Jouzel, J., et al.: The EDC3 chronology for the EPICA Dome C ice core, *Climate of the Past*, 3, 485–497, 2007.
- Petit, J., Jouzel, J., Raynaud, D., Barkov, N., Barnola, J., Basile, I., Bender, M., Chappellaz, J., Davis, J., Delaygue, G., et al.: Vostok ice core data for 420,000 years, IGBP pages/world data center for paleoclimatology data contribution series #2001–076, NOAA/NGDC Paleoclimatology Program, Boulder CO, USA, 2001.
- 770 Petit, J.-R., Jouzel, J., Raynaud, D., Barkov, N. I., Barnola, J.-M., Basile, I., Bender, M., Chappellaz, J., Davis, M., Delaygue, G., et al.: Climate and atmospheric history of the past 420,000 years from the Vostok ice core, *Antarctica, Nature*, 399, 429–436, 1999.
- Pollard, D. and DeConto, R.: Description of a hybrid ice sheet-shelf model, and application to Antarctica, *Geoscientific Model Development*, 5, 1273–1295, 2012a.
- Pollard, D. and DeConto, R.: A simple inverse method for the distribution of basal sliding coefficients under ice sheets, applied to Antarctica, *The Cryosphere*, 6, 953, 2012b.
- 775 Pollard, D. and DeConto, R. M.: Modelling West Antarctic Ice Sheet growth and collapse through the past five million years, *Nature*, 458, 329–332, 2009.
- Rachmayani, R., Prange, M., and Schulz, M.: Intra-interglacial climate variability: model simulations of Marine Isotope Stages 1, 5, 11, 13, and 15, *Climate of the Past*, 12, 677–695, <https://doi.org/10.5194/cp-12-677-2016>, 2016.
- 780 Rachmayani, R., Prange, M., Lunt, D. J., Stone, E. J., and Schulz, M.: Sensitivity of the Greenland Ice Sheet to Interglacial Climate Forcing: MIS 5e Versus MIS 11, *Paleoceanography*, 32, 1089–1101, <https://doi.org/10.1002/2017PA003149>, <http://doi.wiley.com/10.1002/2017PA003149>, 2017.
- Raymo, M. E. and Mitrovica, J. X.: Collapse of polar ice sheets during the stage 11 interglacial, *Nature*, 483, 453–456, <https://doi.org/10.1038/nature10891>, 2012.
- 785 Raynaud, D., Barnola, J.-M., Souchez, R., Lorrain, R., Petit, J.-R., Duval, P., and Lipenkov, V. Y.: The record for Marine Isotopic Stage 11, *Nature Communications*, 436, 39–40, <https://doi.org/10.1038/43639b>, 2005.
- Reyes, A. V., Carlson, A. E., Beard, B. L., Hatfield, R. G., Stoner, J. S., Winsor, K., Welke, B., and Ullman, D. J.: South Greenland ice-sheet collapse during Marine Isotope Stage 11, *Nature*, 510, 525–528, <https://doi.org/10.1038/nature13456>, 2014.
- Robinson, A., Alvarez-Solas, J., Calov, R., Ganopolski, A., and Montoya, M.: MIS-11 duration key to disappearance of the Greenland Ice
- 790 Sheet, *Nature Communications*, 8, 16 008, <https://doi.org/10.1038/ncomms16008>, 2017.
- Sato, T. and Greve, R.: Sensitivity experiments for the Antarctic Ice Sheet with varied sub-ice-shelf melting rates, *Annals of Glaciology*, 53, 221–228, 2012.
- Scherer, R. P.: Quaternary interglacials and the West Antarctic Ice Sheet, in: *Geophysical Monograph Series*, edited by Droxler, A. W., Poore, R. Z., and Burckle, L. H., vol. 137, pp. 103–112, American Geophysical Union, Washington, D. C., <https://doi.org/10.1029/137GM08>,
- 795 2003.
- Scherer, R. P., Aldahan, A., Tulaczyk, S., Possnert, G., Engelhardt, H., and Kamb, B.: Pleistocene collapse of the West Antarctic Ice Sheet, *Science*, 281, 82–85, 1998.

- Shackleton, N. J., Sánchez-Goñi, M. F., Pailler, D., and Lancelot, Y.: Marine isotope substage 5e and the Eemian interglacial, *Global and Planetary change*, 36, 151–155, 2003.
- 800 Spratt, R. M. and Lisiecki, L. E.: A Late Pleistocene sea level stack, *Climate of the Past*, 12, 1079–1092, 2016.
- Steig, E. J. and Alley, R. B.: Phase relationships between Antarctic and Greenland climate records, *Annals of Glaciology*, 35, 451–456, 2002.
- Sutter, J., Fischer, H., Grosfeld, K., Karlsson, N. B., Kleiner, T., van Liefferinge, B., and Eisen, O.: Modelling the Antarctic Ice Sheet across the mid-Pleistocene transition—implications for Oldest Ice, *The Cryosphere*, 13, 2023–2041, 2019.
- Swanger, K. M., Lamp, J. L., Winckler, G., Schaefer, J. M., and Marchant, D. R.: Glacier advance during Marine Isotope Stage 11 in the  
805 McMurdo dry valleys of Antarctica, *Scientific reports*, 7, 41 433, 2017.
- Tigheelaar, M., Timmermann, A., Pollard, D., Friedrich, T., and Heinemann, M.: Local insolation changes enhance Antarctic interglacials: Insights from an 800,000-year ice sheet simulation with transient climate forcing, *Earth and Planetary Science Letters*, 495, 69–78, <https://doi.org/10.1016/j.epsl.2018.05.004>, 2018.
- Tigheelaar, M., Timmermann, A., Friedrich, T., Heinemann, M., and Pollard, D.: Nonlinear response of the Antarctic Ice Sheet to late  
810 Quaternary sea level and climate forcing, *The Cryosphere*, 13, 2615–2631, 2019.
- Turney, C. S., Fogwill, C. J., Gollledge, N. R., McKay, N. P., van Sebille, E., Jones, R. T., Etheridge, D., Rubino, M., Thornton, D. P., Davies, S. M., et al.: Early Last Interglacial ocean warming drove substantial ice mass loss from Antarctica, *Proceedings of the National Academy of Sciences*, 117, 3996–4006, 2020.
- Tzedakis, P. C., Wolff, E. W., Skinner, L. C., Brovkin, V., Hodell, D. A., McManus, J. F., and Raynaud, D.: Can we predict the duration of an  
815 interglacial?, *Climate of the Past*, 8, 1473–1485, <https://doi.org/10.5194/cp-8-1473-2012>, <https://www.clim-past.net/8/1473/2012/>, 2012.
- Uemura, R., Motoyama, H., Masson-Delmotte, V., Jouzel, J., Kawamura, K., Goto-Azuma, K., Fujita, S., Kuramoto, T., Hirabayashi, M., Miyake, T., et al.: Asynchrony between Antarctic temperature and CO<sub>2</sub> associated with obliquity over the past 720,000 years, *Nature communications*, 9, 961, 2018.
- Waelbroeck, C., Labeyrie, L., Michel, E., Duplessy, J., McManus, J., Lambeck, K., Balbon, E., and Labracherie, M.: Sea-level and  
820 deep water temperature changes derived from benthic foraminifera isotopic records, *Quaternary Science Reviews*, 21, 295–305, [https://doi.org/10.1016/S0277-3791\(01\)00101-9](https://doi.org/10.1016/S0277-3791(01)00101-9), 2002.
- WAIS Divide Project Members: Onset of deglacial warming in West Antarctica driven by local orbital forcing, *Nature*, 500, 440–444, <https://doi.org/10.1038/nature12376>, 2013.
- Willerslev, E., Cappellini, E., Boomsma, W., Nielsen, R., Hebsgaard, M. B., Brand, T. B., Hofreiter, M., Bunce, M., Poinar, H. N., Dahl-  
825 Jensen, D., Johnsen, S., Steffensen, J. P., Bennike, O., Schwenninger, J.-L., Nathan, R., Armitage, S., de Hoog, C.-J., Alfimov, V., Christl, M., Beer, J., Muscheler, R., Barker, J., Sharp, M., Penkman, K. E. H., Haile, J., Taberlet, P., Gilbert, M. T. P., Casoli, A., Campani, E., and Collins, M. J.: Ancient Biomolecules from Deep Ice Cores Reveal a Forested Southern Greenland, *Science*, 317, 111–114, <https://doi.org/10.1126/science.1141758>, <http://www.sciencemag.org/cgi/doi/10.1126/science.1141758>, 2007.
- Wilson, D. J., Bertram, R. A., Needham, E. F., van de Flierdt, T., Welsh, K. J., McKay, R. M., Mazumder, A., Riesselman, C. R., Jimenez-  
830 Espejo, F. J., and Escutia, C.: Ice loss from the East Antarctic Ice Sheet during late Pleistocene interglacials, *Nature*, 561, 383–386, <https://doi.org/10.1038/s41586-018-0501-8>, <http://www.nature.com/articles/s41586-018-0501-8>, 2018.
- Yang, H. and Zhu, J.: Equilibrium thermal response timescale of global oceans, *Geophysical Research Letters*, 38, <https://doi.org/10.1029/2011GL048076>, 2011.